RESEARCH & DEVELOPMENT

Final Report

Performance Evaluation of Cable Barriers on a 6:1 Sloped Median under MASH TL-3 Conditions

Prepared By

Howie Fang, Ph.D.

Emre Palta

Zheng Li

Oyeboade Fatoki

University of North Carolina at Charlotte
Department of Mechanical Engineering & Engineering Science
Department of Civil & Environmental Engineering
Charlotte, NC 28223-0001

March 31, 2019

Technical Report Documentation Page

1. Report No. **NCDOT 2017-13**	2. Government Accession No.	3. Recipient's Catalog No.	
4. Title and Subtitle ***Performance Evaluation of Cable Barriers on a 6:1 Sloped Median under MASH TL-3 Conditions***		5. Report Date **March 31, 2019**	
		6. Performing Organization Code	
7. Author(s) **Howie Fang, Emre Palta, Zheng Li, Oyeboade Fatoki**		8. Performing Organization Report No.	
9. Performing Organization Name and Address **The University of North Carolina at Charlotte** 9201 University City Boulevard Charlotte, NC 28223-0001		10. Work Unit No. (TRAIS)	
		11. Contract or Grant No.	
12. Sponsoring Agency Name and Address **North Carolina Department of Transportation** Research and Analysis Group 1 South Wilmington Street Raleigh, North Carolina 27601		13. Type of Report and Period Covered **Final Report** **August 1, 2016 – February 28, 2019**	
		14. Sponsoring Agency Code **NCDOT 2017-13**	
Supplementary Notes:			

16. Abstract

In this study, non-linear finite element simulations were conducted to evaluate the performance of the current NCDOT cable median barrier (CMB) and two retrofit CMB designs (named "Sixth Design Retrofit" and "Four-cable Design Retrofit") placed on a 6H:1V sloped median. The aim of this research was to investigate possibility of replacing the current CMB design with one of the two retrofit designs. All three CMB designs were evaluated under MASH TL-3 conditions, i.e., under the impacts of a 1100C passenger car and a 2270P pick-up truck at 100 km/hr (62 mph) and a 25-degree impact angle. The CMBs were impacted from both front-sides and backsides at two different impact locations: 1) on a post in the CMB mid-span, and 2) at the midpoint between two adjacent posts in the mid-span. The CMB performance was evaluated using vehicular responses specified in MASH, i.e., the exit-box criterion, MASH evaluation criteria A, D and F, exit angle, yaw, pitch and roll angles, and transverse velocities.

The simulation results demonstrated the effectiveness of each of the three CMB designs on a 6H:1V sloped median under vehicular impacts. The simulation results showed that cable heights and the number of cables played an important role in the effectiveness of CMBs when placed on sloped medians. The finite element modeling and simulation works were shown to be both effective and efficient and can be used to study crash scenarios that are difficult and/or extremely expensive to conduct with physical crash testing.

17. Key Words *Cable systems; Median barriers; Roadside structures; Highway safety; Retrofitting; Finite element method*	18. Distribution Statement		
19. Security Classify. (of this report) Unclassified	20. Security classify. (of this page) Unclassified	21. No. of Pages 77	22. Price

Form DOT F 1700.7 (8-72) **Reproduction of completed page authorized**

Disclaimer

The contents of this report reflect the views of the authors and not necessarily the views of the university. The authors are responsible for the facts and the accuracy of the data presented herein. The contents do not necessarily reflect the official views or policies of either the North Carolina Department of Transportation or the Federal Highway Administration. This report does not constitute a standard, specification, or regulation.

Acknowledgments

This study was supported by the North Carolina Department of Transportation (NCDOT) under Project No. 2017-13. The authors would like to thank NCDOT personnel from the *Traffic Engineering and Safety Systems*, *Roadway Design Unit*, *Highway Division 5 – District 1*, *FHWA – NC Division*, and the *Research and Development Unit* for their support and cooperation during the grant period.

Executive Summary

In this study, non-linear finite element simulations were conducted to evaluate the performance of the current NCDOT cable median barrier (CMB) and two retrofit CMB designs (named "*Sixth Design Retrofit*" and "*Four-cable Design Retrofit*") placed on a 6H:1V sloped median. The aim of this research was to investigate possibility of replacing the current CMB design with one of the two retrofit designs. All three CMB designs were evaluated under MASH TL-3 conditions, i.e., under the impacts of a 1100C passenger car and a 2270P pick-up truck at 100 km/hr (62 mph) and a 25-degree impact angle. The CMBs were impacted from both front-sides and backsides at two different impact locations: 1) on a post in the CMB mid-span, and 2) at the midpoint between two adjacent posts in the mid-span. The CMB performance was evaluated using vehicular responses specified in MASH, i.e., the exit-box criterion, MASH evaluation criteria A, D and F, exit angle, yaw, pitch and roll angles, and transverse velocities.

The simulation results demonstrated the effectiveness of each of the three CMB designs on a 6H:1V sloped median under vehicular impacts. The simulation results showed that cable heights and the number of cables played an important role in the effectiveness of CMBs when placed on sloped medians. The finite element modeling and simulation works were shown to be both effective and efficient and can be used to study crash scenarios that are difficult and/or extremely expensive to conduct with physical crash testing.

Table of Contents

List of Tables

List of Figures

1. Introduction

Roadside safety barriers are important devices to enhance transportation safety. Over the years, different types of barriers have been developed and can be categorized into rigid, semi-rigid, and flexible systems. Roadside barriers serve the purpose of safely redirecting run-out-of-way vehicles and preventing vehicles from intruding into oncoming traffic. All barriers used on U.S. highways are designed following the guidelines of the American Association of State Highway and Transportation Officials (AASHTO) (AASHTO 2002, 2005) and must be tested to satisfy the safety requirements specified by Manual for Assessing Safety Hardware (MASH).

1.1 Background

Commonly used barrier systems include concrete barriers, W-beam and thrice-beam guardrails, and cable barriers. Concrete barriers belong to the rigid category; they have relatively higher initial costs, require less maintenance, and are less forgiving in severe crashes than other barrier systems. The W-beam or thrive-beam guardrails consist of steel rails mounted on wood or steel posts with end treatments and transitions. W-beam and thrie-beam guardrails are intended to be sacrificial; therefore, substantial replacements and/or repairs are required after major vehicular crashes. Even low-energy impacts can bend and damage the rails and displace the posts enough for the barrier not to perform properly in a subsequent crash event. The cost of maintaining these systems is generally high.

NCDOT currently has approximately 750 miles of low-tension cable median barriers (CMBs) installed across the state's highways as shown in Fig. 1.1. The CMB system has been shown to be generally effective with a high rate of success in reducing cross-median crashes and fatalities since the first installations in the mid 1990's. Although these low tension CMBs have satisfied the safety requirements of NCHRP Report 350, they should be evaluated under conditions of MASH which specifies more severe impact conditions than those in the NCHRP Report 350. In a current data analysis of the low-tension CMB hits from January 2011 through December 2013, the CMBs received 4731 hits in which 151 crashes resulted in system penetration (3.2 percent of the total hits). NCDOT would like to explore a solution to minimize the percentage of crashes that may result in penetrations on the CMBs.

Figure 1.1: In-service three-strand, low-tension cable barriers in North Carolina

In 2009, UNC Charlotte completed a research project, *Finite Element Evaluation of Two Retrofit Options to Enhance the Performance of Cable Median Barriers*, for NCDOT. In this project, two retrofit designs to the current NCDOT CMB were evaluated using finite element (FE) modeling and simulations and were found to have a potential to reduce the penetration occurrences compared to the current CMB design. The two retrofit designs, named "*Sixth Design Retrofit*" and "*Four-cable Design Retrofit*" as illustrated in Fig. 1.2, have not been evaluated using the crash testing

criteria specified by MASH. NCDOT would like to gain knowledge of the performance of the three CMB systems under MASH testing criteria. If the "*Four-cable Design Retrofit*" performs better than the "*Sixth Design Retrofit*", NCDOT would like to know how the fourth cable would be added to the current design in terms of cable height and anchor block fixtures. Finally, NCDOT would envision a follow-up project to complete a real-life crash test of the selected CMB retrofit design under MASH testing conditions in order to apply for federal approval to install the low-tension CMB retrofit.

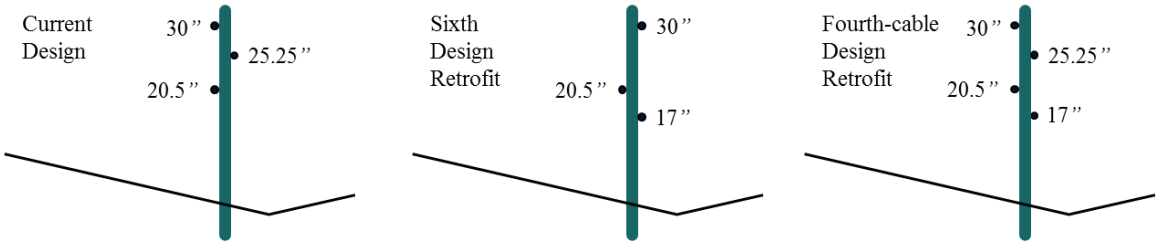

Figure 1.2: Current and the two retrofit CMB designs.

1.2 Research Objectives and Tasks

In this study, full-scale FE simulations were employed to evaluate the performance of the current CMB design and two retrofit designs under MASH testing criteria. The evaluations were based on MASH TL-3 conditions, i.e., under the impact of a 1100C small passenger car and a 2270P pickup truck. All three CMB designs were placed on a 6H:1V sloped median and impacted by these two vehicles at 100 km/hr and a 25-degree impact angle. The simulation results were analyzed to determine the effectiveness of the two retrofit designs compared to the current design. The research project had six major tasks as stated below.

Task 1: Literature Review and Data Collection

A comprehensive literature review was conducted on crash testing, modeling and simulations that are related, in particular, to CMBs to assist with model validation and crash simulations. Literature on performance evaluation of other roadside barrier systems as well as FE modeling work on roadside safety was also collected to assist the research of this study.

Task 2: FE Model Development and Validation

In this task, FE models for the three CMB designs were created and integrated with the median and vehicle models according to NCDOT specifications and the crash scenarios of this study. The two vehicles used in the modeling and simulation work for this study were a 1996 Dodge Neon with a mass of 1,090 kg (2,400 lbs) and a 2006 Ford F250 pickup truck with a mass of 2,270 kg (5,504lbs). Finite element models of the two vehicles and the three CMBs, including the soil and anchor blocks, were discussed in details in Section 3.1.

Task 3: Evaluation of the "Sixth Design Retrofit"

In this task, the "Sixth Design Retrofit" CMB was evaluated at MASH TL-3 conditions (i.e., at an impact speed of 100 km/hr and a 25-degree impact angle). The differences between the "Sixth Design Retrofit" and the current design lie in the cable heights and cable placement on the sides

of the post (see Fig. 1.2.). In the "Sixth Design Retrofit," the top cable was placed on the opposite side of the post but at the same height as that in the current design. The middle cable in the "Sixth Design Retrofit" is on the same side of the post and at the same height as the bottom cable in the current design. The bottom cable in the "Sixth Design Retrofit" was placed at 17 inches and on the same side on the post as the top cable. The "Sixth Design Retrofit" CMB was placed on a 6H:1V sloped median and impacted by the 1100C and 2270P vehicles from both front-side and backside. Figure 1.3 shows the definition of front-side and backside impacts as well as initial impact conditions when the vehicle leaves the shoulder/travel lane and moves down the slope.

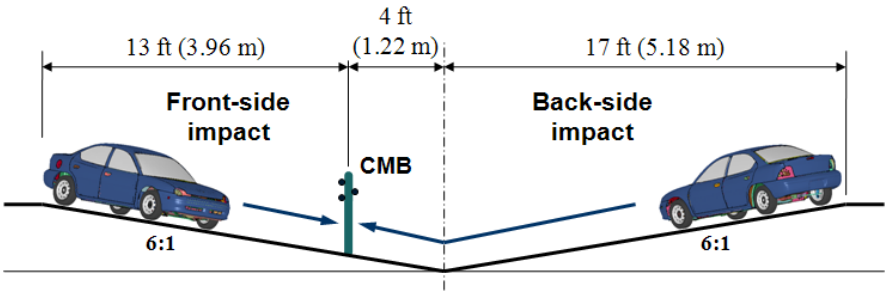

Figure 1.3: Illustration of the CMB placed on a 6H:1V sloped median and impacted by a passenger car from both front- and back- sides.

FE simulations were performed for vehicles impacting the CMB at two locations: on the post and at the mid-point of two adjacent posts, all in the mid-span of the CMB. Simulation results at these impact locations were compared to determine the worst-case scenario of vehicular impacts. The vehicle's responses in terms of redirection, rollover, lateral displacements, and velocities were analyzed to determine the effectiveness of the cable median barriers. Figure 1.4 shows the definition of the three rotational responses (roll, pitch, and yaw) along with the corresponding translational responses (surge, sway, and heave). In evaluating the vehicle's responses, the MASH evaluation criterion *N* (i.e., the exit box criterion) was adopted. Additionally, the MASH evaluation criterion *F* requires that vehicle remains upright and the maximum roll and pitch angles of the impacting vehicle do not exceed 75°. The time histories of roll, pitch, and yaw angles were recorded in the simulations for the entire period of the impacts. The maximum roll and pitch angles were compared to the MASH valuation criterion *F*. In addition to the above-mentioned MASH evaluation criteria, the time histories of the vehicle's transverse displacements and velocities were also examined for performance evaluation.

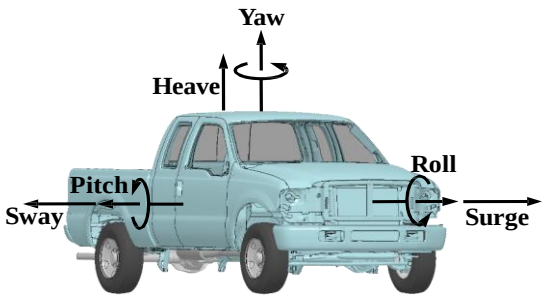

Figure 1.4: Definition of vehicle responses.

Task 4: Evaluation of the "Four-cable Design Retrofit"

In this task, the "Four-cable Design Retrofit" CMB was evaluated at MASH TL-3 conditions. The impact conditions for this design were the same as those used in Task 3. The "Four-cable Design Retrofit" was obtained by simply adding a fourth cable at 17-inch height to the current design and on the same side of the post as the middle cable in the current design (see Fig. 1.2). The "Four-cable Design Retrofit" CMB was placed at the same location on a 6H:1V sloped median and having the same impact points as those for the "Sixth Design Retrofit" CMB.

Task 5: Final Report

This final report provides a comprehensive summary of research activities, findings, and outcomes for this project. It synthesizes the literature review, FE modeling efforts, simulation results, and research findings on the performance of the CMB designs under MASH safety criteria. The final report also includes recommendations on the retrofit design to be crash tested and, if successful, installed on North Carolina highways.

2. Literature Review

Highway median barriers have been developed and used on U.S. highways for decades to contain and redirect errant vehicles and prevent secondary vehicular crashes. These median barriers are generally categorized into three main types: rigid (e.g., concrete barriers), semi-rigid (e.g., W-beam and Thrie-beam guardrails), and flexible systems (e.g., cable barriers). In this section, a comprehensive summary is provided on studies related to CMBs and other barrier systems. The topics cover performance evaluation (in-service and crash testing) and the application of FE modeling and simulations in highway safety research.

2.1 Performance Evaluation of Cable Barriers

In the 1960s, Jehu (1968) published a study on safety barrier development that outlined full-scale dynamic testing conducted in the United States, Germany, Netherlands, and the United Kingdom. In the United States, New York State pioneered the development of weak-post barrier systems through analytical models and full-scale crash tests. In 1965, the state's roadside and median barrier standards were changed to include only weak-post barriers. In the early 1970s, Zweden and Bryden (1977) conducted a study to evaluate the field performance of older strong-post barriers and newly developed weak-post barriers based on accident data collected in New York State from 1967 to 1970. A statistical analysis was conducted to compare the performance of the barrier systems based on accident data including occupant injury, vehicular responses, and post-impact maintenance. This study generated a number of significant conclusions on the performance of weak- and strong-post barriers. Although there was no significant difference in fatality rates between the two barrier systems, weak-post barriers exhibited a combined fatality/serious injury rate significantly lower than that for strong-post barriers. The resulting occupant injury appeared to be linked to barrier stiffness since both barrier systems had lower injury severity rates than other stiffer median barriers. With respect to barrier penetrations, the weak-post barriers demonstrated a lower penetration rate than the strong-post barriers, which could be due to the lack of consistency between early strong-post barrier designs. The study also indicated that barrier penetrations on weak-post systems were typically due to the low rail heights, and that barrier end terminals (i.e., the first and the last 50 feet of the barrier) had higher rates of penetration and serious injury than the mid-sections. The study also related barrier damage to their stiffness. It was found that stiffer barriers (e.g., strong-post barriers) had less damage or shorter damaged sections than weaker barriers (e.g., weak-post barriers). The study also determined that despite their longer damage lengths, weak-post barriers were on average less expensive to repair than strong-post barriers.

In the early 1980's, there were significant changes in vehicle designs with smaller and lighter vehicles constituting a large portion of the road traffic. A study was initiated by the New York State Department of Transportation (DOT) in 1983 to determine the impact severity on traffic barriers in relation to vehicle sizes and weights, barrier types and mounting heights, and roadway features (Hiss and Bryden 1992). Several conclusions were drawn regarding the performance of cable barriers, W-beam guardrails, and box-beam guardrails. For example, injury severities were found to be insensitive on cable barriers with rail heights over 24 in. (0.61 m). For cable and W-beam median barriers, however, the sample sizes were too small to assess their performance due to their limited usage and exposure to possible accidents.

Ross et al. (1984) investigated the performance of longitudinal barriers placed on sloped terrains

using both crash tests and computer simulations by the highway vehicle object simulation model (HVOSM). In the study, they determined typical conditions to place longitudinal barriers on sloped terrains, evaluated the performance of commonly used barrier systems, and developed guidelines for the selection and placement of barriers on sloped terrains. It was found from the study that W-beam and thrie-beam guardrails were more sensitive to terrain slopes than cable barriers. In the study conducted by Ross et al. (1993), uniform procedures were developed for evaluating the safety performance of candidate roadside hardware systems, including longitudinal barriers, crash cushions, breakaway supports, truck-mounted attenuators, and work zone traffic control devices. The report from this study, the NCHRP Report 350, was adopted as the standard guideline for evaluating the safety performance of roadside safety devices. The evaluation of safety devices was facilitated through three main criteria: 1) structural adequacy; 2) occupant risk; and 3) post-impact trajectory. Structural adequacy refers to how well the device performed its intended tasks (i.e., a guardrail preventing a vehicle from striking a shielded object). The occupant risk criterion was intended to quantify the potential of severe occupant injury. The post-impact vehicle trajectory ensured that the device would not cause subsequent harm (i.e., a vehicle being redirected back into the travel lane). The guideline recognized the infinite number of roadside hardware installations and crash configurations; therefore, standardized installations and practically representative impact scenarios were used to provide a basis for comparing the performance of similar devices. Of particular note was the multi-service-level concept that provides six different test levels to allow for more or less stringent performance evaluations (ideally depending on the ultimate usage/placement of the hardware).

Although the NCHRP Report 350 specified six different test levels, the warrants for devices satisfying an individual test level was outside the scope of the document and was left to the judgment of transportation agencies implementing the hardware. Generally speaking, devices tested to the lower test levels, i.e., TL-1 and TL-2, were mostly used on roadways with smaller traffic volumes and lower travel speeds, and devices tested to the higher levels, i.e., TL-3 to TL-6, were typically used on roadways with larger volumes and higher speeds.

In the early 1990s, the Traffic Engineering Branch of the North Carolina DOT (NCDOT) conducted a study of accidents on North Carolina's interstate highways in which vehicles crossed the median and entered opposing travel lanes (Lynch et al. 1993). The study analyzed accidents that occurred during the period from April 1, 1988 to October 31, 1991. The objectives of this study were to identify interstate locations with unusually high cross-median accidents, to determine possible safety improvements, to develop a priority listing of these locations with recommended improvements, and to develop a model for identifying potentially dangerous locations on North Carolina interstate highways. Data collected in the study showed that 105 fatalities resulted from 751 cross-median crashes took place in North Carolina. These crashes represented three percent of total crashes but 32% of total fatalities on interstate highways during the study period. One of the outcomes of this study was the recommendation to construct median barriers at 24 locations along the interstate highways in North Carolina.

Following three fatalities from a cross-median accident in 1996, the Oregon DOT installed CMBs along a session of I-5 to reduce the potential of future occurrences. Sposito and Johnston (1999) evaluated the cost-effectiveness of this system in preventing cross-median crashes. By comparing frequency/severity data from pre- and post-installations, the CMBs were found to reduce both the

fatality rate and susceptibility of cross-median collisions. The study also indicated that the number of accidents with minor injuries increased from 0.7 to 3.8 per year since the installation of CMBs. Based on a cost-analysis including maintenance cost, the annual cost of CMBs was found to always be less than those of concrete median barriers. The report showed that the cost-effectiveness of CMBs in reducing cross-median crashes was in agreement with similar studies performed in North Carolina, Iowa, and New York.

In the early 1990's, the Washington State DOT (WSDOT) started installing the generic low-tension CMBs on medians wider than 32 ft (9.75 m). Subsequently, the WSDOT sponsored crash tests to evaluate the performance of this barrier system in accordance with the NCHRP Report 350. In the two crash tests (Bullard and Menges 1996, 2000), the vehicles were contained by the cables and brought to a stop with relatively minor damages and the occupant risk values were within the preferred limits set by the NCHRP Report 350 (Albin et al. 2001).

Using data collected from Connecticut, Iowa, and North Carolina from 1997 to 1999, Ray and Weir (2001) conducted an in-service performance evaluation of four guardrail systems: the G1 cable guardrail, G2 weak-post W-beam guardrail, and the G4(1S) and G4(1W) strong-post W-beam guardrails. The study primarily focused on estimating the number of unreported collisions and the true distribution of occupant injuries. The collisions were measured in terms of collision characteristics, occupant injury, and barrier damage. Within the sample size limitations of the data collected in the study, no statistically significant difference was found between the performance of the guardrails in the three states, and there was no difference between the performance of G1 and G2 guardrails and between G1 and G4(1W) guardrails.

Hunter et al. (2001) evaluated the generic three-strand CMBs installed on a nine-mile stretch on interstate freeway I-40 in North Carolina. Data extracted from the Highway Safety Information System between 1990 and 1997 was used in a before-after comparison by several regression models that used a reference population (e.g., all freeway locations without CMBs) to predict the number of accidents at locations with CMB treatments. The predicted number of accidents was then compared to the actual number of collisions at sites with CMBs. Although a statistically significant increase was found in the total number of crashes on sections after the installation of CMBs, a significant reduction was also found in the number of serious and fatal collisions. These safety studies by NCDOT "provided a great deal of momentum" towards the installation of more barriers in North Carolina (Stasburg and Crawley 2005), with three-strand CMBs the most commonly used median barriers. North Carolina had approximately 550 miles (885 km) of low-tension CMBs by year 2006, with approximately 3.6% of the impacts resulting in cross-median penetrations (Troy 2007).

Based on a review of previous research and testing of CMBs, Alberson et al. (2003) developed a new terminal to improve the lateral deflection, maintenance, and crash performance of the generic low-tension CMBs. By replacing the single, large concrete anchorage block with three specially designed posts, the new terminal eliminated spring connectors and was expected to withstand higher tensile loads. Full-scale crash testing on the new terminal showed reduced lateral cable deflections and suggested a performance improvement. This newly developed cable barrier system was expected to (partially) address the issue of cable heights in backside hits by changing the cable heights in the terminal section. A recommendation was made for further investigation of cable

heights in the length-of-need sections in relation to vehicle profiles.

In a project funded by the New Jersey DOT, Gabler et al. (2005) evaluated the post-impact performance of two median barrier systems in New Jersey: a three-strand CMB and a modified thrie-beam guardrail. FE modeling was used as a major tool for the investigation. The project also included field investigation of crashes involving the subject barriers and a survey of median barrier experiences of other state DOTs. This study concluded that three-strand CMBs were capable of containing and redirecting passenger vehicles, that the CMBs were effective at reducing the incidence of cross-median collisions in wider medians, and that the CMBs reduced the overall collision severity despite the typically increased total number of accidents.

Cable barriers in Washington State successfully restrained 95 percent of errant vehicles without involving a second vehicle (WSDOT 2006). By comparison, W-beam guardrails and concrete barriers only restrained 67 to 75 percent of errant vehicles without involving a second vehicle in the crash. From 1990 to 2008, WSDOT had installed 181 miles of cable barriers on Washington's highways. Despite the overall increased number of collisions, serious injuries from highway crashes were reduced by nearly 59 percent while the vehicle miles increased by 29 percent. It was also reported that the annual cross-median collisions decreased by 61 percent. Based on WSDOT's data, CMBs were more likely to contain vehicles than concrete barriers. In addition, CMBs reduced the rollover collisions by approximately 28 percent.

Despite the statewide success of CMBs, the public had strong concerns about the increasing number of crashes and cross-median collisions on I-5 in Marysville, WA. As a result, the WSDOT (2006) conducted a comprehensive review of traffic safety on I-5 in Marysville from 1999 through 2004. This study showed that the cross-median penetrations occurred where the CMB was placed within five feet from the bottom of the ditch, which caused the vehicle's suspension to be compressed right after crossing the bottom of the ditch. Consequently, the vehicle was not able to engage with the cables, particularly the bottom cable, and thus under-rode the CMB. While recommending the continuous use of CMBs, a few suggestions were also made for future research including placement of CMBs on sloped medians and CMB anchor designs (MacDonald and Batiste 2007).

Alberson et al. (2007) completed a study in which a preliminary guideline was developed for the selection of CMB systems. The project reviewed cable barrier installations in the U.S. and overseas including the generic low-tension CMBs and five proprietary high-tension cable systems. A survey was also conducted in the study to identify experiences, practices, and design and construction standards for cable barrier systems in various states. The study indicated a continuously increased usage of CMBs with a total of 1,645 miles of installation. As expected, the severity of accidents was found to decrease at locations where CMBs were installed, while the total number of accidents was found to increase. The study indicated that the placement of CMBs was critical to minimizing the number of fatal accidents and maximizing the performance of the systems, and that these issues were sometimes at odds and deserved further research.

In 2009, the Manual for Assessing Safety Hardware (MASH) was published to supersede the previous roadside safety standard, NCHRP Report 350. MASH presented uniform guidelines for crash testing permanent and temporary highway safety features and recommends evaluation

criteria to assess test results. MASH does not supersede any guidelines for the design of roadside safety hardware, which are contained within the AASHTO Roadside Design Guide. As of January 1, 2011, the Federal Highway Administration (FHWA) has required that all new product designs be tested using MASH test criteria for use on the National Highway System. A few of the significant changes from NCHRP Report 350 to MASH include:

- The weight of the small car test vehicle was increased from 1,800 lbs. (820C) to 2,420 lbs. (1100C)
- The impact angle of the small test vehicle (1100C) was increased from 20° to 25°
- The weight of the pickup truck test vehicle was increased from 4,400 lbs. (2000P) to 5,000 lbs. (2270P)
- The mass of the single-unit truck in TL-4 was increased from 18,000 lbs. (8,000 kg) to 22,000 lbs. (10,000 kg) and the impact speed was increased from 50 mph (80 km/h) to 56 mph (90 km/h).

In the work of Gabauer and Gabler (2009), they performed a statistical study on the risk of vehicle rollovers on different barrier and vehicle types. Observations from limited crash data showed that concrete barriers were less likely to cause rollovers than other types of barrier systems, and that SUVs were more likely (more than three times) to roll over than pickup trucks and passenger cars.

In a study conducted by Hu and Donnell (2010), they analyzed the severity of median barrier crashes using five years of data from rural divided highways in North Carolina. The criteria used for the analysis included median barrier type, the barrier's offset distance from the edge of the travel lane, roadway segment characteristics, roadway surface conditions, driver and vehicle characteristics, median barrier placement, and median cross-slope data. The major conclusion of this study was that less severe crash outcomes pertained to those on CMBs when compared to concrete barriers and W-beam guardrails. It was also observed that the barrier's offset distance from the travel lane was associated with a lower probability of severe crashes.

Stolle et al. (2013) conducted a study to evaluate the performance of in-service CMBs and determine the reasons of CMB failures using data collected from 12 different states. They found that the main reasons causing penetrations on the CMBs were: 1) diving underride, in which the front end of the vehicle dropped below the bottom cable; 2) prying, in which the vehicle profile caused cable separation or lifting; 3) bouncing override, in which the vehicle rebounded after contact with the back slope and bounced over the top of the barrier; and 4) system failure, in which one component failure or design failure prevented the cables from adequately engaging the vehicle. They also found that steep median slope was the main reason for vehicles' rollovers.

In a recent study by Alluri et al. (2015), the performance of CMBs installed on freeways in Florida was evaluated based on the percentages of barrier and median crossovers by vehicle type, crash severity, and CMB type. Using data from 101 miles of CMBs placed on 23 different locations, they found that 2.6% of vehicles hitting the CMBs penetrated the barriers and entered into the opposite travel lane. Among all vehicles hitting the barriers, 98.1% of cars and 95.5% of light trucks were prevented from crossing the median. They also found that, in terms of crash severity, overrides were more severe compared to underrides and penetrations.

In the work by Savolainen et al. (2018), they evaluated the effectiveness of CMBs installed in Iowa

using 6,718 median related crashes that were occurred from 2007 to 2015. They developed a series of severity-based statistical models to assess the safety and effectiveness of the CMBs installed in Iowa. Results from their statistical models demonstrated that the CMBs could reduce the frequency of crashes with fatal, incapacitating, and non-incapacitating injuries while increasing the frequency of crashes with only possible injuries and property damage.

2.2 Finite Element Modeling and Simulations of Vehicular Crashes

Mackerle (2003) provided a bibliography of 271 references published between 1998 and 2002 on finite element (FE) simulations of crashes and on impact-induced injuries. This bibliography categorized the references into four different topic areas: 1) Crash and impact simulations where occupants were not included; 2) Impact-induced injuries; 3) Human surrogates; and 4) Injury protection. Topics in the first area included crashworthiness of aircrafts and helicopters, automobiles, and vehicle rail structures. The second area of research utilized two major types of models for humans, the crash dummy and real human body models. Research topics in this area were mainly on biomechanics and impact analyses for various human injuries. Topics on human surrogates focused on the development FE models of hybrid and other types of human dummies. These dummy models were used to obtain dynamic responses of the whole human body during impacts, which were difficult to measure experimentally. In the area of injury protection, FE modeling and simulations were utilized to analyze injury protection systems such as seat belts, air bags, and collapsible structures to reduce serious or fatal injuries. The references included in Mackerle's bibliography were generally useful to the work on FE crash simulations; however, only a few references under injury protection were related to roadside safety.

Most publicly available FE models of vehicles and roadside safety structures were initially developed at the National Crash Analysis Center (NCAC) at George Washington University. Since the 1990s, significant efforts have been put on the development of FE models for crash analysis. Most of these models are available as LS-DYNA input files from NCAC's website (NCAC web1). A list of references on these modeling efforts and the simulation work performed at NCAC is also available from NCAC's website (NCAC web2).

The modeling and simulation efforts from NCAC can be found in several representative works. Marzougui et al. (2000) developed the FE model of an F-shaped portable concrete barrier (PCB) and validated the model with full-scale crash test data. With the proven fidelity and accuracy of the modeling methodology, models for two modified PCB designs were created and used to evaluate their safety performance. A third design was then developed based on the simulation results. In the work by Zaouk et al. (2000a, 2000b), a detailed FE model of a 1996 Dodge Neon was developed. The three-dimensional geometric data of each component were obtained by passive digitizing and were imported into a preprocessor to generate mesh, connect parts, and assign material properties. Tensile tests were conducted on specimens to obtain the material properties of the various sheet metal components. The body-in-white model was used in the simulation of a frontal impact and the results were compared with test data to evaluate the accuracy and validity of the model. Kan et al. (2001) developed an integrated FE model that included the vehicle's main structure, interior components, a Hybrid III dummy, and an airbag for crashworthiness evaluation. The integrated model was then used in a case study to demonstrate the potential benefit of the integrated simulation and analysis approach. This approach would further improve the engineering practice with cost savings, while also producing more accurate

and consistent analysis results. Marzougui et al. (2004) developed a detailed suspension model and incorporated it into the previously developed FE model of a Chevrolet C2500 pickup truck (Zaouk et al. 1997). Pendulum tests were conducted at the FHWA Federal Outdoor Impact Laboratory (FOIL) and the test data were compared with simulation results of deformations, displacements, and accelerations at various locations. Crash simulations were performed using the upgraded vehicle model and the results were compared with crash data from previously conducted full-scale tests.

To facilitate the use of FE simulations in the evaluation of roadside safety structures at higher test levels specified by NCHRP Report 350, Mohan et al. (2007) improved and validated a previously developed model of a 1996 Ford F800 single-unit truck. This 18,000-lb (8,172-kg) truck was used as the standard TL-4 vehicle in NCHRP Report 350. Simulations were performed using the improved model and the results were compared with those from a full-scale crash test. The global kinematics and time histories of the truck's accelerations from simulations were found to correlate well with test data. The research also suggested that considering frictions between the tires and barrier and between the tires and ground could improve the correlation of simulation results to test data on the vehicle's yaw angles.

In the work by Marzougui et al. (2007a), they investigated the penetrations of low-tension CMBs placed on flat and sloped medians using FEA and vehicle dynamics analysis coupled with full-scale crash testing. The FE model of a Chevrolet C2500 pickup truck was used in the crash simulation of a CMB placed on a flat terrain and the results showed that the vehicle was retained by the barrier. The FE model of a Ford Crown Victoria was used in the simulation of a CMB placed on a 6H:1V sloped median and at 1.22 m (4 ft) from the ditch centerline. The Crown Victoria was found to under-ride the CMB with almost no resistance from the cables. The simulation results using the Crown Victoria model were confirmed by full-scale crash tests (No. 04010 and 04011) performed at the FHWA/FOIL. The simulation results showed that the vehicle's front profile was relatively lower than the cables and hence reduced the effectiveness of the CMB. In both simulations, the impact speed was 62 mph (100 km/hr) and the impact angle was 25°.

Marzougui et al. (2007a) also performed vehicle dynamics analysis using the two models noted above along with the model of a small sedan, a Mitsubishi Mirage, to further investigate the effect of sloped median (6H:1V) on CMB performance. It was determined that the suspension of the mid-sized vehicle tended to be fully compressed due to the dynamic forces imposed by the terrain, speed, and angle after the vehicle crossed the bottom of the sloped median and started moving up the median. These conditions were likely to place the nose of the vehicle below the lowest cable and hence caused the vehicle to under-ride the barrier. Future work recommended by Marzougui et al. (2007a) was to further analyze alternative designs and barrier placement retrofits to improve the CMB performance on sloped median. Their suggested retrofits included adding a fourth cable, using a closer post spacing, using a stronger cable/post connection, and incorporating ties to connect the three cables.

In the study of Marzougui et al. (2007b), they developed an FE model of a W-beam guardrail and validated it using full-scale crash testing data. The model was shown to give an accurate representation of the real system by comparing the roll and yaw angles. Using the validated model, they performed four simulations of a passenger truck impacting the W-beam guardrail with

different rail heights. The simulation results showed that the effectiveness of the barrier to redirect a vehicle could be compromised when the rail height was lower than recommended. Using vehicle dynamics simulations, Marzougui et al. (2009) investigated the performance of a three-strand CMB placed behind a curb. Five different curbs, three different vehicles (small passenger car, mid-sized passenger car and pickup truck), three impact angles (5º, 15º, 25º), and three impact speeds (50 km/hr, 70 km/hr, 100 km/hr) were considered. For each of the five curbs studied, the maximum height of the bottom cable and the minimum height of the top cable were determined as functions of the distance from the curb to the cable barrier. It should be noted that vehicle dynamics simulations could not take into account the contact between the vehicle and cable barrier. In fact, there was no cable barrier model in the vehicle dynamics simulation models. Therefore, deformations of the vehicle and cable barrier were not considered. Although the study provided insights into the placement of CMB behind curbs, the lack of vehicle-barrier interactions in the simulation raised concerns on the effectiveness of the recommended placements.

Opiela et al. (2009) developed the FE model of a 2007 Chevrolet Silverado 1500 2WD, which had 942,491 nodes, 872,960 shell elements, 2,654 beam elements, and 53,286 solids elements. Detailed front and rear suspension systems were modeled with the intension of obtaining good behavior in oblique impact situations. This FE model was further validated by Marzougui et al. (2010) using crash test data and simulation results of an oblique impact into a New Jersey concrete barrier that was in compliance with MASH testing conditions. Extended validations were subsequently performed by Marzougui et al. (2012) to include interior components attached to the door in the FE model. The standard full-frontal, offset-frontal, and side impacts specified by the Federal Motor Vehicle Safety Standards (FMVSS) were simulated and the simulation results were compared to test data. The FE model was also used to simulate the centerline pole impact to demonstrate the robustness of the model.

Researchers from the roadside safety group at Worcester Polytechnic Institute (WPI) utilized FE models in a number of roadside safety studies. Ray (1996a) analyzed full-scale crash test data and developed a criterion using statistical parameters to assess the repeatability of full-scale crash tests and to evaluate simulation results compared to crash test data. Ray (1996b) reviewed the history of using FE analysis in roadside safety research, and presented the vehicle, occupant, and roadside hardware models that were developed to date. Ray and Patzner (1997) developed a nonlinear FE model of a modified eccentric loader breakaway cable terminal and used it in simulating a full-scale crash test involving a small passenger car. The simulation results were analyzed and compared to crash test data, and the FE model was recommended to be used in the evaluation of new design alternatives. Plaxico et al. (1997) developed a 3D FE model of a modified thrie-beam guardrail and simulated the impact of a compact automobile. The computational model was then calibrated with data from an actual field test that was previously conducted as part of a full-scale crash test program carried out under the auspices of FHWA. Plaxico et al. (1998) developed the FE model of a breakaway timber post and soil system used in the breakaway cable terminal (BCT) and the modified eccentric loader BCT. The simulation results were compared and found to correlate well to test data. Patzner et al. (1999) examined the effects of post strength and soil strength on the overall performance of the terminal system using a nonlinear FE model. A matrix of twelve simulations of particular full-scale crash test scenarios was used to establish the combinations of post and soil strengths that produce favorable results. The parametric study showed that certain combinations of soil and post strengths increased the hazardous possibilities

of wheel snagging, pocketing, or rail penetration, while other combinations produced more favorable results.

In the work of Plaxico et al. (2000), the impact performance of two strong-post W-beam guardrails, the G4 (2W) and G4 (1W), were compared. After validating the FE model of the G4 (2W) guardrail with data of a full-scale crash test, the FE model of the G4 (1W) guardrail was developed. The two guardrails were compared with respect to deflection, vehicle redirection, and occupant risk factors. The two systems were found to perform similarly in collisions, and both satisfied the requirements of the NCHRP Report 350 for Test 3-11 conditions. Using LS-DYNA simulations and laboratory experiments, Plaxico et al. (2003) investigated the failure mechanism of the bolted connection of a W-beam rail to a guardrail post, which could have a significant effect on the performance of a guardrail system. A computationally efficient and accurate FE model of the rail-to-post connection was developed to be used in the analysis of guardrail performance using LS-DYNA. Orengo et al. (2003) presented a method to model tire deflation in LS-DYNA simulations along with examples of using the model. Deflated tires have significantly different behaviors from those of inflated tires, as observed in real world crashes and in full-scale crash tests. A vehicle's kinematics is strongly coupled to the behaviors of deflated tires; therefore, modeling such behaviors is critical to accurate simulations of roadside hardware. Ray et al. (2004) used LS-DYNA simulations to determine if an extruded aluminum bridge rail will pass the full-scale crash tests for test levels three and four conditions of the NCHRP Report 350. The simulation results, which were supported by a subsequent AASHTO LRFD analysis, indicated a high likelihood of passing the crash tests.

FE simulations have also been used by researchers at the Midwest Roadside Safety Facility (MwRSF). Reid (1996) utilized FE models to study the effects of material properties on automobile crashing into structures and attempted to develop crashworthiness guidelines for design engineers. In one of his later works, Reid (1998) demonstrated through two simple examples the potential modeling issues that could be easily overlooked in FE impact simulations: contact definition and damping. He also suggested ways to check for modeling errors and to make improvements. In the work of Reid and Bielenberg (1999), FE simulations were performed for a bullnose median barrier impacted by a 2000-kg (4405-lb) pickup truck to determine the cause of failure and to evaluate a potential solution to the problem. Reid and Coon (2002) presented details on the development of the hook-bolt model used in the CMBs. In a collaborative work to improve the FE model of a Chevrolet C2500 pickup truck (Reid and Marzougui 2002; Tiso et al. 2002), structural modeling methods were introduced for model improvement through refining meshes, using better material models, adding details to simplified components, and improving connections between components. Suspension modeling, which is critical to the correct vehicle dynamics, was also investigated in this collaborative work, and a new model was successfully developed with significant improvements.

To educate roadside safety engineers and promote the use of simulation, Reid (2004) summarized ten years of the simulation efforts at MwRSF on the development of new roadside safety appurtenances. In the work by Reid and Hiser (2004), they studied the friction effects, particularly between solid elements, on component connections and interactions in crash modeling and analysis. In their work on modeling bolted connections that allowed for slippage, Reid and Hiser (2005) investigated two modeling techniques that were based on discrete-spring clamping and stressed clamping models with deformable elements, respectively. The simulation results for both

models compared well with test data, with the stressed clamping model with deformable elements having better accuracy accompanied by significantly increased computational cost. Hiser and Reid (2005) also investigated improved FE modeling methods for slip base structures, which could have a considerable potential for reducing the amount of crash resistance and thus occupant injury when struck by errant vehicles. They developed and evaluated two bolt preloading methods, with one using discrete spring elements and the other using pre-stressed solid elements. Similar to their findings in the work of modeling hook-bolts, they found that the method using solid elements was more accurate than that using discrete spring elements when the impact conditions became more severe. As a result, the model using pre-stressed solid elements was incorporated into the FE model of a cable guardrail system. The results showed that the slip base model was acceptable in both end-on impact and length-of-need impact simulations.

In the study by Reid et al. (2009), they investigated the potential of increasing the suggested flare rates for strong post W-beams to reduce guardrail installation lengths, which could potentially reduce the impact frequency and guardrail construction and maintenance costs. Both computer simulation and full-scale crash tests were used in the evaluation of increased flare rates up to 5:1. Simulation results indicated that the conventional G4(1S) guardrail modified to incorporate a routed wood block could not successfully meet the crash test criteria by NCHRP Report 350 when installed at any flare rates larger than the 15:1 recommended in the Roadside Design Guide. Their study also showed that the Midwest Guardrail System (MGS) could meet the test criteria of NCHRP Report 350 when installed at a 5:1 flare rate, yet with greater impact severities during testing than anticipated. Reid et al. also indicated that whenever roadside or median slopes were relatively flat (10H:1V or flatter), increasing the flare rate on guardrail installations would become practical and have some major advantages including significantly reducing guardrail lengths and associated costs. The study, however, did not give any indications of guardrail performance on steeper slopes.

FE simulations were also found in the work of other researchers in roadside safety research. Whitworth et al. (2004) evaluated the crashworthiness of a modified W-beam guardrail using detailed FE models of the guardrail and a Chevrolet C2500 pickup truck. The simulation results were found to match well to crash test data in terms of roll and yaw angles. Simulations were also performed to evaluate the effect of certain guardrail design parameters, such as rail mounting height and routed/non-routed blockouts, on the crashworthiness and safety performance of the system. In the work by Bligh et al. (2004), FE models were utilized to develop new roadside features to address three roadside safety issues. An alternative to the popular T6 tubular W-beam bridge rail was developed to address problems with vehicle instability observed in full-scale crash tests. A retrofit connection to TxDOT's grid-slot portable concrete barrier was developed to limit dynamic barrier deflections to levels that were more practical for work zone deployment. Finally, crashworthy mow strip configurations were developed for use when vegetation control around guard fence systems was desired to reduce the cost and risk associated with hand mowing. In a project funded by the New Jersey DOT, Gabler et al. (2005) evaluated the post-impact performance of two median barrier systems in New Jersey: a three-strand CMB and a modified thrie-beam guardrail. FE modeling was adopted as a major means for the investigation. The project also included field investigations of crashes into the subject barriers and a survey of the median barrier experience of other state DOTs. This study concluded that the three-strand CMB was capable of containing and redirecting passenger vehicles, that the CMB was effective at reducing the

incidence of cross-median collisions in wider medians, and that the CMB reduced the overall collision severity despite typically increasing the total number of hits on the barrier.

Computer simulations were also used by researchers around the world on roadside safety research. Using LS-DYNA simulations, Atahan (2002) analyzed a strong-post W-beam system that had failed in a previously full-scale crash test. After identifying the cause of failure and incorporating necessary improvements, a new W-beam system was developed and showed improved performance based on simulation results. Atahan (2003) performed LS-DYNA simulations to study the impact performance of G2 steel weak-post W-beams installed at the slope break point on non-leveled terrains. The results showed that there was a risk of increased vehicle instability when the roadside slope adjacent to the W-beam guardrail became steeper than 6H:1V. Atahan and Cansiz (2005) investigated the failure of a bridge rail-to-guardrail transition design in a full-scale crash test in which the vehicle rolled over the guardrail. They used full-scale LS-DYNA simulations to replicate the crash test and identified the cause of failure attributed to the low height of the W-beam rails. In the work by Atahan (2007), LS-DYNA simulation was used to study the crashworthiness behavior of a bridge rail-to-guardrail transition structure under 8,000 kg of impact load. This work demonstrated the effectiveness of FE simulations for its replications of the actual dynamic interactions and crash mechanism. Atahan also pointed out that the use of a real soil model other than the simplified spring soil model could improve the accuracy of FE simulations but would significantly increase the computational costs.

Since 2007, researchers at the University of North Carolina at Charlotte (UNC Charlotte) have worked on a number of roadside safety projects in which nonlinear FE modeling and simulations were used to evaluate the performance of CMBs and W-beam guardrails. In the work by Fang et al. (2012) and Fang et al. (2015), they analyzed the in-service performance of the generic three-strand CMBs installed on 6H:1V and 4H:1V sloped medians. Based on simulation results, two retrofit CMB designs were developed to reduce the potential of small vehicles penetrating through the CMBs. In addition, the effect of horizontal median curvature on CMB performance was also studied. In the work by Gutowski et al. (2017a, 2017b), they studied the performance of W-beam guardrails placed on sloped medians and behind curbs using full-scale FE simulations. Other modeling and simulation work included the efficient modeling method for slender members used in crash analysis (Wang et al. 2013), evaluation of occupant safety in vehicular crashes into roadside barriers (Li et at. 2015), design optimization of a MASH TL-3 concrete barrier (Yin et al. 2016), and design optimization of a new W-beam guardrail (Yin et al. 2017).

FE modeling and simulations, particularly with LS-DYNA, have been increasingly used in roadside safety research. In addition to the abovementioned references, FHWA published several manuals on using LS-DYNA material models and evaluation of these models (Lewis 2004; Murray et al. 2005; Murray 2007; Reid et al. 2004). These references are also useful in crash modeling works using LS-DYNA.

3. Finite Element Modeling of Vehicles and Cable Median Barriers

The simulation work of this project involved FE models of two vehicles (i.e., a 1996 Dodge Neon and a 2006 Ford F250) and three CMB systems (i.e., the current NCDOT design, the *Sixth Design Retrofit*, and the *Four-cable Design Retrofit*). All crash simulations were conducted at MASH TL-3 conditions by which the CMBs were impacted by the vehicles at 100 km/h (62 mph) and an impact angle of 25 degree. In all the impact cases, the vehicles departed from the travel lane at the prescribed speed and angle before impacting the CMBs. The impact speed was defined in the vehicle's travel direction, and the impact angle was defined as the angle between the vehicle's travel direction and the CMB's longitudinal direction.

3.1 FE Models of a Passenger Car and Pickup Truck

The FE models of the two vehicles used in this project were a 1996 Dodge Neon passenger car and a 2006 Ford F250 pickup truck, as shown in Fig. 3.1. Table 3.1 gives the specifications of the two vehicles relevant to this study.

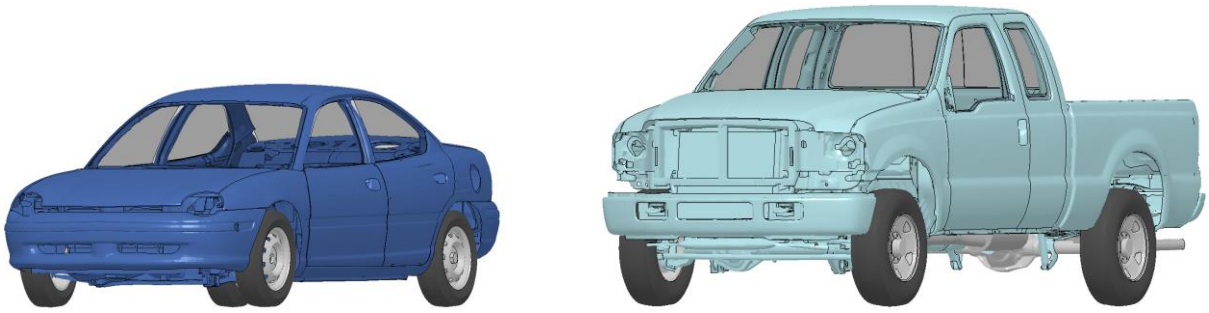

a. 1996 Dodge Neon b. 2006 Ford F250

Figure 3.1: Finite element models of two MASH compliant vehicles used in this study.

Table 3.1: Specifications of the two test vehicles used in crash simulations

Specification	Test Vehicle	
	1996 Dodge Neon	**2006 Ford F250**
Curb weight *	2,403 lb (1,090 kg)	5,504 lb (2,499 kg)
Overall length	171.8 in (4.36 m)	226.4 in (5.75 m)
Overall width	67.5 in (1.71 m)	79.9 in (2.03 m)
Overall height	52.8 in (1.34 m)	76.5 in (1.94 m)
Ground clearance	5.7 in (145 mm)	8.3 in (211 mm)

* The curb weight is the weight of the vehicle with all standard equipment and amenities, but without any passengers, cargo or any other separately loaded items.

The FE model of the 1996 Dodge Neon had a total of 339 parts that were discretized into 283,683 nodes and 270,727 elements (2,852 solid, 92 beam, 267,775 shell, and 8 discrete elements). Ten

different constitutive models were used, including the piecewise linear plasticity model for most steel components, the rigid model for mounting hardware, the elastic model for the tires and other rubber components, the Blatz-Ko rubber model for nearly incompressible rubber cushions, the viscous damping model for the shock absorbers, the low-density foam model for the radiator core, the spot-weld model for sheet metal connections, the null material model defined for contact purposes, the linear elastic spring model for the spring-damper connection of the front suspension, and the crushable foam model for the bumper energy absorber. Hourglass control was used on components that could potentially experience large deformations. The FE model of the Dodge Neon was originally developed at NCAC and validated with the NHTSA's New Car Assessment Program (NCAP) Frontal-Impact Test 2320 (NCAC, 2007a).

The FE model of the 2006 Ford F250 was composed of a total of 746 parts that were discretized into 737,986 nodes and 735,895 elements (25,905 solid, 2,305 beam, 707,656 shell, and 29 discrete elements). Eleven different constitutive models were used, including the piecewise linear plasticity model defined for most steel components, the rigid model for mounting hardware, the elastic model for the tires and other rubber components, the linear and nonlinear elastic spring model for the suspension springs, the viscous damping model for the shock absorbers, the low-density foam model for the radiator core, the spot-weld model for sheet metal connections, the viscoelastic model for radiator support mounts, the Blatz-Ko rubber model for nearly incompressible rubber cushions, and the null material model for contact purposes. Hourglass control was used on various components that could potentially experience large deformations. The FE model of the Ford F250 was originally developed at NCAC and validated with the NHTSA's New Car Assessment Program (NCAP) Frontal-Impact Test 5820 (NCAC 2008).

Simulations of the vehicles crashing into roadside barriers imposed significant challenges to the numerical models due to the large, nonlinear deformations and the large numbers of components contacting each other. One of dauting task was to define appropriate contacts between the vehicles and the cable median barriers. For example, in the simulations of the Ford F250 crashing into the CMB, the CBM and the vehicle's fender experienced severe deformations. The vehicle's wheel, fender, bumper cover, suspension, and several other parts were in contact with the post and cables. These contacts needed to be handled by selecting the appropriate contact algorithms to eliminate the unrealistic penetrations of these parts when contacting each other. Otherwise, the simulations would encounter great numerical difficulties, resulting in premature termination and unrealistic behaviors of the vehicle and/or CMB. The FE model of the Dodge Neon experienced a similar issue with the bumper cover penetrating the CMB and becoming entangled due to a contact definition that was used in the original model but inappropriate for the simulations of this project. These contact issues were resolved for both the FE models of the Ford F250 and Dodge Neon before they were used in the simulations of this project.

3.2 FE Models of the Cable Median Barriers

The FE models of the CMBs used in this study included three CMB designs: the current NCDOT CMB design, the *Sixth Design Retrofit*, and the *Fourth-cable Design Retrofit*. The initial FE model of the CMB was obtained from NCAC, which was developed based on the Washington State CMB design. This CMB model was modified by Fang et al. (2015) in a previous NCDOT research project to conform to the NCDOT design specifications. Several modifications were made to the NCAC CMB model to create current CMB design of NCDOT. First, the post spacing was changed

from 16 ft - 4.85 in. (5 m) to 16 ft (4.88 m) in accordance with the specifications (NCDOT 2002,2006). Secondly, due to the change of post locations (spacing), the cable model in the region of the posts was regenerated. Thirdly, the CMB in the NCAC model was placed on flat terrain and thus was modified to a 6:1 sloped median. Finally, the meshes of the cables and J-hooks were regenerated and new contact algorithms were adopted to improve both the numerical accuracy and computational efficiency (Wang et al. 2013).

In the afore-mentioned NCDOT research project, Fang et al. (2015) evaluated five different retrofit designs to assess possibility of replacing the current CMB design. Among those retrofit designs, two designs had superiority over others; these two retrofit designs were named as *Sixth Design Retrofit* and *Four-cable Design Retrofit*. To create the *Sixth Design Retrofit*, the middle cable of the current design (i.e., at 25.25 in above grade) was lowered by 8.25 in (209.55 mm) and placed on the opposite side of the post; thus it became the bottom cable of the *Sixth Design Retrofit* as depicted in Fig. 3.2. The top cable in the *Sixth Design Retrofit* was placed on the opposite side of the post but at the same height above grade as the top cable in the current design. The *Four-cable Design Retrofit* was obtained by adding a fourth cable to the current design at 17 inches above grade (see Fig. 3.2).

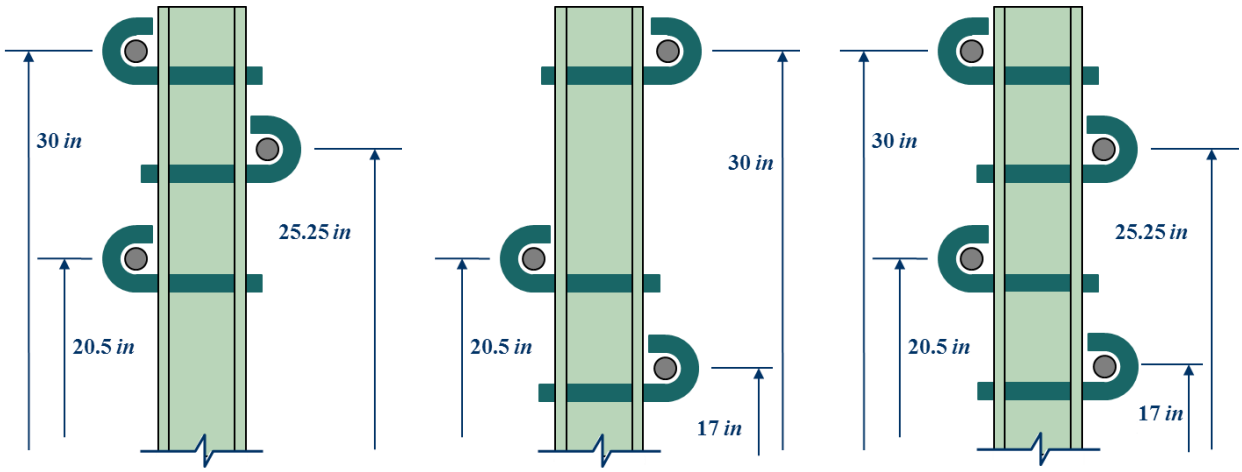

a. Current Design b. Sixth Design Retrofit c. Four-cable Design Retrofit

Figure 3.2: Sketch of the three CMB designs for this project.

The FE models of the CMBs used in this project were taken from the previous NCDOT projects (Fang et al. 2009, 2012). The cables and hook-bolts were modeled using Hughes-Liu beam elements, the posts were modeled using shell elements, and the soils and anchor blocks were modeled using hexahedron solid elements. Figure 3.3 shows close-up views of the cable, hook-bolt, and a single post-soil model used in this project. Some improvements were made on the existing FE models of the CBMs for this project. For example, null shell elements around the cables, which were used for contact purpose in the previous projects (Fang 2009, 2012), were eliminated and more robust contact algorithm (i.e., AUTOMATIC_GENERAL_INTERIOR) were adopted between the cable and vehicles. Furthermore, the terminal posts and anchor blocks of the retrofit designs were recreated for this project, as shown in Fig. 3.4. A sensitivity analysis was

conducted to study effect of coefficient of friction between the anchor block and the soil. Based on the sensitivity analysis, the static coefficient of friction was determined as 0.5 for compacted soils around the anchor blocks. The FE models had five different constitute material models: piecewise linear plasticity (MAT_024) for the hook-bolts, posts, and the bolts and nuts on the terminal post, elastic (MAT_001) for cables, elastic spring (MAT_S01) for bolt-tensioning springs in the bolts, soil and foam with failure (MAT_014) for soils, and concrete (MAT_159) for anchor blocks.

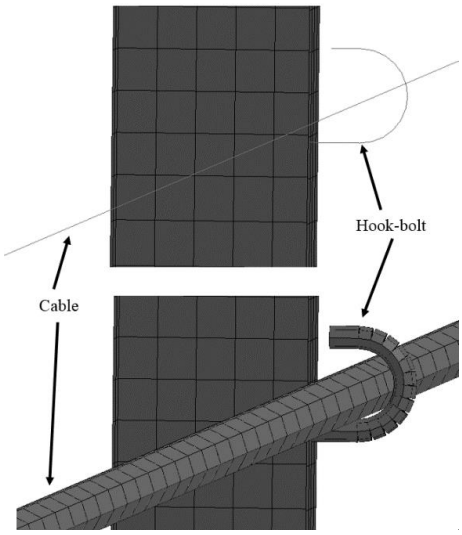

a. Cable and hook-bolt. (virtual thickness of the beam elements highlighted for ease of view)

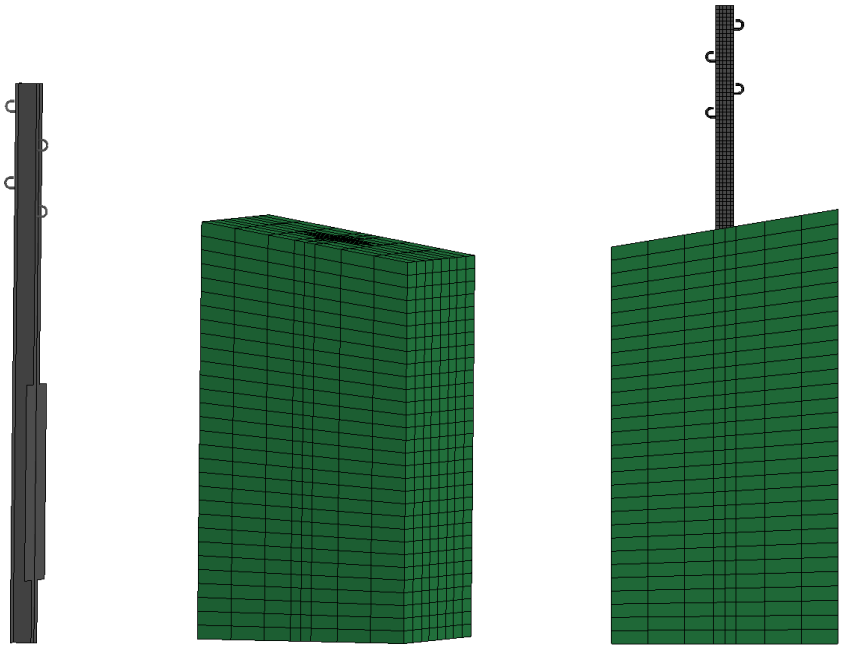

a. Entire post, soil block, and a single integrated post-soil, from left to right.

Figure 3.3: Components of the FE model of CMB.

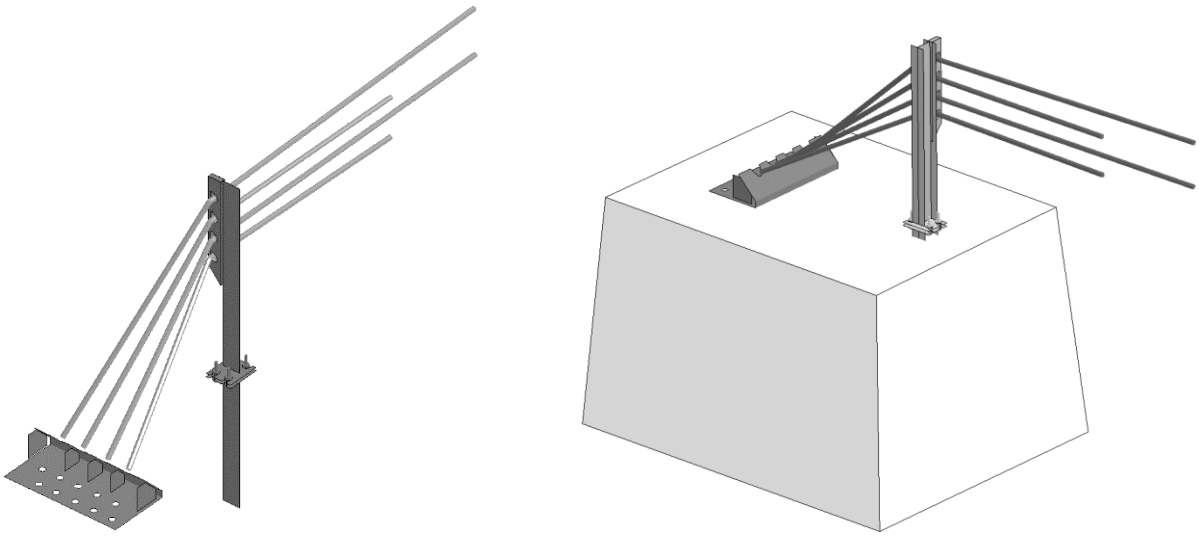

a. Terminal post

b. Anchor block

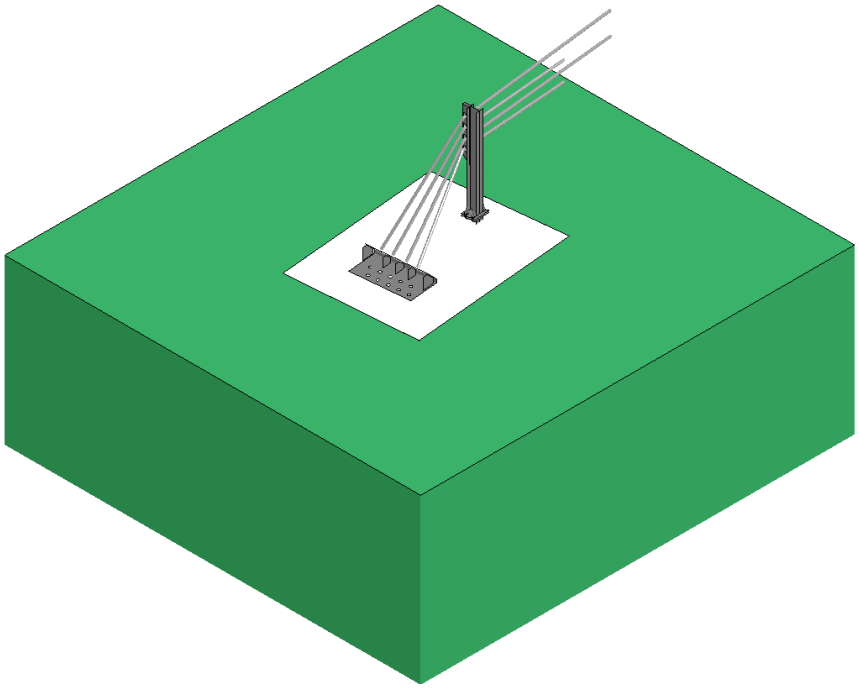

c. Integrated terminal post-anchor block-soil model.

Figure 3.4: The FE model of the four-cable CMB anchor block.

Figure 3.5 shows the FE models of the three CMB models on the slope soil. The first CBM configuration, Figure 3.5a, is the current CMB design. The second configuration, Figure 3.5b, is the Sixth Design Retrofit where the 25.25 in height cable of the current design lowered by 8.25 in as a result it became the 17 in height cable. The third configuration, Figure 3.5c, is the Four-cable Design Retrofit where a 17 in height cable was added to the current design CMB.

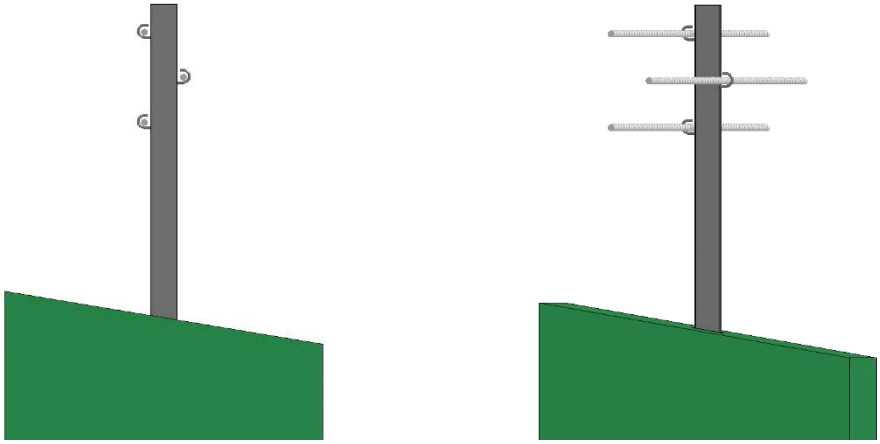

a. The current design CMB.

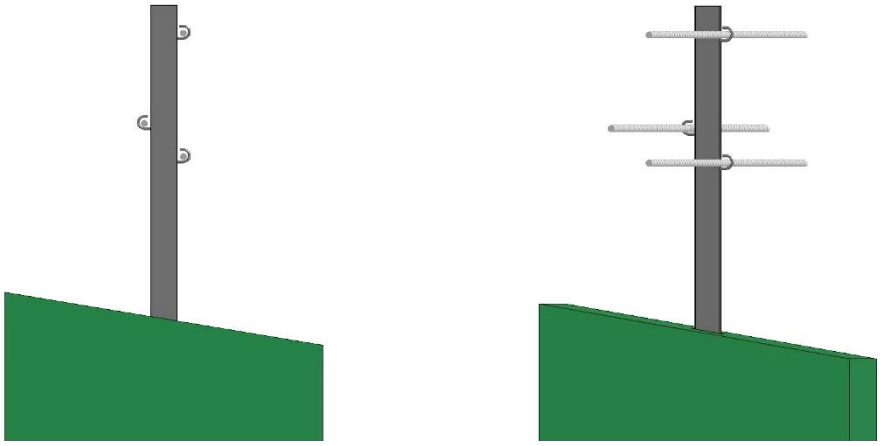

b. The *Sixth Design Retrofit*.

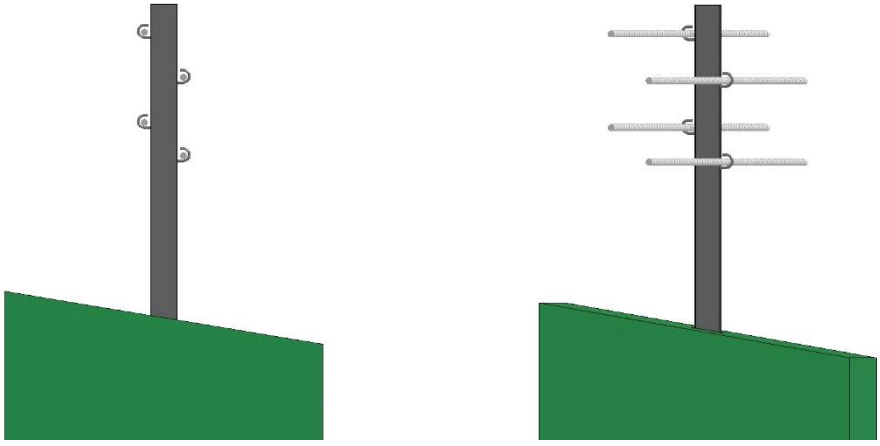

c. The *Four-cable Design Retrofit*.

Figure 3.5: FE models of the three CMB designs.

The FE model of a single CMB segment was duplicated to create the entire 400-ft (122-m) CMB section required for this project. The duplication of the guardrail sections was completed with an in-house code developed to replicate not only the parts, nodes, elements, and material properties, but also the contact definitions defined among the parts in each segment as well as between parts of adjacent CMB segments. The FE models of two end terminal posts were then attached to the CMB section to create a full CMB model. Figures 3.6 to 3.8 illustrate the full FE models of the current CMB design, *Sixth Design Retrofit*, and *Four-cable Design Retrofit* placed on a 6H:1V sloped median.

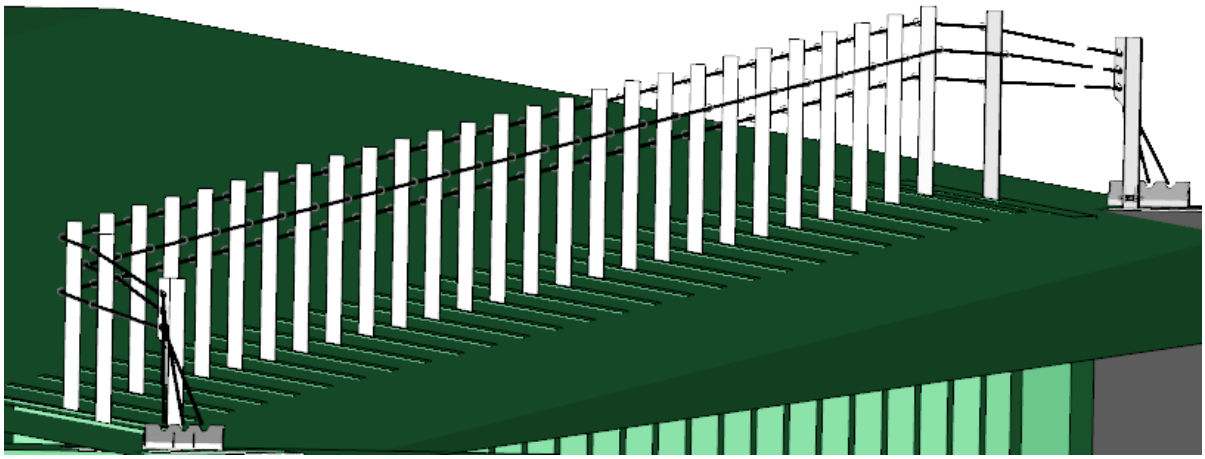

Figure 3.6: FE model of entire section of the current CMB design.

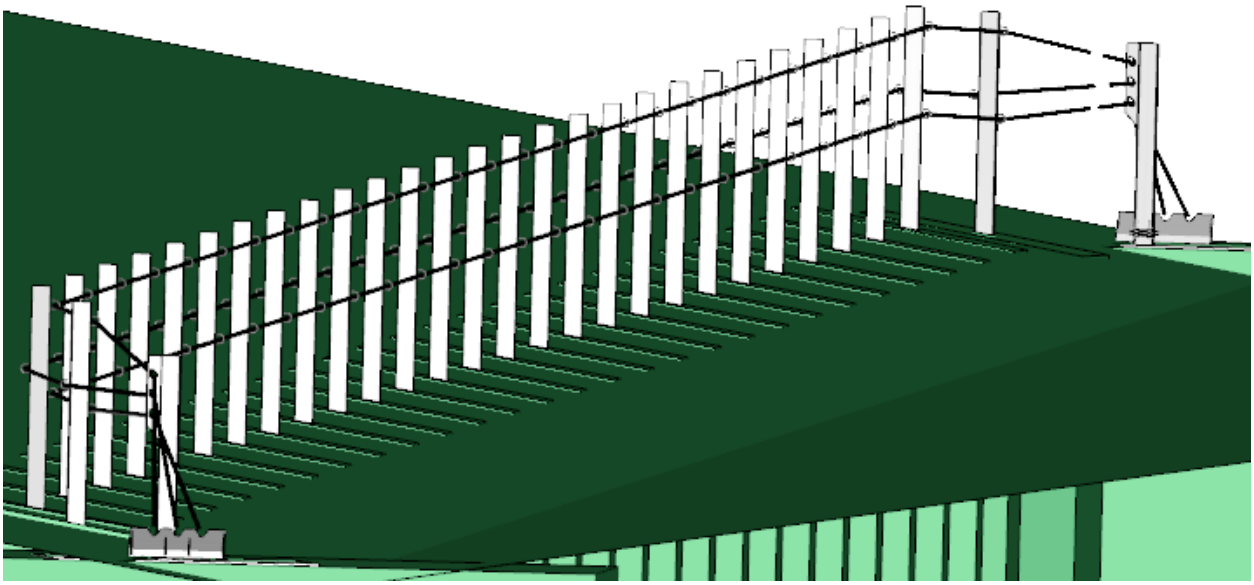

Figure 3.7: FE model of entire section the sixth CMB design retrofit.

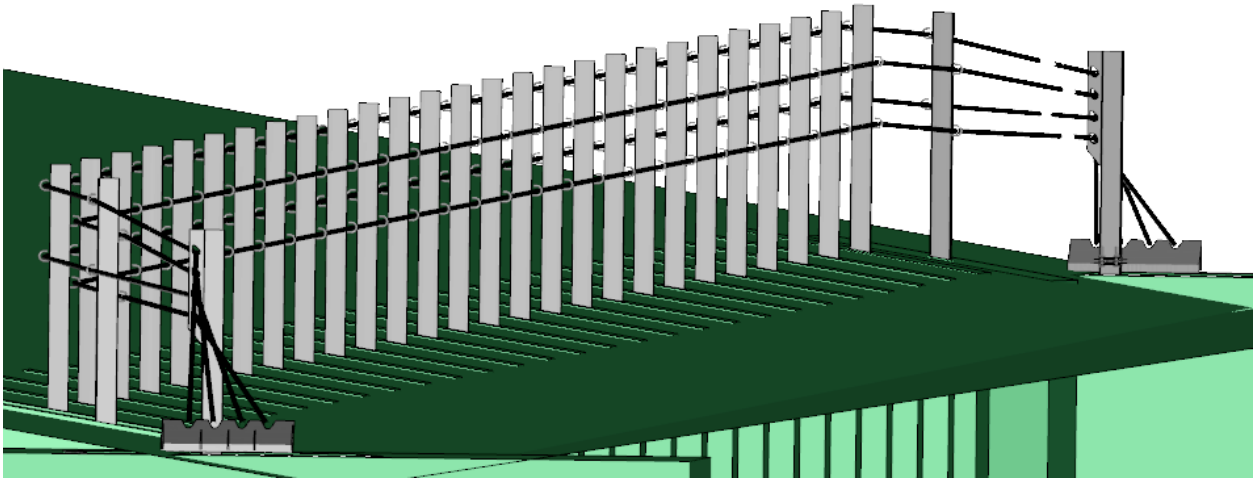

Figure 3.8: FE model of entire section of the "Four-cable Design Retrofit".

3.3 Simulation Setup

The three CMB models were combined with the two vehicle models to conduct the simulation work of this project. For ease of discussion, the simulations and corresponding results were divided into three cases based on the CMB designs.

Case 1: The current design.
Case 2: The "*Sixth Design Retrofit*."
Case 3: The "*Four-cable Design Retrofit*."

In all the simulations, the CMBs were placed on a 6H:1V slope median and evaluated at MASH TL-3 conditions (i.e., at a speed of 62mph (100 km/hr) and a 25-degree angle). For each case, the CBM was impacted from both the front-side and backside by the two vehicles. Based on the previous NCDOT research projects (Fang et al. 2009,2012), two impact locations were considered: 1) a post in the middle of the entire CMB section; and 2) the point at the mid-span of the CMB section. The two impact locations are illustrated in Fig. 3.9 where a Dodge Neon impacting the CMB at the post and mid-span. Table 3.2 give a summary of all the impact cases along with the impact conditions. A total of 24 simulations were required for the three cases.

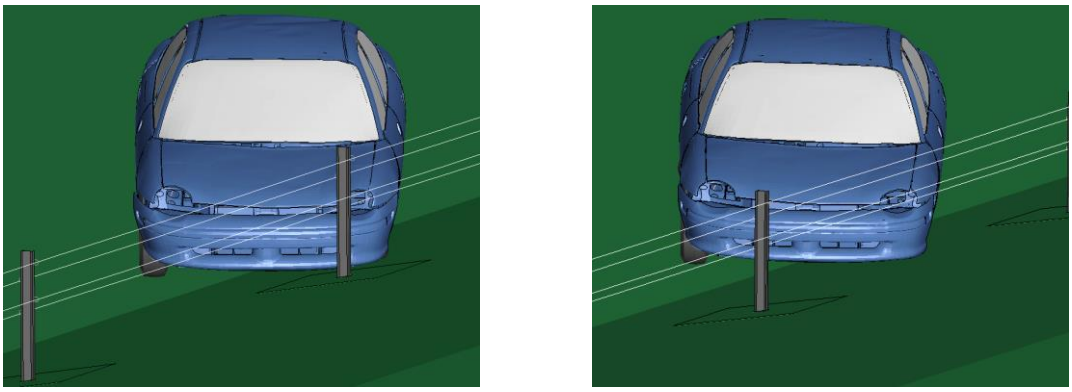

Figure 3.9: A Dodge Neon impacting the CMB at a post (left) and the mid-span (right).

Table 3.2: Simulation conditions for all cases

Case No	Barrier Design	Impact Side	Impact Location	Impacting Vehicles	Impact Speed	Impact Angle
1	Current Design	Front-side	Post	Dodge Neon Ford F250	62 mph (100km/h)	25°
			Mid-span			
		Backside	Post			
			Mid-span			
2	*Sixth Design Retrofit*	Front-side	Post	Dodge Neon Ford F250	62 mph (100km/h)	25°
			Mid-span			
		Backside	Post			
			Mid-span			
3	*Four-cable Design Retrofit*	Front-side	Post	Dodge Neon Ford F250	62 mph (100km/h)	25°
			Mid-span			
		Backside	Post			
			Mid-span			

4. Simulation Results and Analysis

The FE simulation results for the three cases in Table 3.2 are presented in this section. The performance of the CMBs under vehicular impacts were evaluated using vehicular responses specified by the MASH exit box criterion. The simulation results of the vehicles' yaw, pitch, and roll angles as well as transverse displacements and velocities were also examined to provide a comprehensive understanding of vehicular responses.

The exit box criterion is designed to determine the redirection characteristics of the vehicle after impacting a longitudinal barrier. Figure 4.1 illustrates the definition of the exit box, which is a rectangular area begins at the vehicle's last contact point with the barrier's initial face location (i.e., the upper left corner of the exit box shown in Fig. 4.1). The size of the exit box is determined by the type and size of the impacting vehicle. Table 4.1 gives the definition of the exit box dimensions, A and B, specified in MASH.

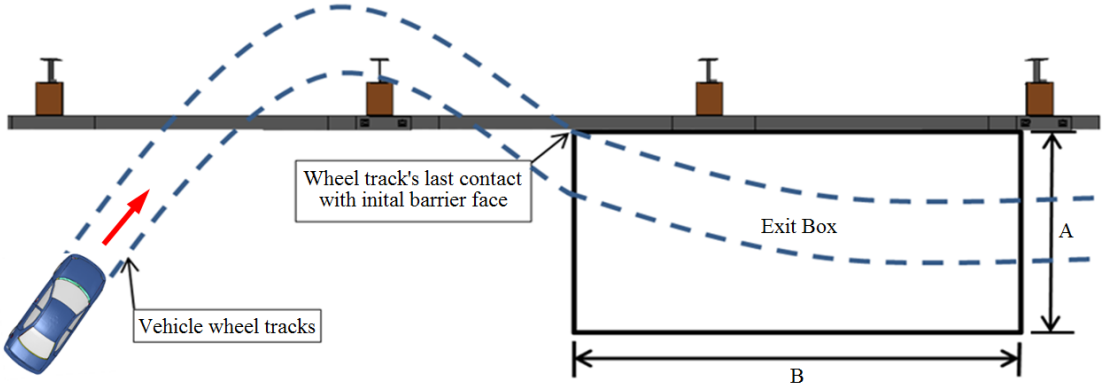

Figure 4.1: The exit-box criterion in MASH.

Table 4.1: The exit box criterion defined in MASH

Vehicle Type	Exit Box Dimension	
	A	**B**
Cars or Pickup Trucks	$7.2 + V_W + 0.16V_L$ (*ft*)	32.8 *ft* (10 m)
Other Vehicles	$14.4 + V_W + 0.16V_L$ (*ft*)	65.6 *ft* (20 m)

In Table 4.1, V_W and V_L stand for the vehicle's width and length, respectively. According to the exit box criterion, if all four wheels of the vehicle remain inside the exit box for the distance *B*, the case is considered a safe redirection, meaning that the exit angle of the impacting vehicle is small enough to effectively eliminate the possibility of the vehicle returning to the roadway and causing a second crash. Although the exit box criterion is a useful tool for determining the post-impact vehicular trajectories, use of this criterion alone is not enough to determine if the vehicle has been safely redirected. In addition, a large exit angle and/or spin-out, which may be caused by pocketing and/or snagging of the vehicle on the guardrail posts, may still be present even for a case determined as a safe redirect by the exit box criterion. Another scenario that is considered safe by the MASH evaluation criterion *N* is when the vehicle remains in contact with the guardrail

while reducing its velocity to zero. When this scenario is present, no exit box is required. Additionally, the MASH criterion *F* requires that the vehicle remains upright during and after collision with a maximum of 75 degree on roll and pitch angles.

The exit box dimensions for the Dodge Neon and Ford F250, as given in Table 4.2, were obtained using the formula in Table 4.1 and the vehicle data in Table 3.1. These two exit boxes were used to assess the post-impact vehicular responses from the simulation results.

Table 4.2: Exit box dimensions for the test vehicles of this project

Vehicle	**Exit Box Dimension**	
	A	**B**
1996 Dodge Neon	15.1 *ft* (4.6 m)	32.8 *ft* (10.0 m)
2006 Ford F250	16.9 *ft* (5.15 m)	32.8 *ft* (10.0 m)

4.1 Case 1: Evaluation of the Current CMB Design

In this section, the current CMB design were evaluated under MASH TL-3 conditions where two vehicles, a small passenger car and pickup truck, impacting at a speed of 100 km/h (62 mph) and a 25-degree angle. Table 4.3 summarizes the vehicular responses for all the simulations in Case 1.

Table 4.3: Summary of simulation results for Case 1

Test Vehicle	**Impact Side**	**Impact Location**	**Vehicular Response**
Dodge Neon	Front-side	Post	The vehicle passed the exit box criterion and was safely redirected
		Mid-span	The vehicle passed the exit box criterion and was safely redirected
	Back-side	Post	The vehicle under-rode and penetrated the CMB, and consequently entered the oncoming traffic lane
		Mid-span	The vehicle under-rode and penetrated the CMB, and consequently entered the oncoming traffic lane
Ford F250	Front-side	Post	The vehicle remained in contact with the barrier and was engaged with the top cable
		Mid-span	The vehicle passed the exit box criterion and was safely redirected
	Back-side	Post	The vehicle passed the exit box criterion but failed to pass MASH criterion *A*
		Mid-span	The vehicle passed the exit box criterion but failed to pass MASH criterion *A*

4.1.1 Dodge Neon Impacts from the Front-side

Figures 4.2 and 4.3 show the top-view vehicle trajectories of the Dodge Neon impacting the CMB (current design) from the front-side at a post and mid-span, respectively. In Figs. 4.2 and 4.3, the CMB was shown in its un-deformed state with the vehicle's tire tracks outlined in white. The exit boxes, shown by the yellow rectangle, were placed from the last point of contact of the vehicle's

tire tracks with the initial CMB face. In both cases, the exit angles were small enough to allow the vehicle travelling through the entire length of the exit box and exiting from the right-hand side. The current CMB design in these two impact cases met the MASH exit box criterion and the vehicle was considered to be safely redirected.

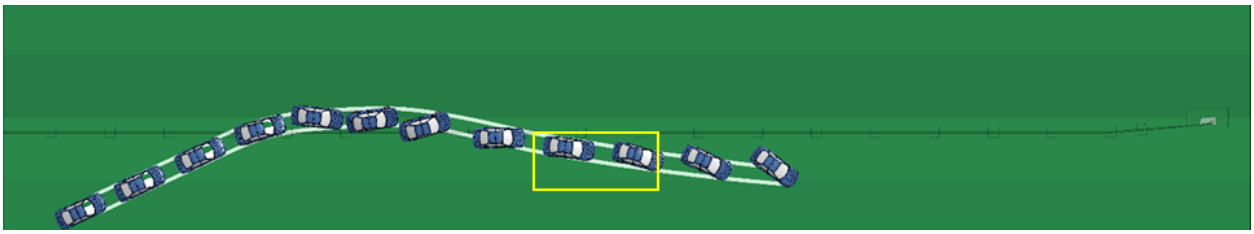

Figure 4.2: A Dodge Neon impacting the current CMB design at a post from front-side.

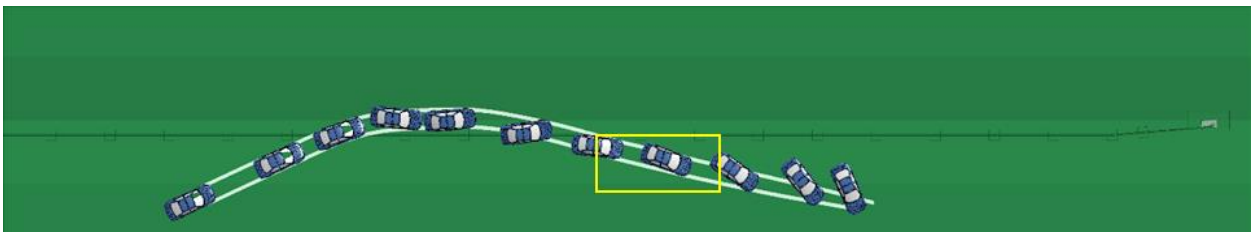

Figure 4.3: A Dodge Neon impacting the current CMB design at mid-span from front-side.

Figures 4.4a and 4.4b show the yaw, pitch, and roll angles of the Dodge Neon impacting the front-side of the CMB at post and mid-span, respectively. The exit angles were determined to be 6° and 9° for the impacts at post and mid-span, respectively, using the yaw and initial impact angles. The roll and pitch angles were found to be less than ten degrees in both positive and negative directions for both cases and thus passed the MASH evaluation criterion *F*, which specified a maximum of 75° roll or pitch angle.

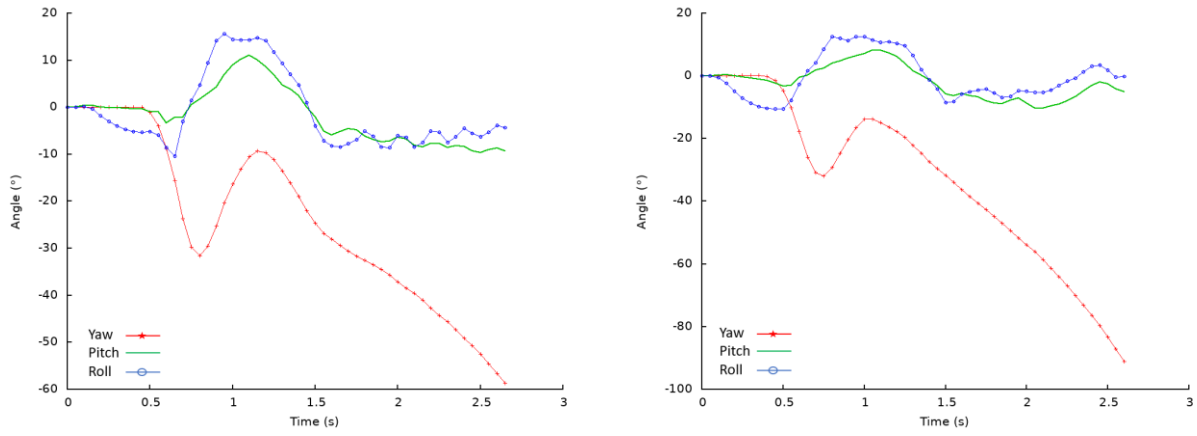

(a) At a post (b) At mid-span

Figure 4.4: Yaw, pitch, and roll angles of a Dodge Neon impacting the current CMB design from front-side.

The maximum dynamic deflections of the CMB were determined to be 2.28 m (7.48 ft) and 2.45 m (8.03 ft) for impacting at the post and mid-span, respectively. Figures 4.5a and 4.5b show Dodge Neon impacting the front-side of current CMB design at the time instants of maximum CMB deflections. As seen in Fig. 4.5, the vehicle was engaged with all three cables in both impact cases. The engaged cables continued holding the vehicle until the vehicle was redirected.

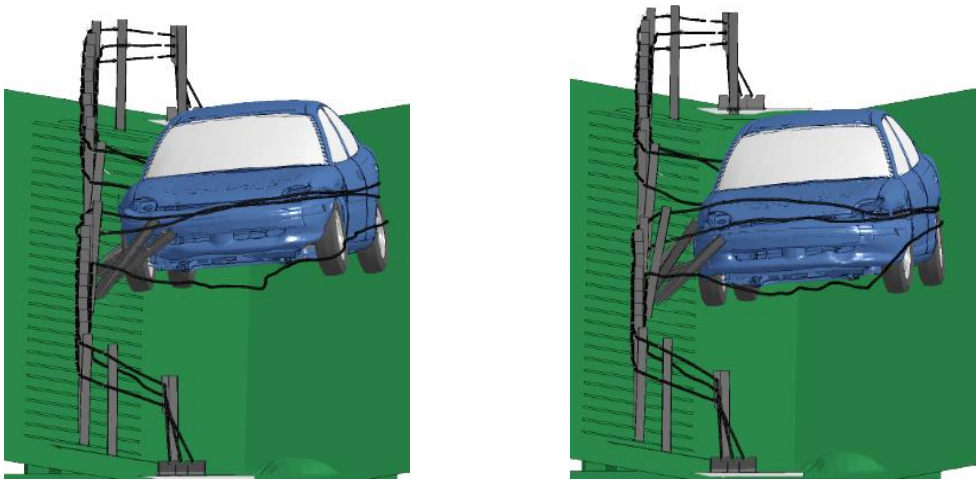

(a) At a post (b) At mid-span

Figure 4.5: Vehicle-barrier interactions for Dodge Neon impacting the current CMB design from front-side.

Figure 4.6 shows the time histories of transverse velocities measured at the center of gravity (CG) of the Dodge Neon impacting the CMB at the post and mid-span, respectively. The transverse velocities were less than 15 km/hr (9.3 mph) after the vehicle was redirected in both cases, indicating a small probability of getting involved in a secondary collision.

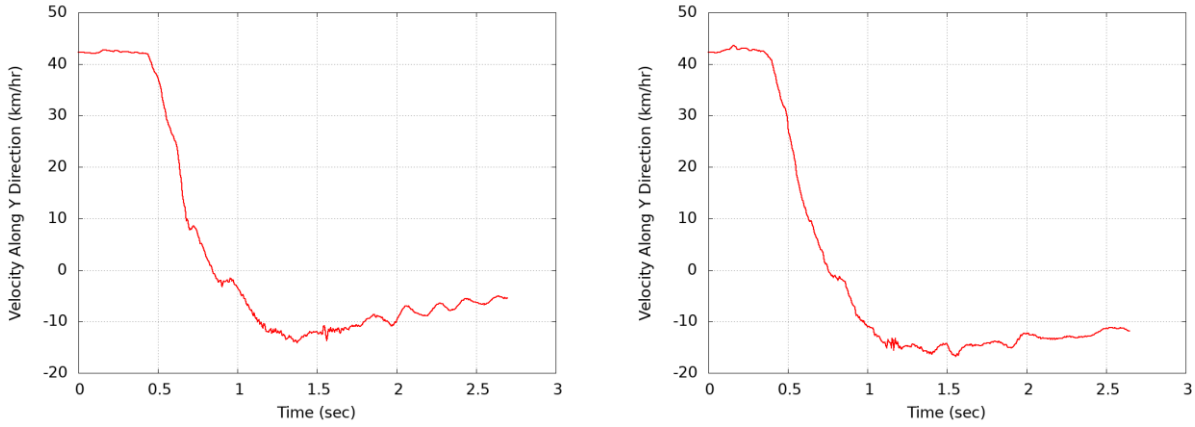

(a) At a post (b) At mid-span

Figure 4.6: Transverse velocity of a Dodge Neon impacting the current CMB design from front-side.

4.1.2 Dodge Neon Impacts from the Backside

In backside impacts by the Dodge Neon, the current CMB design failed to stop the vehicle in both impact cases, i.e., at the post and mid-span; the vehicle under-rode and penetrated the CMB, crossed the median, and entered the oncoming traffic. Figures 4.7 and 4.8 show the vehicle trajectories of the Dodge Neon impacting the current CMB design from the back-side at the post and mid-span, respectively.

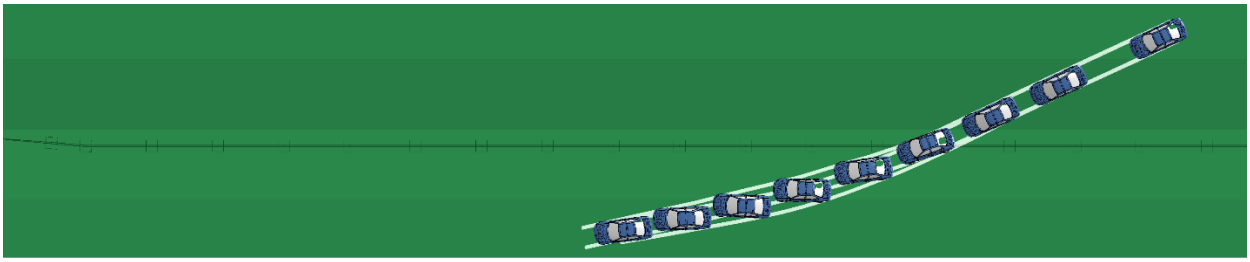

Figure 4.7: A Dodge Neon impacting the CMB (current design) at the post from backside.

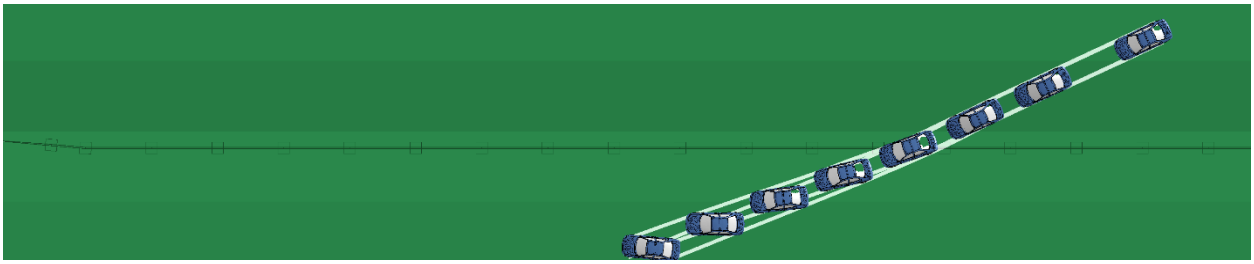

Figure 4.8: A Dodge Neon impacting the CMB (current design) at mid-span from backside.

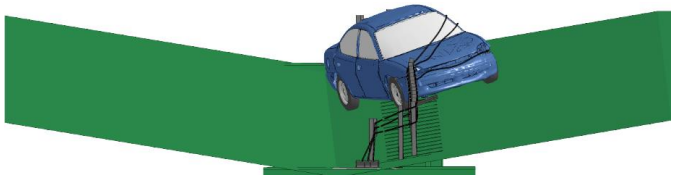

0.7 sec

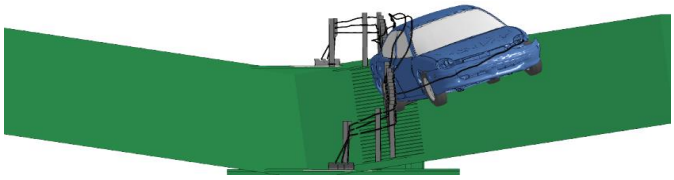

0.8 sec

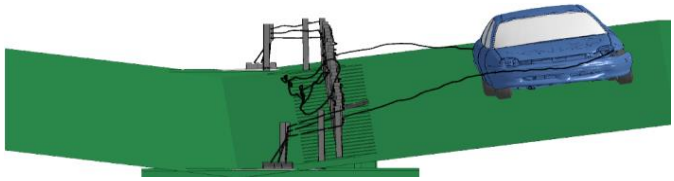

1.0 second

Figure 4.9: A Dodge Neon impacting the current CMB design at a post from backside.

Figure 4.9 shows three sequential instants of the Dodge Neon impacting the current CMB design at a post from the backside. As seen in Figure 4.9, the vehicle did not engage with the top two cables, and the bottom cable was not enough to redirect the vehicle, resulting in an under-riding of the CMB. In the case of the Dodge Neon impacting the current CMB design at mid-span from the backside (see Fig. 4.10), the vehicle did not engage with any cable and under-rode the barrier.

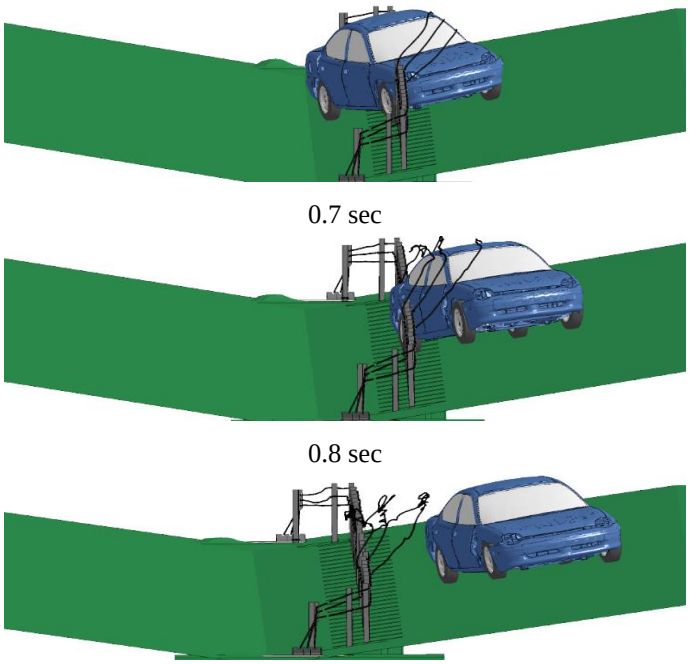

0.7 sec

0.8 sec

0.9 sec

Figure 4.10: A Dodge Neon impacting the current CMB design at mid-span from backside.

Figure 4.11 shows yaw, pitch, and roll angles of the Dodge Neon impacting the backside of the current CMB design at a post and mid-span. Since the vehicle under-rode the CMB and was not redirected, the exit angles of the vehicle and the maximum transverse displacements of the CMB could not be determined. Although the CMB failed to meet the MASH exit box criterion, the pitch and roll angles of the vehicle met with the MASH evaluation criterion *F*, which specified a 75° maximum pitch or roll angle.

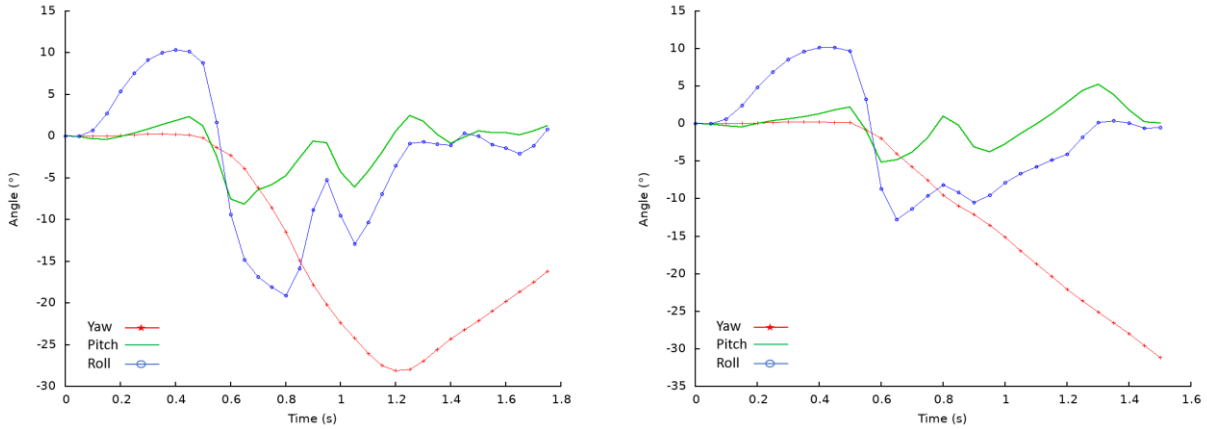

(a) At a post (b) At mid-span

Figure 4.11: Yaw, pitch, and roll angles of a Dodge Neon impacting the current CMB design from front-side.

4.1.3 Ford F250 Impacts from the Front-side

Figures 4.12 and 4.13 show the top-view vehicle trajectories of the Ford F250 impacting the current CMB design from the front-side at a post and at mid-span, respectively. In the case of impacting the CMB at a post, the vehicle remained in contact with the barrier; therefore, it was unnecessary to check with the MASH exit box criterion and the case was still considered safe according to MASH. In the case of impacting the CMB at mid-span (Fig. 4.13), the vehicle was redirected with a small exit angle and the MASH exit box criterion was met.

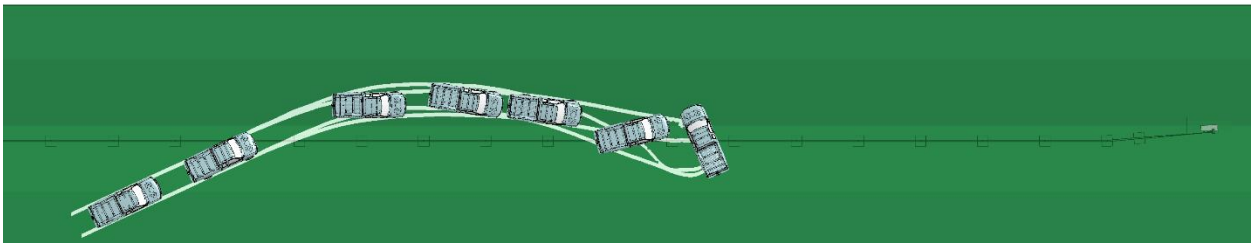

Figure 4.12: A Ford F250 impacting the current CMB design at a post from front-side.

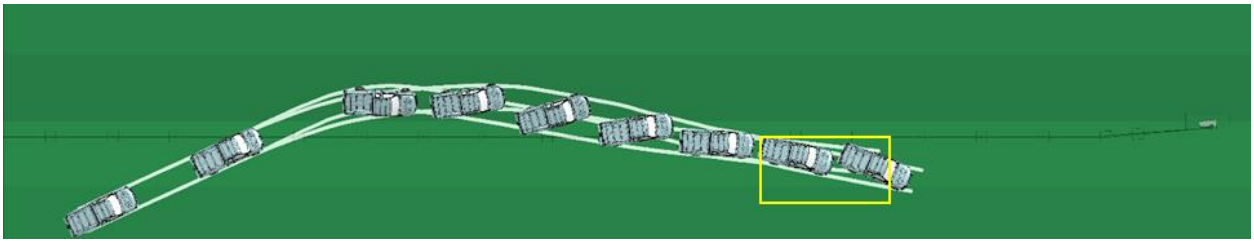

Figure 4.13: A Ford F250 impacting the current CMB design at mid-span from front-side.

Figure 4.14 shows the yaw, pitch, and roll angles of the Ford F250 impacting the current CMB design from front-side at a post and at mid-span. When impacting the CMB at a post, the vehicle remained in contact with the barrier; therefore, the exit angle was not determined. The exit angle was determined to be -7° in the case of impacting the CMB at mid-span. In both front-side impacts

by the Ford F250, the roll and pitch angles in the vehicle were less than 20 degrees in either positive or negative direction and thus passed the MASH evaluation criterion *F*.

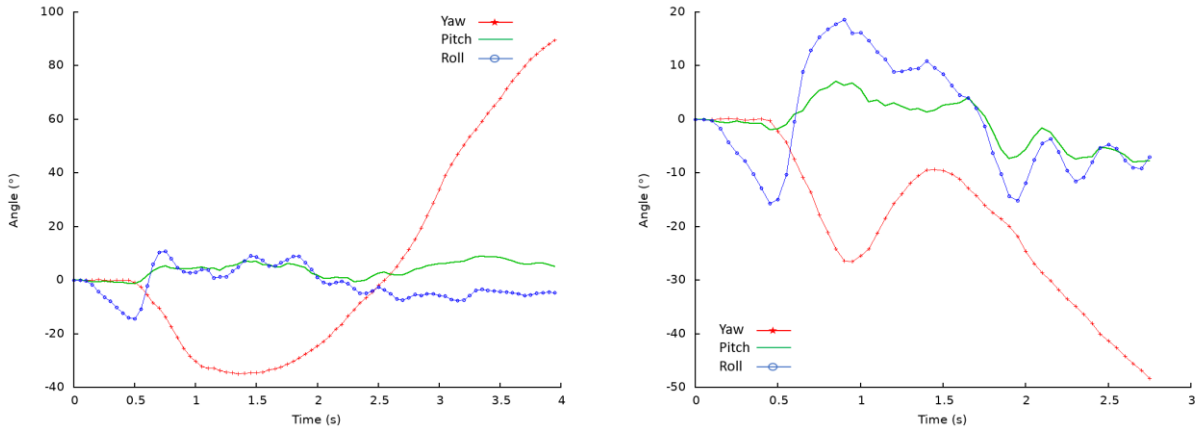

(a) At a post (b) At mid-span

Figure 4.14: The yaw, pitch, and roll angles of the Ford F250 impacting the current CMB design from front-side.

Figure 4.15 shows the vehicle-barrier interactions at instants with maximum dynamic deflections, approximately 2.28 m (7.48 ft) when impacting the CMB at the post and 2.55 m (8.36 ft) when impacting at mid-span. In the case of impacting at the post (Fig. 4.14a), the vehicle fully engaged with the top cable and partially engaged with the middle cable by the right-side tires. This type of engagement caused the vehicle to spin counterclockwise and the middle cable was later on released from the vehicle. In the case of impacting at mid-span (Fig. 4.14b), the vehicle fully engaged with all three cables during the entire course of the impact until the vehicle lost contact with the CMB.

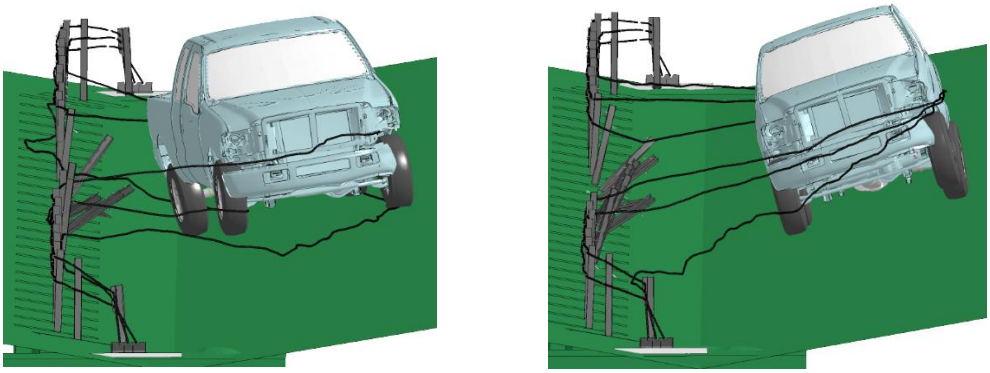

(a) At a post (b) At mid-span

Figure 4.15: Vehicle-barrier interactions for Ford F250 impacting the current CMB design from front-side.

Figure 4.16 shows the time histories of transverse velocities measured at the CG point of Ford F250 while impacting the current CMB design from the front-side. After being redirected, the transverse velocities of the vehicle were less than 15 km/hr (9.3 mph) in both cases, indicating a relatively very small chance of getting involved in a secondary collision.

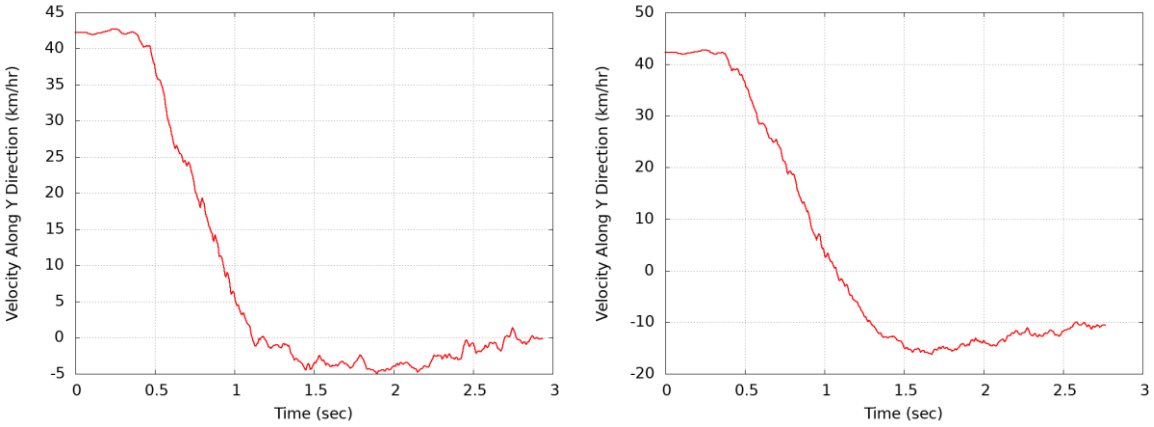

(a) At a post (b) At mid-span

Figure 4.16: Transverse velocities of the Ford F250 impacting the current CMB design from front-side.

4.1.4 Ford F250 Impacts from the Backside

Figures 4.17 and 4.18 show the top-view vehicle trajectories of the Ford F250 impacting the backside of the current CMB design at a post and at mid-span, respectively. It can be seen that the MASH exit box criterion was met in both impact cases, but the vehicle entered the oncoming travel land and thus violated the MASH Evaluation Criterion *A* in both backside impacts.

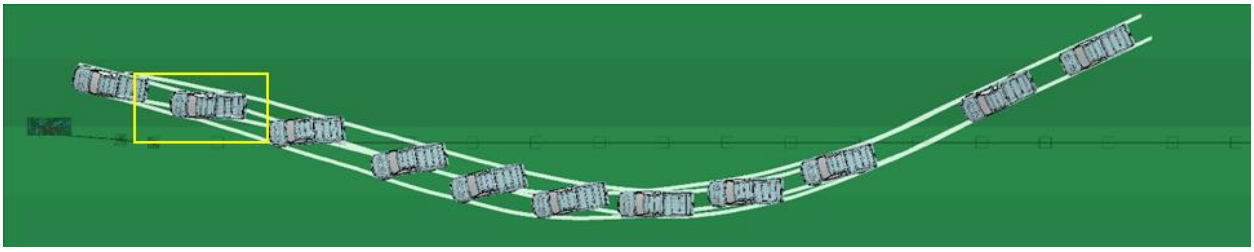

Figure 4.17: A Ford F250 impacting the current CMB design at a post from backside.

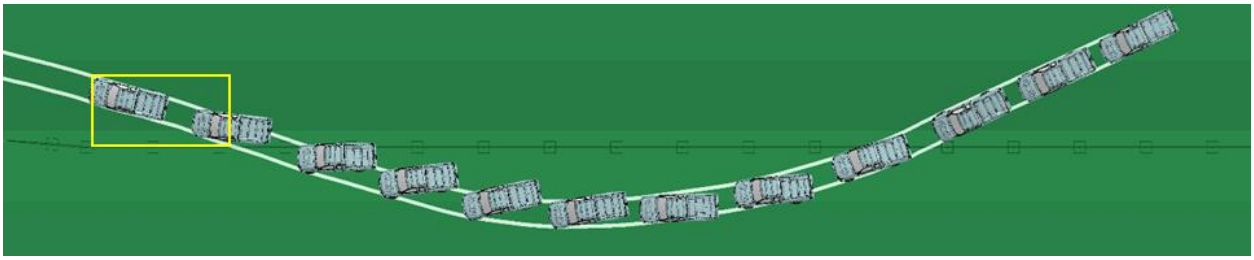

Figure 4.18: A Ford F250 impacting the current CMB design at mid-span from backside.

Figure 4.19 shows the yaw, pitch, and roll angles of the Ford F250 impacting the backside of the current CMB design at a post and mid-span. The exit angles were determined to be 13° and 12° for the impacts at a post and mid-span, respectively. The roll and pitch angles of the Ford F250

were less than 15° in both positive and negative directions for both cases and thus passed the MASH evaluation criterion *F*, which specified a maximum 75° roll or pitch angle.

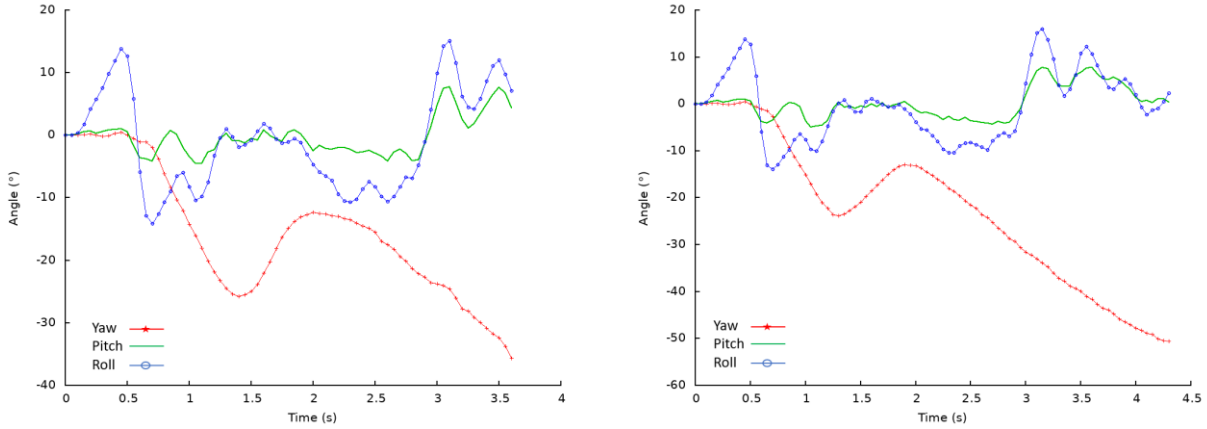

(a) At a post (b) At mid-span

Figure 4.19: Yaw, pitch, and roll angles of the Ford F250 impacting the current CMB design from backside

Although the current CMB design met the MASH exit box criterion and evaluation criterion *F* for the impacts of Ford F250 from the backside, it did not meet the requirement of MASH evaluation criterion *A*, which required a reasonable maximum lateral displacement of the barrier. The maximum lateral displacements of the CMB were found to be 5.77 m (18.93 ft) for the both cases; therefore, the vehicle entered the oncoming traffic lane at the maximum lateral displacements, as shown in Fig. 4.20. Although the vehicle engaged with all three cables and did not penetrate through the CMB, the large lateral deflections of the CMB allowed the vehicle to enter the oncoming traffic lane, resulting in a high probability of getting involved in a secondary collision.

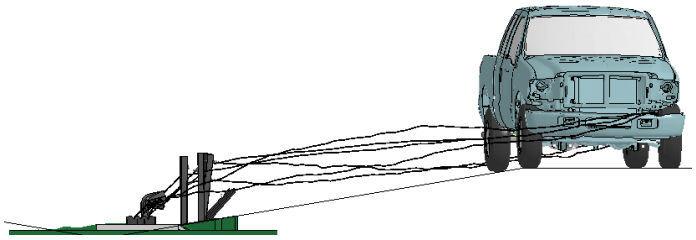

(a) At a post

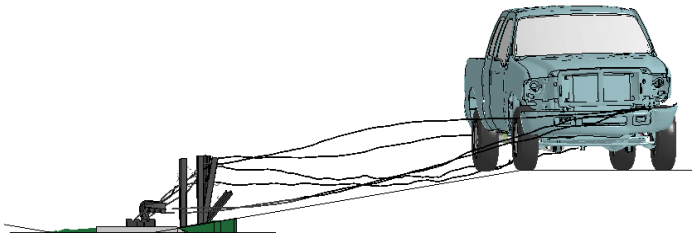

(b) At mid-span

Figure 4.20: Vehicle-barrier interactions for Ford F250 impacting the current CMB design from backside.

Figure 4.21 shows the time histories of transverse velocities at the CG point of Ford F250 impacting the backside of current CMB design at post and mid-span. The transverse velocities of Ford F250 was approximately 15 km/hr (9.3 mph) towards the travel lane, indicating a relatively small chance of getting involved in a secondary collision.

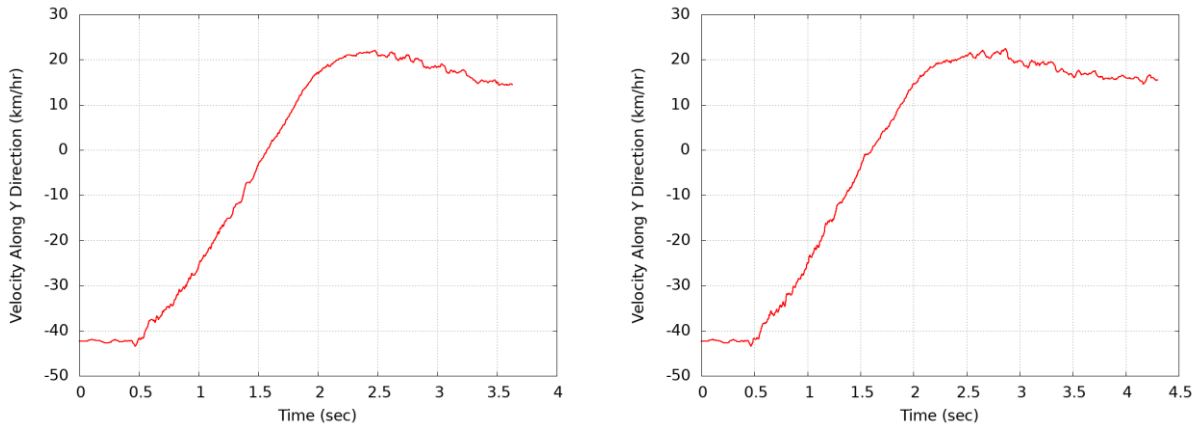

(a) At a post (b) At mid-span

Figure 4.21: Transverse velocities of the Ford F250 impacting the current CMB design from backside.

Overall, the current CBM design could meet the MASH evaluation criteria under impacts of Dodge Neon from both front-side and backside, and of Ford F250 from the front-side. The current CMB design, however, failed to meet the MASH evaluation criterion *A* when impacted by the Ford F250 from the backside both at post and at amid-span.

4.2 Case 2: Evaluation of the "Sixth Design Retrofit"

In this section, the "*Sixth Design Retrofit*" was evaluated under MASH TL-3 conditions, i.e., under impacts of a small passenger car (1100C) and pickup truck (2270P) at an impact speed of 100 km/hr (62 mph) and a 25° angle. Table 4.4 summarizes the simulation results for Case 2 on the performance of "*Sixth Design Retrofit*" in terms of vehicular responses.

4.2.1 Dodge Neon Impacts from the Front-side

Figures 4.22 and 4.23 show the top-view vehicle trajectories of the Dodge Neon impacting the front-side of the "*Sixth Design Retrofit*" at a post and at mid-span, respectively. The CMB was shown in its undeformed state with the vehicle's tire tracks outlined in white in Figs. 4.22 and 4.23. The exit boxes, shown by the yellow rectangle, were placed at the last point of contact of the vehicle's tire tracks with the initial CMB face.

Table 4.4: Summary of simulation results for Case 2

Test Vehicle	Impact Side	Impact Location	Vehicular Response
Dodge Neon	Front-side	Post	The vehicle was redirected but did not meet the exit box criterion
		Mid-span	The vehicle passed the exit box criterion but with a large rotation
	Back-side	Post	The vehicle passed the exit box criterion but with a large rotation
		Mid-span	The vehicle passed the exit box criterion and was safely redirected
Ford F250	Front-side	Post	The vehicle penetrated the CMB and entered oncoming traffic
		Mid-span	The vehicle penetrated the CMB and entered oncoming traffic
	Back-side	Post	The vehicle passed the exit box criterion and was safely redirected
		Mid-span	The vehicle passed the exit box criterion and was safely redirected

In the case of Dodge Neon impacting at the post (Fig. 4.22), the "*Sixth Design Retrofit*" did not meet the MASH exit box criterion because the vehicle did not traverse though the length of the exit box before leaving the box. Due to the high exit angle of the post-impact trajectory, the chance of a secondary collision was high. In the case of impacting at mid-span (Fig. 4.23), the MASH exit box criterion was met; however, the vehicle exhibited large yaw angles after leaving the exit box.

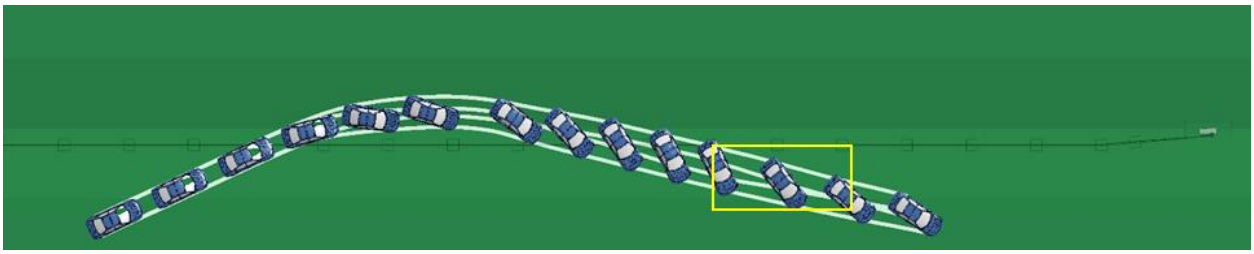

Figure 4.22: A Dodge Neon impacting the "Sixth Design Retrofit" at a post from front-side.

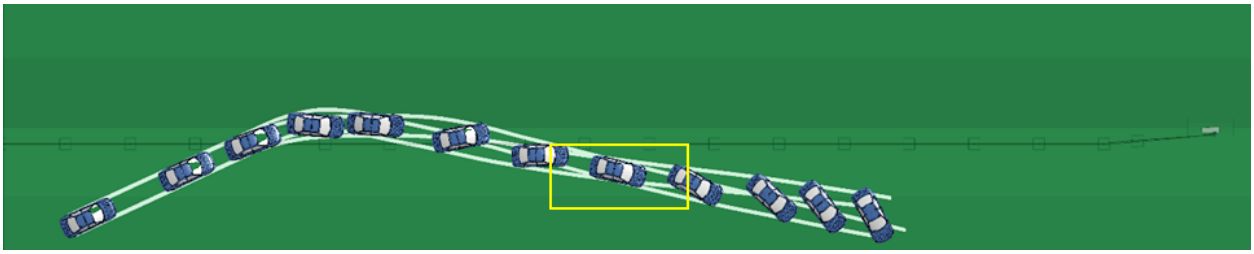

Figure 4.23: A Dodge Neon impacting the "Sixth Design Retrofit" at mid-span from front-side.

The yaw, pitch, and roll angles of the Dodge Neon impacting the front-side of "*Sixth Design*

Retrofit" are shown in Fig. 4.24a. The exit angle was determined to be 54° for the case of impacting the CMB at a post. Although the vehicle was redirected in this impact case, the large exit angle may lead to a secondary collision when the vehicle returned to the travel lane. The exit angle was determined to be 7° for the case of impacting at the mid-span (Fig. 4.24b). However, the vehicle had a large clockwise rotation after losing contact with the CMB, as shown by the continuously increasing yaw angles shown in Fig. 24b. Although this impact case passed the MASH exit box criterion, the vehicle has high likelihood of getting involved in a secondary collision in the travel lane. For both cases of impacting the front-side of the CMB, the "*Sixth Design Retrofit*" passed the MASH evaluation criterion *F* since the roll and pitch angles were less than 10° in the positive and negative directions and were below the 75° maximum allowable degree.

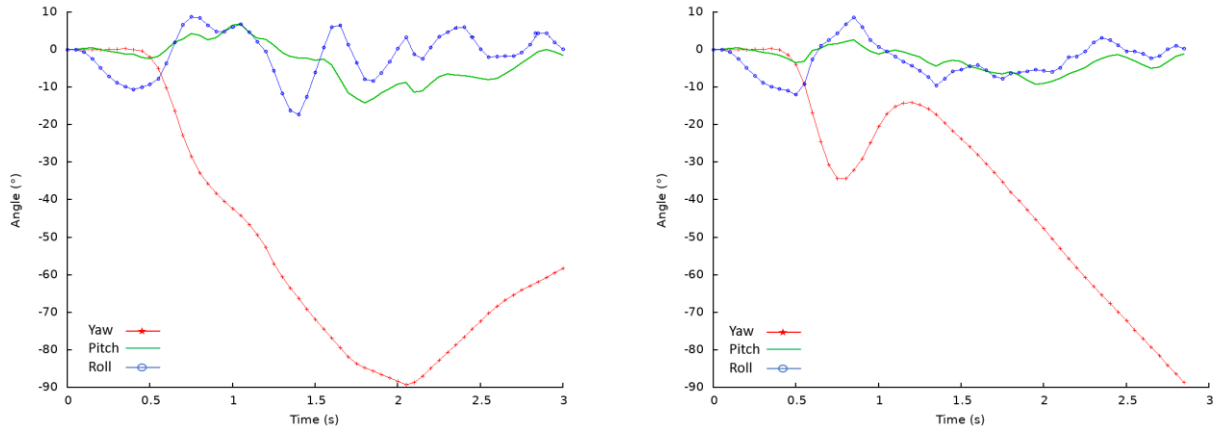

(a) At a post (b) At mid-span

Figure 4.24: Yaw, pitch, and roll angles of a Dodge Neon impacting the "Sixth Design Retrofit" from front-side.

The maximum transverse displacements of the "*Sixth Design Retrofit*" were 3.62 m (11.87 ft) and 2.59 m (8.49 ft) under impacts of the Dodge Neon from the front-side at a post and at mid-span, respectively. Figure 4.25 shows the vehicle-barrier interactions in both cases when the barrier reached maximum deflections. In the case of impacting at a post, the top cable of the CMB fully engaged with the vehicle while the middle cable is seized by the right-front tire of vehicle. In the case of impacting at mid-span, the vehicle engaged with all three cables of the CMB (see Fig. 4.25b) and for this reason, the maximum CMB displacement was less than that of impacting at a post. This observation indicated that the transverse CMB displacements could be affected by cable engagement during the impact. When impacting directly on the cables, e.g., in the case of impacting at mid-span, the vehicle was more likely to get engaged with more cables than in the case of impacting at a post. When impacting at a post, the middle and bottom cables were released from the hook and under-rode by the vehicle before any interaction with the vehicle occurred.

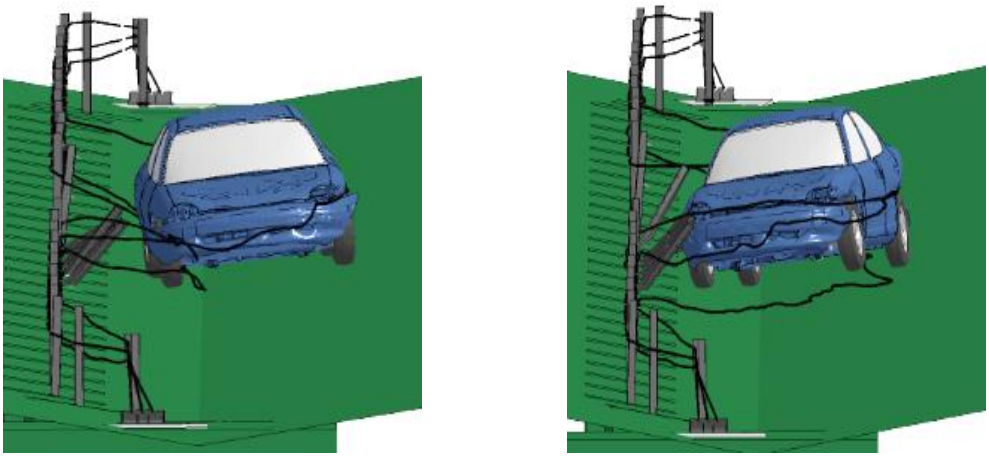

(a) At a post (b) At mid-span

Figure 4.25: Vehicle-barrier interactions for Dodge Neon impacting the "Sixth Design Retrofit" from front-side.

Figure 4.26 shows the time histories of velocities measured at the CG point of the Dodge Neon impacting the front-side of "*Sixth Design Retrofit*." The transverse velocities were less than 15 km/hr (9.32 mph) for both cases (i.e., impacting at a post and at mid-span), indicating a small chance of getting involved in a secondary collision.

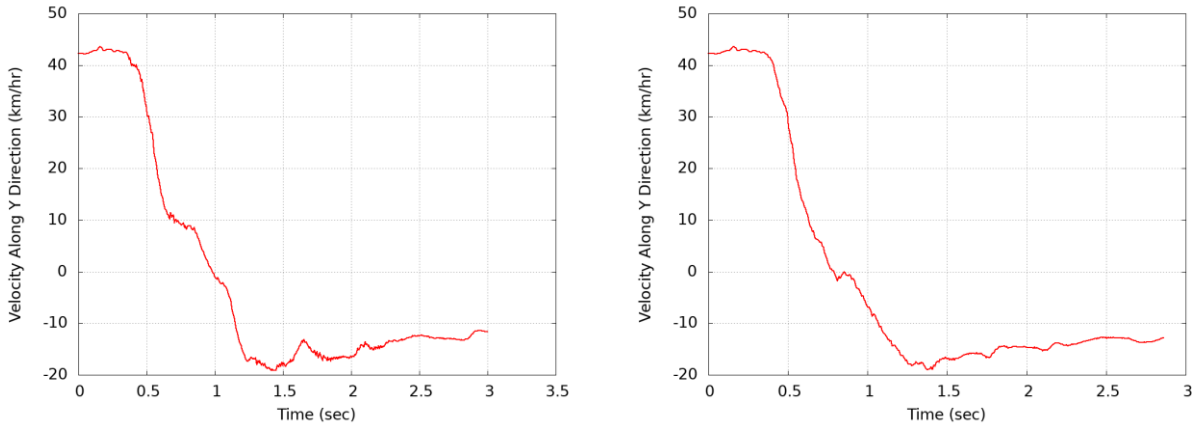

(a) At a post

(b) At mid-span

Figure 4.26: Transverse velocities of a Dodge Neon impacting the "Sixth Design Retrofit" from front-side.

4.2.2 Dodge Neon Impacts from the Backside

Figures 4.27 and 4.28 show the top-view vehicle trajectories of the Dodge Neon impacting the backside of the "*Sixth Design Retrofit*" at a post and at mid-span, respectively. It can be seen from Figs. 4.27 and 4.28 that the vehicle was redirected in both cases and the CMB met the MASH exit box criterion. In the case of impacting the CMB at mid-span, the vehicle had a relatively small exit angle and stayed within the median slop after leaving the exit box. This case can be considered as a safe redirect of the vehicle. However, in the case of impacting at a post, the vehicle entered into the travel lane after leaving the exit box due to a clockwise spinning, indicating a relatively high

chance of getting involved in a secondary collision. Therefore, this case cannot be considered as a safe redirect.

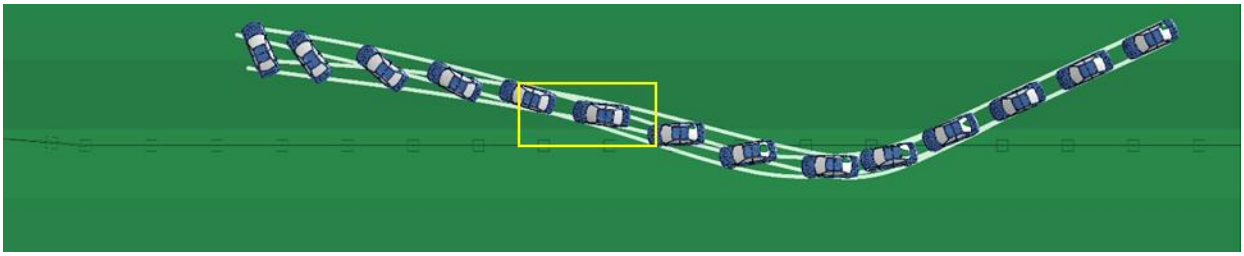

Figure 4.27: A Dodge Neon impacting the "Sixth Design Retrofit" at a post from backside.

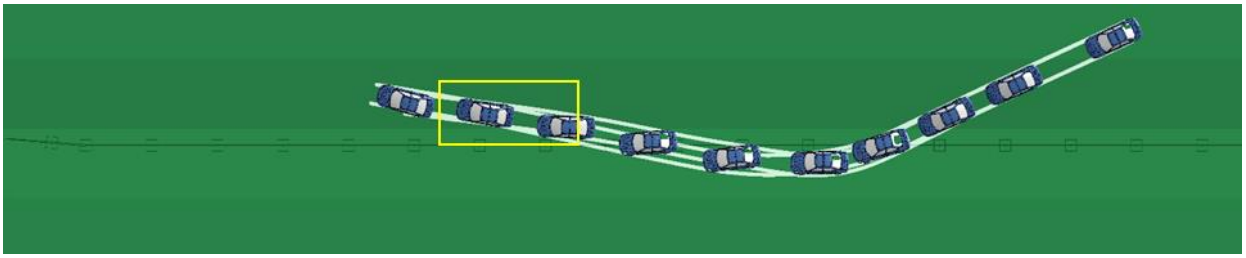

Figure 4.28: A Dodge Neon impacting the "Sixth Design Retrofit" at mid-span from backside.

Figure 4.29 shows the yaw, pitch, and roll angles of Dodge Neon impacting the backside of the "Sixth Design Retrofit" at a post and at mid-span. The exit angles for these two impact cases were determined to be 12° and 7° for impacting at a post and at mid-span, respectively. In both cases, the pitch and roll angles were between plus and minus 20° and thus passed the MASH evaluation criterion *F*, which specified a maximum of 75° for pitch and roll angles.

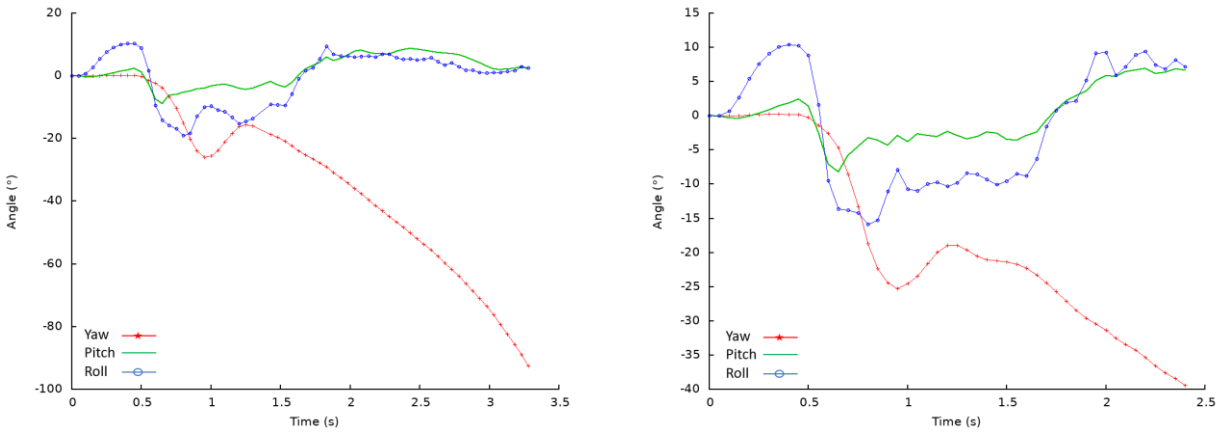

(a) At a post (b) At mid-span

Figure 4.29: Yaw, pitch, and roll angles of a Dodge Neon impacting the "Sixth Design Retrofit" from backside.

Figure 4.30 shows the vehicle-barrier interactions at the maximum displacements of the "*Sixth Design Retrofit*" under impacts of the Dodge Neon at a post and at mid-span from the backside. The maximum displacements of the "*Sixth Design Retrofit*" were found to be 2.42 m (7.93 ft) and 2.29 m (7.59 ft) for impacts at a post and at mid-span, respectively. In both cases, the vehicle was engaged with the middle and bottom cables until the vehicle was redirected. The vehicle only had some initial contacts with the top cable, which did not contribute to the redirection of the vehicle.

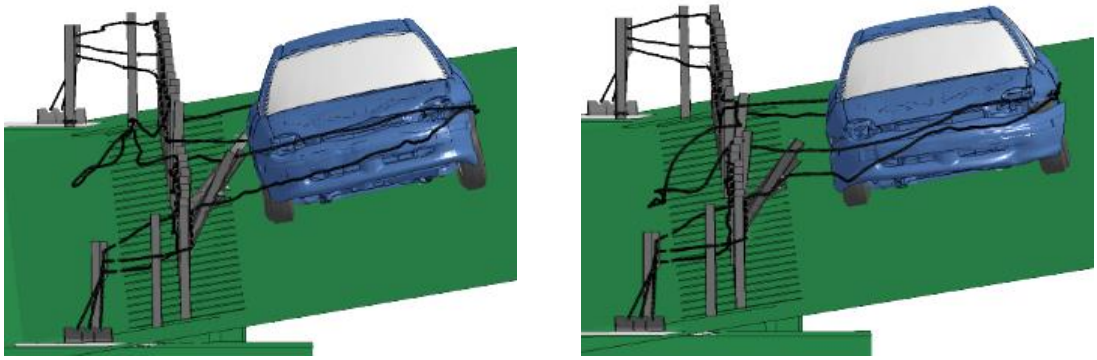

(a) At a post (b) At mid-span

Figure 4.30: Vehicle-barrier interactions for Dodge Neon impacting the "Sixth Design Retrofit" from backside.

Figure 4.31 shows the time histories of velocities measured at the CG point of the Dodge Neon impacting the "*Sixth Design Retrofit*" at a post and at mid-span. The transverse velocities were approximately 10 km/hr (6.2 mph) towards the end of the impacts for both cases. However, the vehicle reached a higher transverse velocity (20 km/hr or 12.4 mph) after being redirected in the case of impacting at a post than that of impact at mid-span. This high transverse velocity causes the vehicle to enter into the travel lane in the case of impacting at a post, even though the vehicle was redirected. Along with its spinning, the vehicle had a relatively high chance of getting involved in a secondary collision.

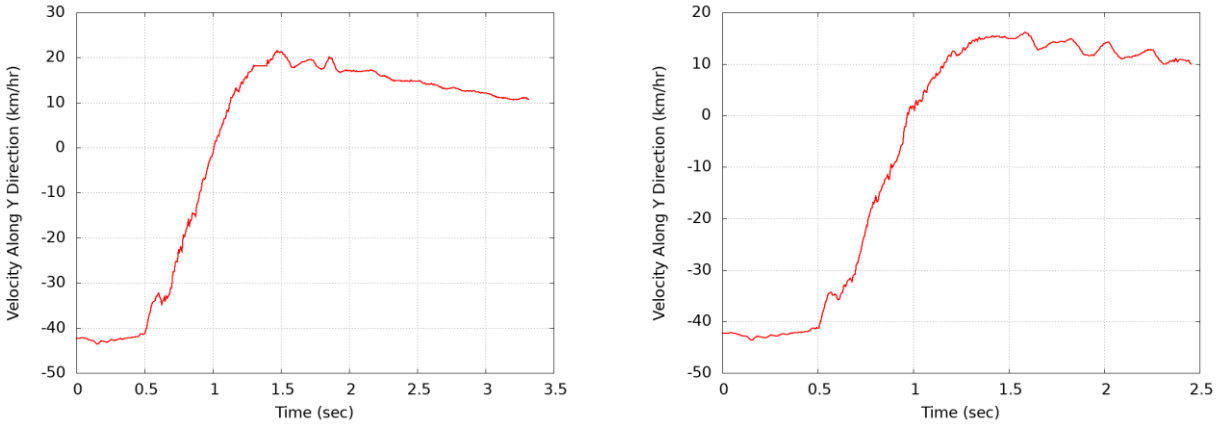

(a) At a post (b) At mid-span

Figure 4.31: Transverse velocities of a Dodge Neon impacting the "Sixth Design Retrofit" from backside.

4.2.3 Ford F250 Impacts from the Front-side

The post-impact trajectories of the Ford F250 impacting the front-side of the "*Sixth Design Retrofit*" at a post and at mid-span are shown in Figs. 4.32 and 4.33, respectively. It can be seen that the Ford F250 penetrated the CMB and entered into the oncoming travel lane in both cases. The post-impact responses of the Ford F250 were similar in both cases: the vehicle did not engage with any cable and overrode the CMB. Figure 4.34 shows three-time instants of vehicle-barrier interactions in the impact at a post.

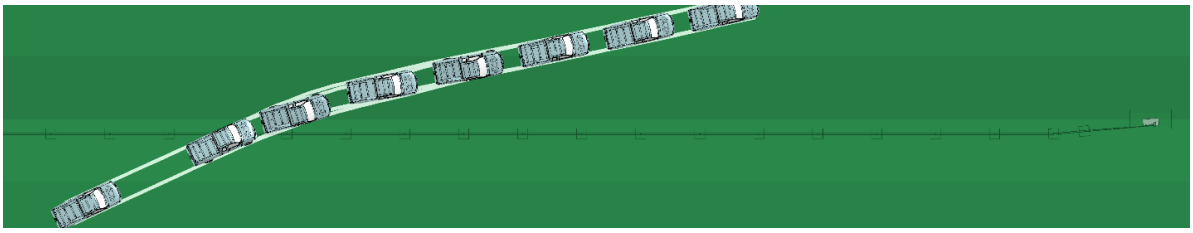

Figure 4.32: A Ford F250 impacting the "Sixth Design Retrofit" at a post from front-side.

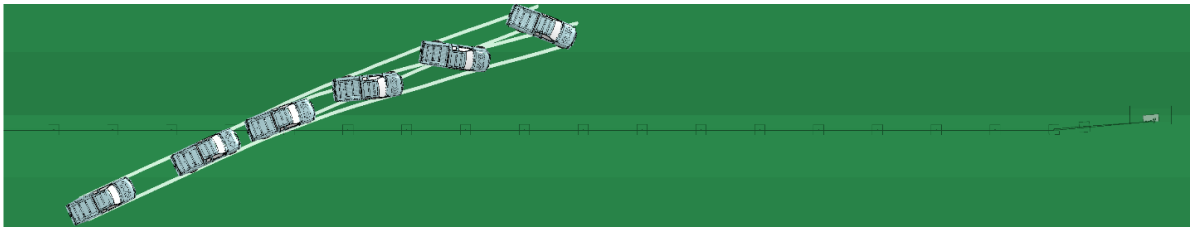

Figure 4.33: A Ford F250 impacting the "Sixth Design Retrofit" at mid-span from front-side.

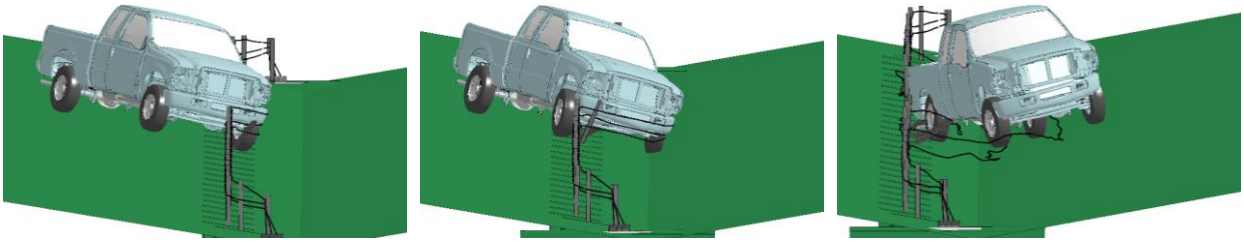

0.8 sec 1.2 sec 1.4 sec

Figure 4.34: Time sequences of the Ford F250 impacting the "Sixth Design Retrofit" at a post from front-side.

The yaw, roll, and pitch angles of the Ford F250 are shown in Fig. 4.35. Due to the lack of retaining forces from the CMB on the vehicle, the roll and pitch angles were relatively small and pass the MASH evaluation criterion *F*, which specified a maximum of 75° roll and pitch angles.

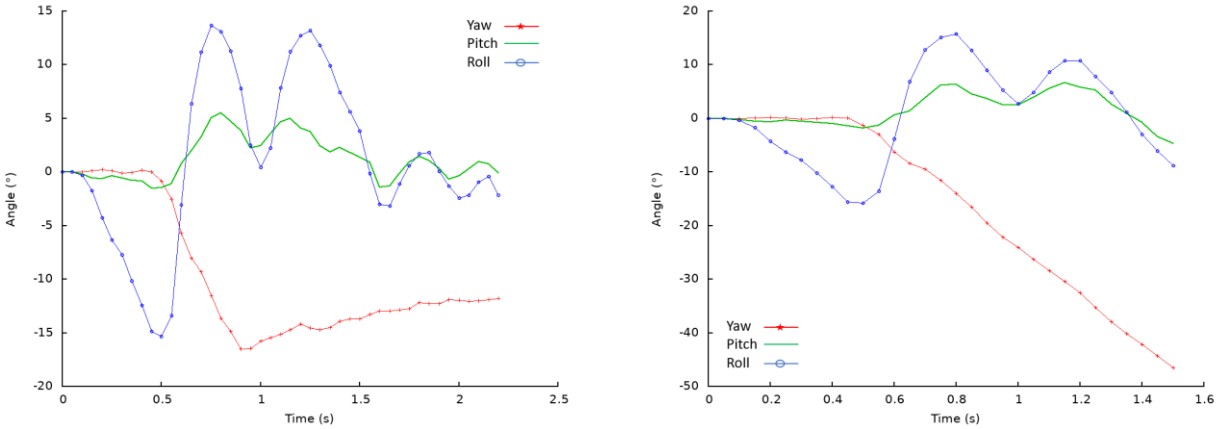

(a) At a post (b) At mid-span

Figure 4.35: Yaw, pitch, and roll angles of the Ford F250 impacting the "Sixth Design Retrofit" from front-side.

Figure 4.36 shows the time histories of transverse velocities measured at the CG point of Ford F250 impacting the front-side of "*Sixth Design Retrofit*" at a post and at mid-span. Due to penetration on the CMB, the vehicle had large transverse velocities in both cases, with 28 km/hr impacting at mid-span and 18 km/hr impacting at a post. In both cases, the vehicle had a high chance of getting involved in a secondary collision.

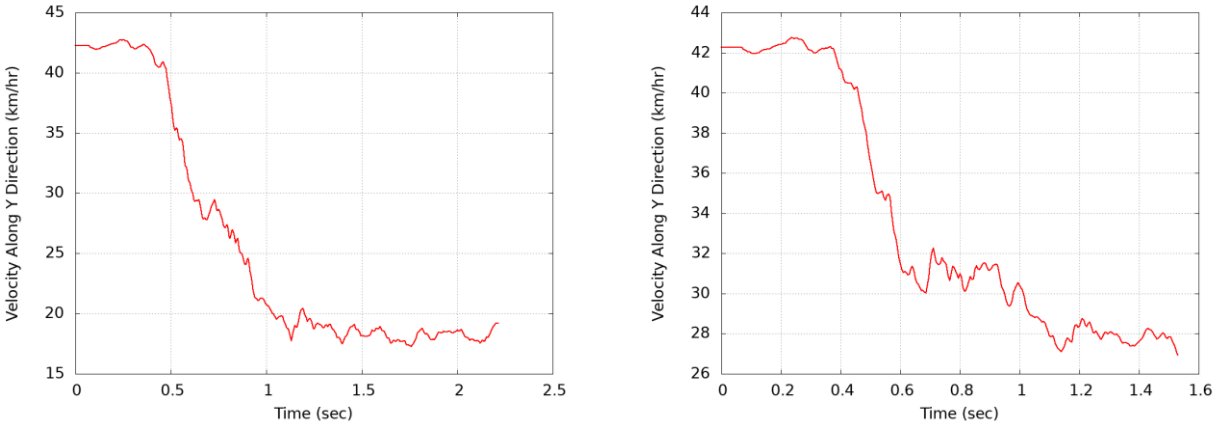

(a) At a post (b) At mid-span

Figure 4.36: Transverse velocities of the Ford F250 impacting the "Sixth Design Retrofit" from front-side.

4.2.4 Ford F250 Impacts from the Backside

When impacted by a Ford F250 from the backside at both a post and mid-span, the "*Sixth Design Retrofit*" passed the MASH exit box criterion and redirected the vehicle with small exit angles, as shown in Figs. 4.37 and 4.38. In both cases, the Ford F250 engaged with all three cables and the vehicular responses were similar to each other.

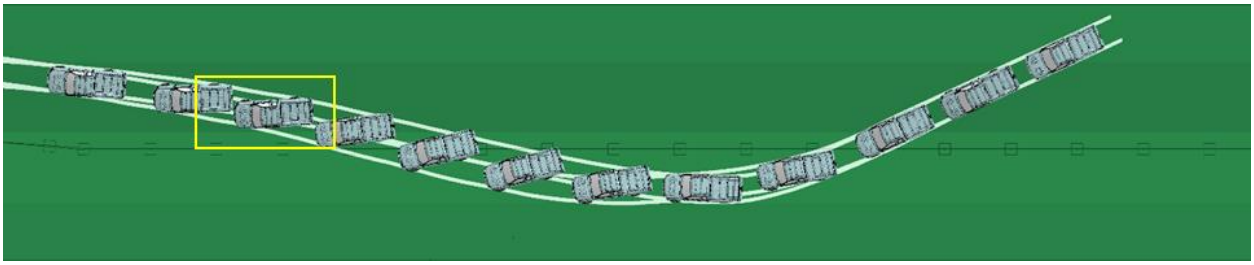

Figure 4.37: A Ford F250 impacting the "Sixth Design Retrofit" at a post from backside.

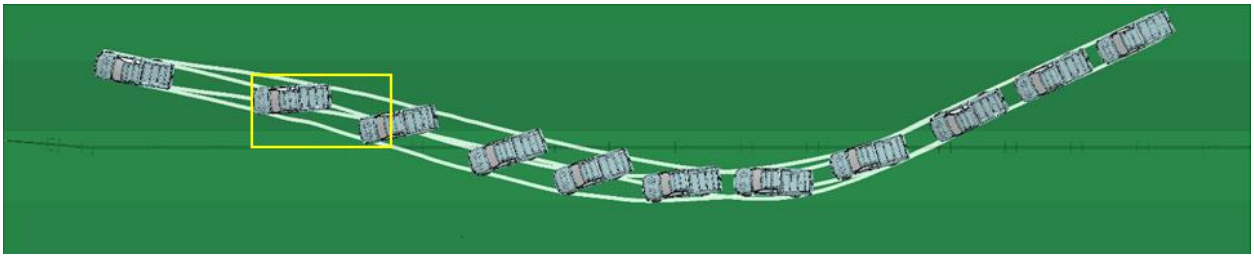

Figure 4.38: A Ford F250 impacting the "Sixth Design Retrofit" at mid-span from backside.

Figure 4.39 shows a comparison of vehicle-CMB interactions during impacts by the Ford F250 on the "*Sixth Design Retrofit*" from the front-side and backside. It can be seen that the Ford F250 had a higher profile when coming from the front-side than coming from the backside (due to suspension compression after crossing the bottom of the ditch). Consequently, the vehicle could not fully engage with all three cables in the front-side impact and eventually overrode the three cable. The vehicle, however, engaged with all three cables in the backside impact and was successfully redirected.

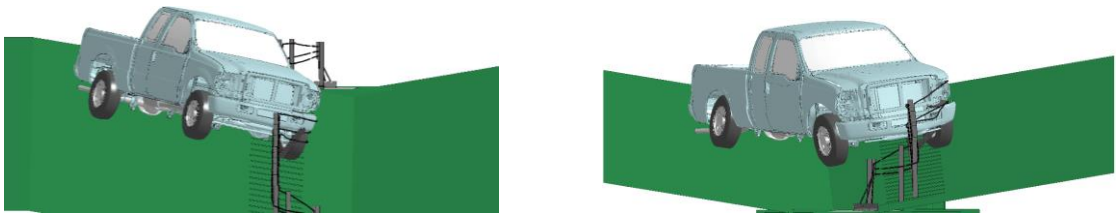

(a) From front-side (b) From backside

Figure 4.39: Vehicle-CMB interactions during impacts by a Ford F250 on the "Sixth Design Retrofit" at a post.

The yaw, pitch, and roll angles of the Ford F250 impacting the backside of "*Sixth Design Retrofit*" at a post and at mid-span are shown in Figure 4.40. The exit angles of the Ford F250 were determined to be 7° and 9° for impacting at a post and at mid-span, respectively. The roll and pitch angles in both impact cases were less than 20° in both positive and negative directions, satisfying the MASH evaluation criterion *F*, which specified a maximum of 75° roll or pitch angle.

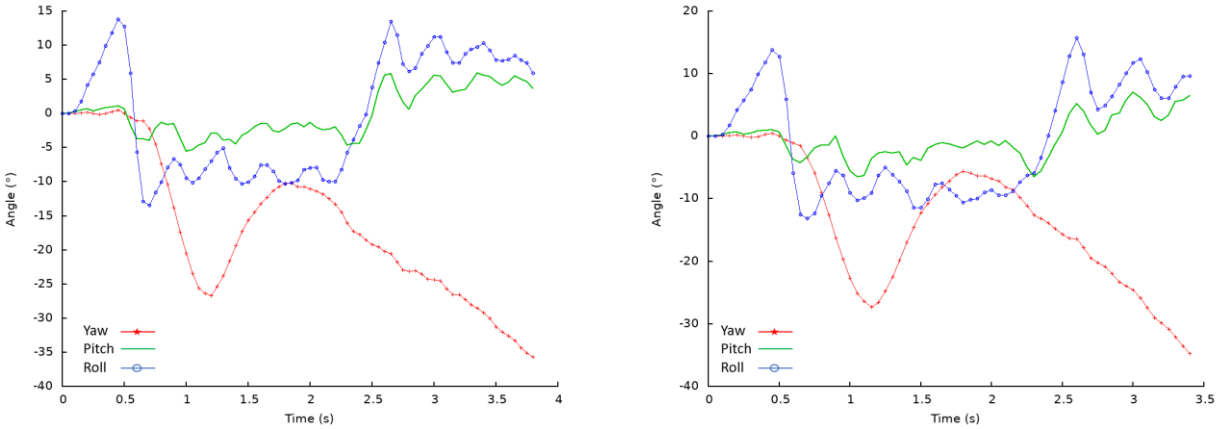

(a) At a post (b) At mid-span

Figure 4.40: Yaw, pitch, and roll angles of the Ford F250 impacting the "Sixth Design Retrofit" from backside.

The maximum dynamic deflections of the "*Sixth Design Retrofit*" were 4.12 m (13.51 ft) and 3.95 m (12.95 ft) during impacts by the Ford F250 at a post and at mid-span, respectively, both from the backside. Figure 4.41 shows the vehicle-barrier interactions at the maximum CMB deflections for both cases for which the overall vehicular responses were similar. In both cases, the vehicle engaged with all three cables and was safely redirected.

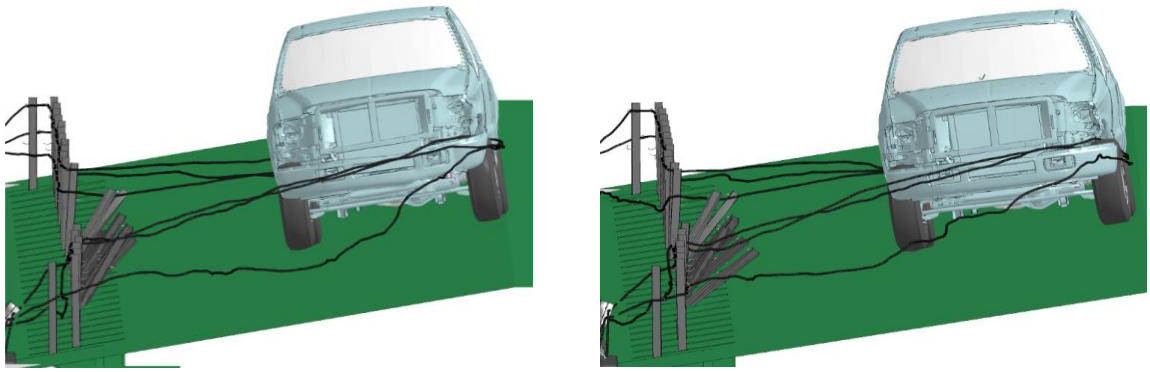

(a) At a post (b) At mid-span

Figure 4.41: Vehicle-barrier interactions for Ford F250 impacting the "Sixth Design Retrofit" from backside.

Figure 4.42 shows the time histories of transverse velocities measured at the CG point of the Ford F250 impacting the backside of the "*Sixth Design Retrofit*" at a post and at mid-span, respectively. The transverse velocities of the Ford F250 were approximately 10 km/hr (6.2 mph) after being redirected for the both cases, indicating a small chance of getting involved in a secondary collision.

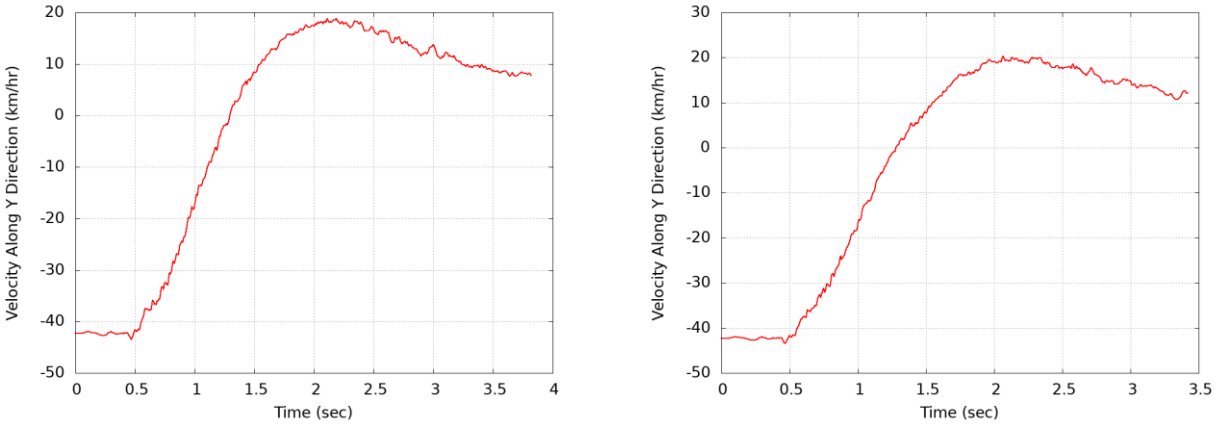

(a) At a post (b) At mid-span

Figure 4.42: Transverse velocities of the Ford F250 impacting the "Sixth Design Retrofit" from backside.

Based on the above simulation results and analysis, the "*Sixth Design Retrofit*" generally worked well under impacts by the Dodge Neon for both front-side and backside impacts, except for one case in which the MASH exit box criterion was not met when impacting the CMB at a post from the front-side. Under impacts by the FORD F250, the "*Sixth Design Retrofit*" met the MASH exit box criterion and MASH evaluation criterion *F* in the two backside impact cases, but failed to prevent the Ford F250 from penetrating in the two front-side impact cases due to vehicle overriding.

4.3 Case 3: Evaluation of the "*Four-cable Design Retrofit*"

In this section, the "*Four-cable Design Retrofit*" was evaluated based on MASH TL-3 conditions. Table 4.5 gives a summary of simulations results on the performance of this design in terms of vehicular responses.

Table 4.5: Summary of simulation results for Case 3

Test Vehicle	Impact Side	Impact Location	Vehicular Responses
Dodge Neon	Front-side	Post	The vehicle passed the exit box criterion and was safely redirected
		Mid-span	The vehicle passed the exit box criterion and was safely redirected
	Back-side	Post	The vehicle remained in contact with the CMB
		Mid-span	The vehicle remained in contact with the CMB
Ford F250	Front-side	Post	The vehicle passed the exit box criterion and was safely redirected
		Mid-span	The vehicle passed the exit box criterion and was safely redirected
	Back-side	Post	The vehicle was redirected but failed to meet the MASH exit box criterion by a small margin
		Mid-span	The vehicle was redirected but failed to meet the MASH exit box criterion by a small margin

4.3.1 Dodge Neon Impacts from the Front-side

Figures 4.43 and 4.44 show the top-view vehicle trajectories of the Dodge Neon impacting the front-side of the "Four-cable Design Retrofit" at a post and mid-span, respectively. It can be seen that the MASH exit box criterion was met in both impact cases and that the vehicle was redirected with small exit angles.

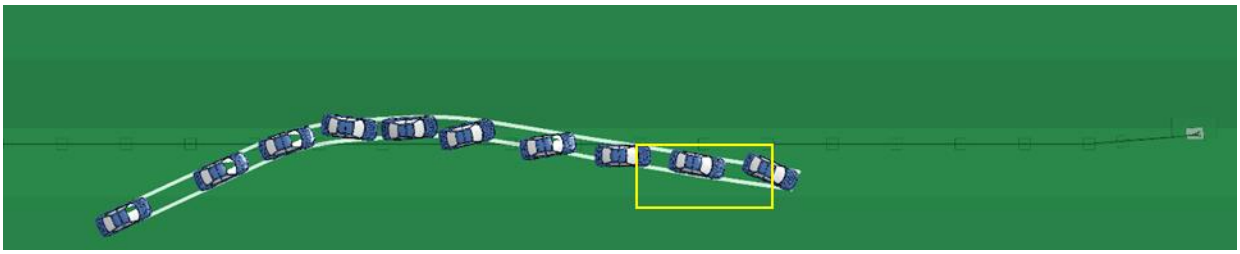

Figure 4.43: A Dodge Neon impacting the "Four-cable Design Retrofit" at a post from front-side.

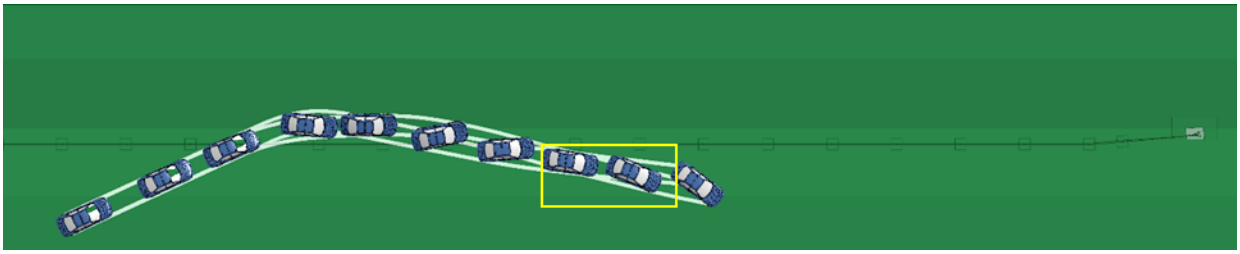

Figure 4.44: A Dodge Neon impacting the "Four-cable Design Retrofit" at mid-span from front-side.

The maximum dynamic displacements of the "*Four-cable Design Retrofit*" were 2.39 m (7.84 ft) and 2.55 m. (8.36 ft) under impacts by the Dodge Neon from the front-side at a post and at mid-span, respectively. Figure 4.45 shows the barrier-vehicle interactions at the maximum dynamic displacements. It can be seen that in both cases, the vehicle engaged with the top two cables and was successfully redirected.

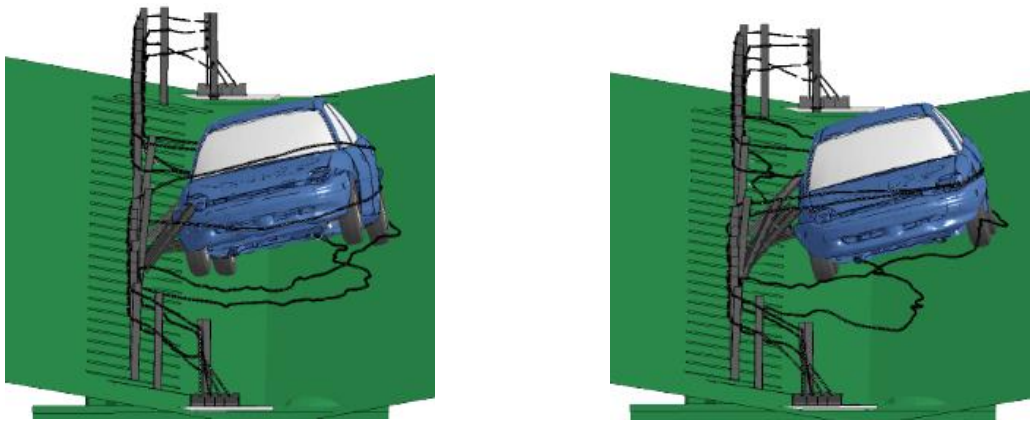

(a) At a post (b) At mid-span

Figure 4.45: Vehicle-barrier interactions at the maximum dynamic displacements for Dodge Neon impacting the "Four-cable Design Retrofit" from front-side.

The yaw, pitch, and roll angles of the Dodge Neon impacting the "*Four-cable Design Retrofit*" from front-side are shown in Figure 4.46. The exit angles were determined to be 5° and 7° for impacting at a post and at mid-span, respectively. The roll and pitch angles were less than 15° for both impact cases, passing the MASH evaluation criterion *F*, which specified a maximum of 75° roll or pitch angle.

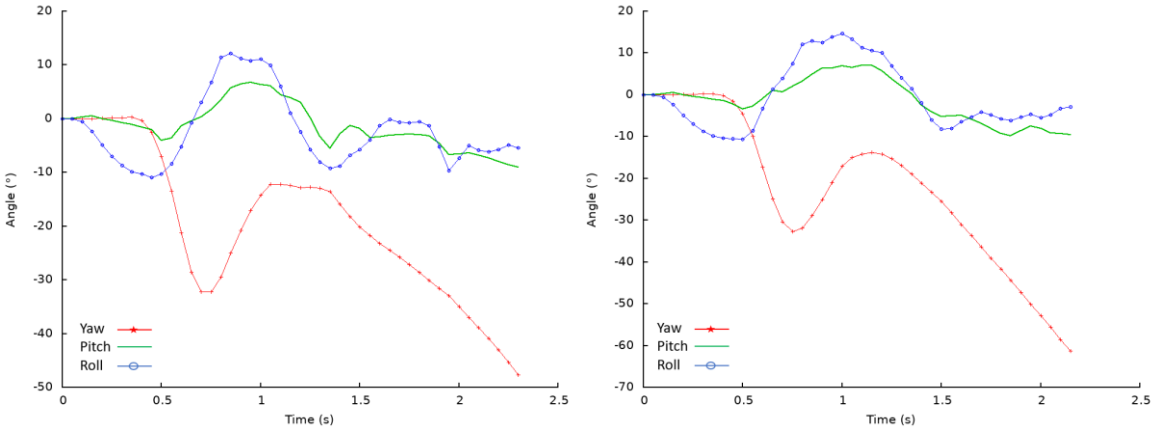

(a) At a post (b) At mid-span

Figure 4.46: Yaw, pitch, and roll angles of Dodge Neon impacting the "Four-cable Design Retrofit" from front-side.

Figure 4.47 shows the time histories of transverse velocities measured at the CG point of the Dodge Neon impacting the "*Four-cable Design Retrofit*" from the front-side. In both cases, the transverse velocities were less than 15 km/hr (9.32 mph) after the vehicle was redirected, indicating a relatively small chance of getting involved in a secondary collision.

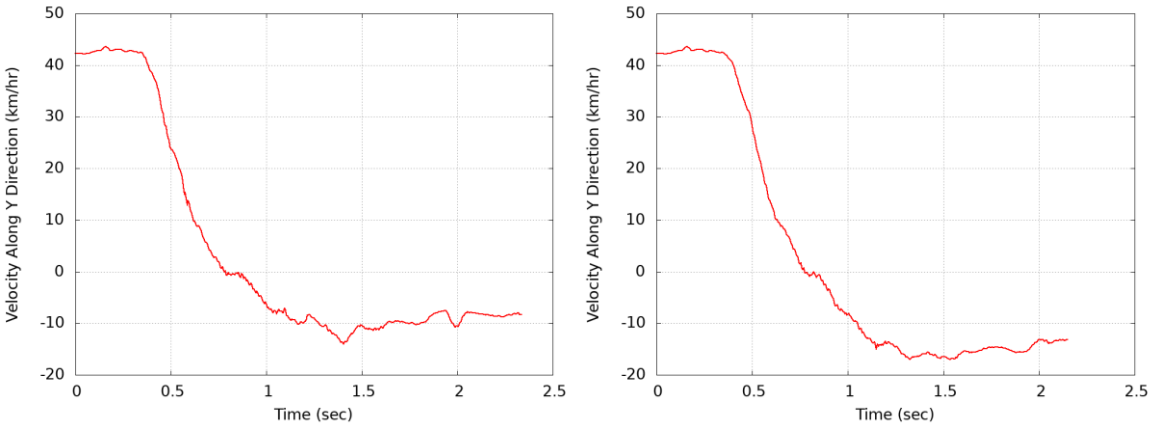

(a) At a post (b) At mid-span

Figure 4.47: Transverse velocities of the Dodge Neon impacting the "Four-cable Design Retrofit" from front-side.

4.3.2 Dodge Neon Impacts from the Backside

For impacts by the Dodge Neon on the "*Four-cable Design Retrofit*" from the backside, the top view vehicle trajectories are shown in Figures 4.48 and 4.49 for impacts at a post and at mid-span, respectively. In both cases, the vehicle was safely redirected and retained. Since the vehicle remained in contact with the CMB, the MASH exit box criterion was not applicable.

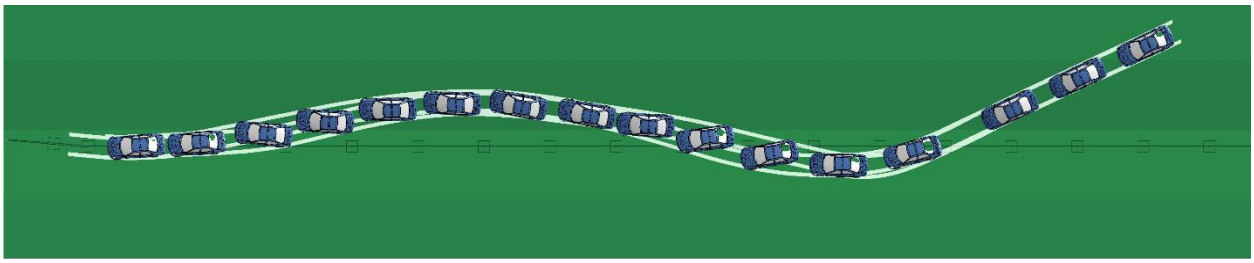

Figure 4.48: A Dodge Neon impacting the "Four-cable Design Retrofit" at a post from backside.

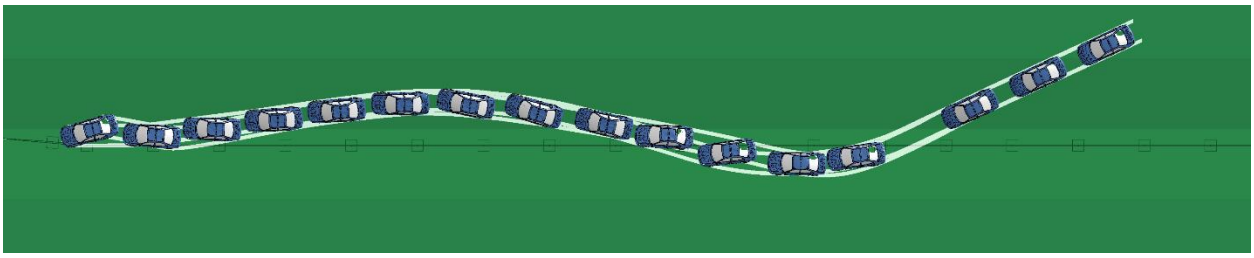

Figure 4.49: A Dodge Neon impacting the "Four-cable Design Retrofit" at mid-span from backside.

The maximum dynamic displacements of the "*Four-cable Design Retrofit*" were 2.94 m (9.64 ft) and 2.78 m (9.12 ft) when impacted by the Dodge Neon from the backside at a post and at mid-span, respectively. Figure 4.50 shows the vehicle-barrier interactions at the maximum dynamic displacements in both cases. In the impact at the post, the vehicle fully engaged with the three lower cables, while the vehicle engaged with one cable in the impact at mid-span. It was also observed that at the maximum dynamic displacements, the vehicle was also redirected in both impact cases.

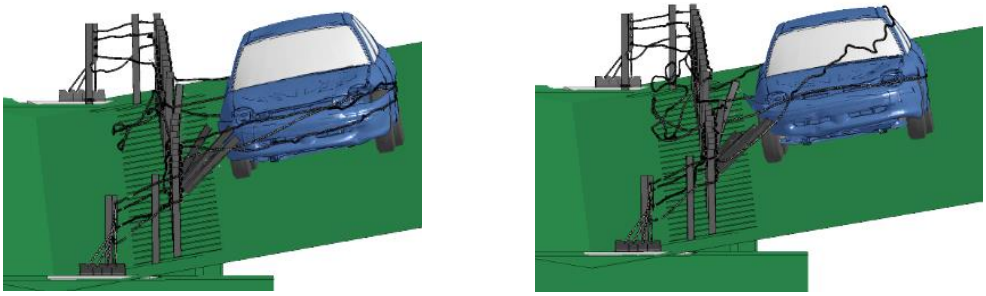

(a) At a post (b) At mid-span

Figure 4.50: Vehicle-barrier interactions at the maximum dynamic displacements for Dodge Neon impacting the "Four-cable Design Retrofit" from backside.

Figure 4.51 shows the yaw, pitch, and roll angles of the Dodge Neon impacting the "*Four-cable Design Retrofit*" from the backside. The pitch and roll angles were less than 15° in both positive and negative directions, passing the MASH evaluation criterion *F*.

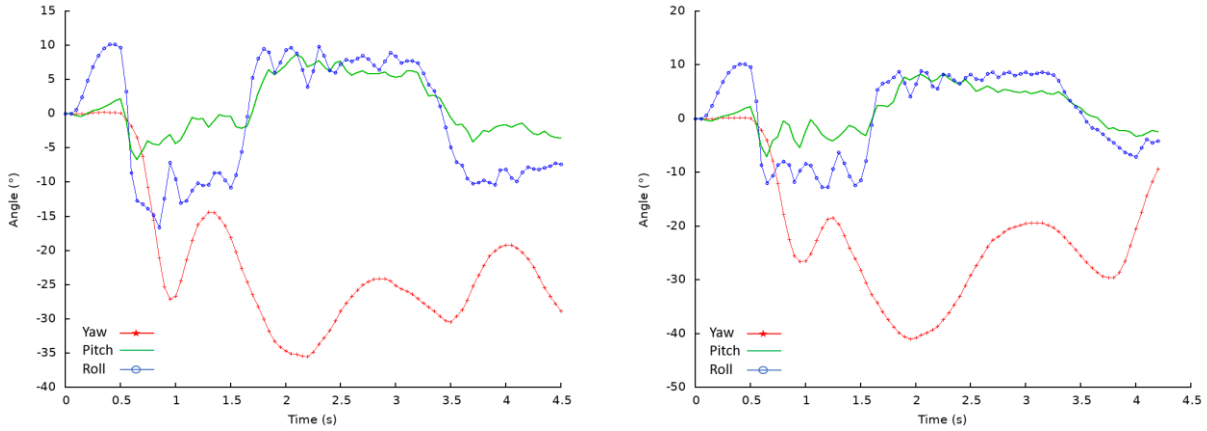

(a) At a post (b) At mid-span

Figure 4.51: Yaw, pitch, and roll angles of the Dodge Neon impacting the "Four-cable Design Retrofit" from backside.

Figure 4.52 shows the time histories of transverse velocities measured at the CG point of the Dodge Neon impacting the "Four-cable Design Retrofit" from the backside. The transverse velocities of the Dodge Neon were less than 5 km/hr (3.2 mph) for both cases, indicating a small chance of getting involved in a secondary collision.

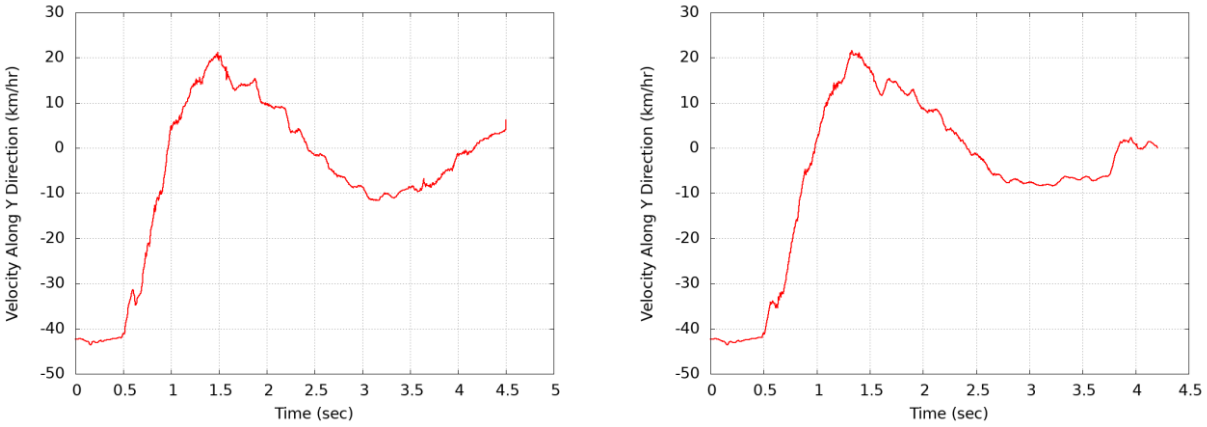

(a) At a post (b) At mid-span

Figure 4.52: Transverse velocities of the Dodge Neon impacting the "Four-cable Design Retrofit" from backside.

4.3.3 Ford F250 Impacts from the Front-side

Figures 4.53 and 4.54 show the top-view vehicle trajectories of the Ford F250 impacting the "*Four-cable Design Retrofit*" from the front-side at a post and at mid-span, respectively. In both cases, the vehicle was redirected, and the MASH exit box criterion was met.

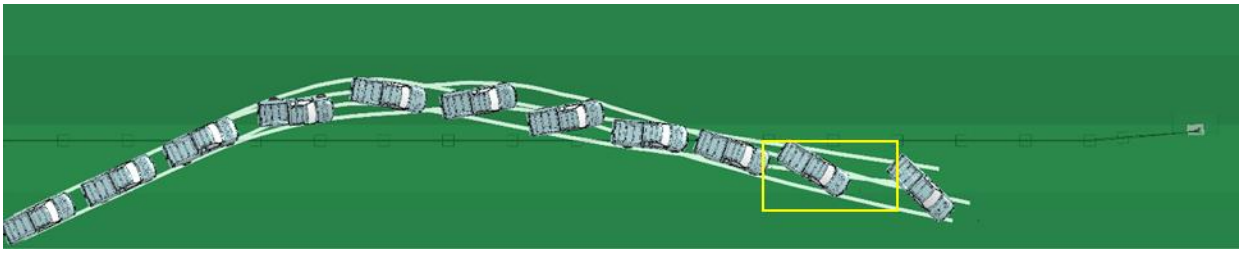

Figure 4.53: A Ford F250 impacting the "Four-cable Design Retrofit" at a post from front-side.

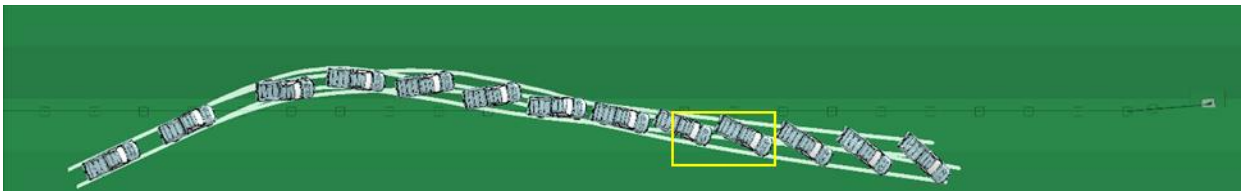

Figure 4.54: A Ford F250 impacting the "Four-cable Design Retrofit" at mid-span from front-side.

The maximum dynamic displacements of the "*Four-cable Design Retrofit*" were 4.8 m (15.75 ft) and 4.4 m (13.12 ft) under impacts by the Ford F250 from front-side at a post and at mid-span, respectively. Figure 4.55 shows the vehicle-barrier interactions at the maximum displacements of the CMB. On both cases, the vehicle engaged with two cables and was redirected.

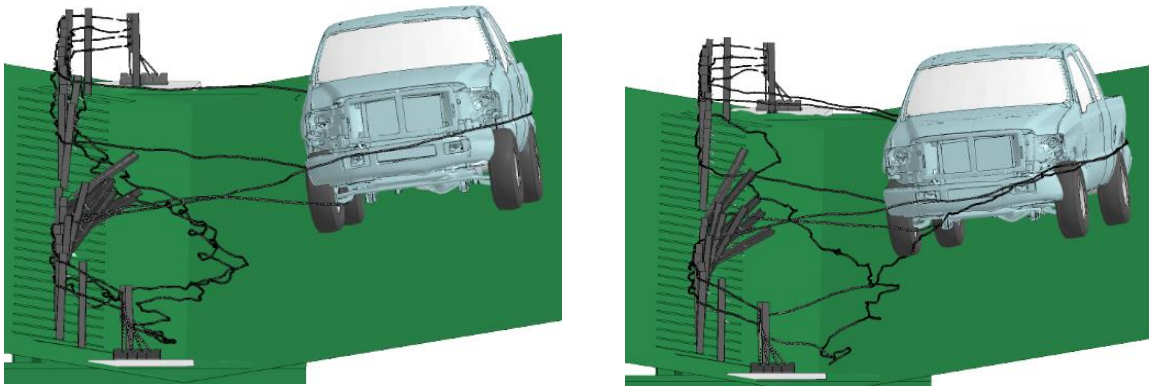

(a) At a post (b) At mid-span

Figure 4.55: Vehicle-barrier interactions at the maximum dynamic displacements for Ford F250 impacting the "Four-cable Design Retrofit" from front-side.

Figure 4.56 shows the yaw, pitch, and roll angles of the Ford F250 impacting the "*Four-cable Design Retrofit*" from the front-side. The exit angles were determined to be 12° and 11° for impacts at a post and at mid-span, respectively. In both impact cases, the roll and pitch angles were less than 15° in both positive and negative directions, passing the MASH evaluation criterion *F*.

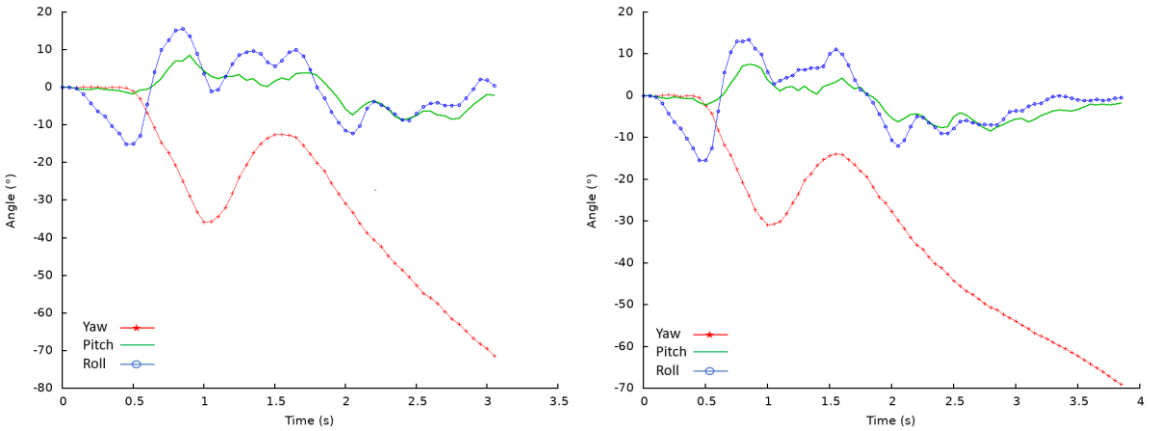

(a) At a post (b) At mid-span

Figure 4.56: Yaw, pitch, and roll angles of the Ford F250 impacting the "Four-cable Design Retrofit" from front-side.

Figure 4.57 shows the time histories of transverse velocities measured at the CG point of the Ford F250 impacting the "*Four-cable Design Retrofit*" from the front-side. The transverse velocities were less than 15 km/hr (9.2 mph) for the both cases, indicating a relatively small chance of getting involved in a secondary collision.

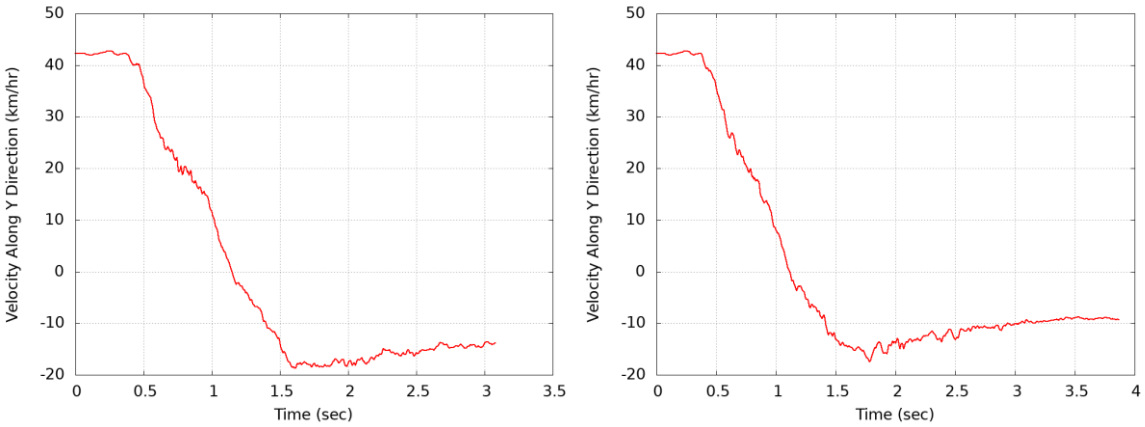

(a) At a post (b) At mid-span

Figure 4.57: Transverse velocities of the Ford F250 impacting the "Four-cable Design Retrofit" from front-side.

4.3.4 Ford F250 Impacts from the Backside

Figures 4.58 and 4.59 show the top-view vehicle trajectories of the Ford F250 impacting the "*Four-cable Design Retrofit*" from backside at a post and at mid-span, respectively. In both cases, the vehicle was redirected, but failed to meet the MASH exit box criterion by a small margin. It should be noted that in both cases, the vehicle turned towards the barrier after leaving the exit box, meaning that the vehicle would remain in the median and would not cause a secondary collision.

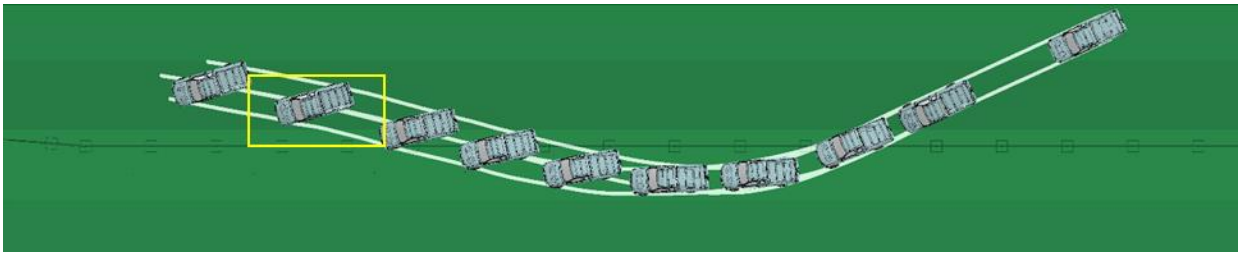

Figure 4.58: A Ford F250 impacting the "Four-cable Design Retrofit" at a post from backside.

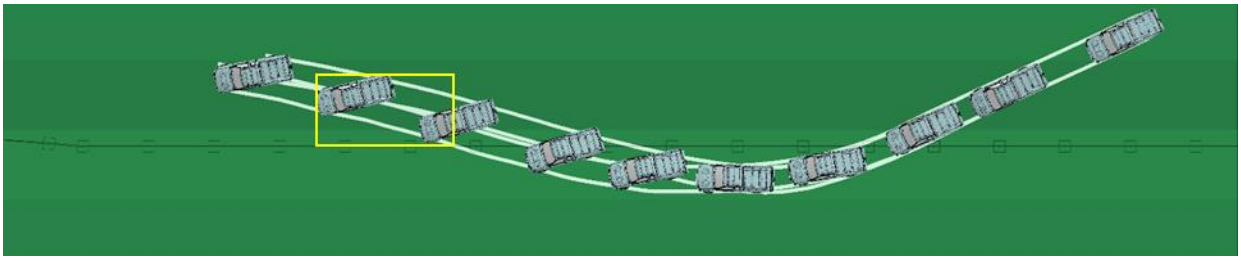

Figure 4.59: A Ford F250 impacting the "Four-cable Design Retrofit" at mid-span from backside.

The maximum dynamic displacements of the "*Four-cable Design Retrofit*" were 3.6 m (11.81 ft) and 3.47 m (11.38 ft) when impacted at a post and at mid-span, respectively, by the Ford F250 from backside. Figure 4.60 shows the vehicle-barrier interactions at the maximum displacements for both impact cases. It can be seen that the vehicle engaged with all four cables and was successfully redirected in both cases.

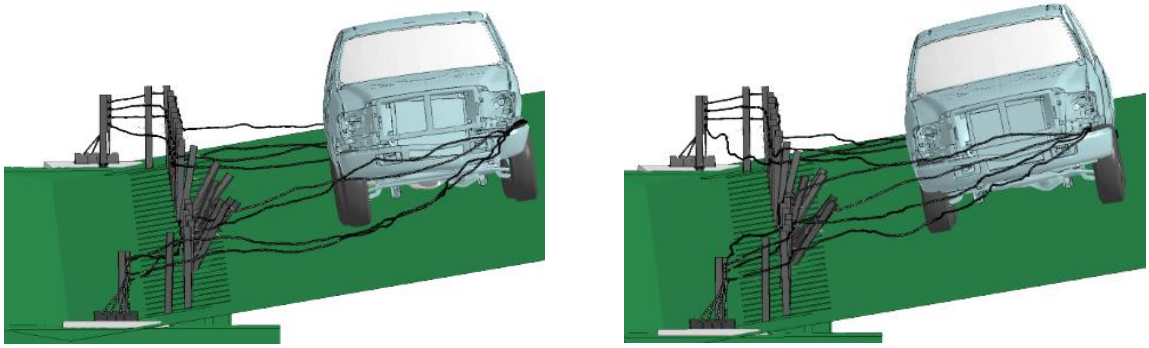

(a) At a post (b) At mid-span

Figure 4.60: Vehicle-barrier interactions at the maximum dynamic displacements for Ford F250 impacting the "Four-cable Design Retrofit" from backside.

The yaw, pitch, and roll angles of the Ford F250 impacting the "Four-cable Design Retrofit" from backside are given in Figure 4.61. In both impact cases, the exit angles were determined to be 12° for the impact at a post and 14° for the impact at mid-span. These relatively low exit angles of the vehicle indicated that the chances of getting involved in a secondary collision were relatively small even though the exit box criterion was not met. The roll and pitch angles were less than 15° in both positive and negative directions, passing the MASH evaluation criterion *F*, which specified a maximum of 75° roll or pitch angle.

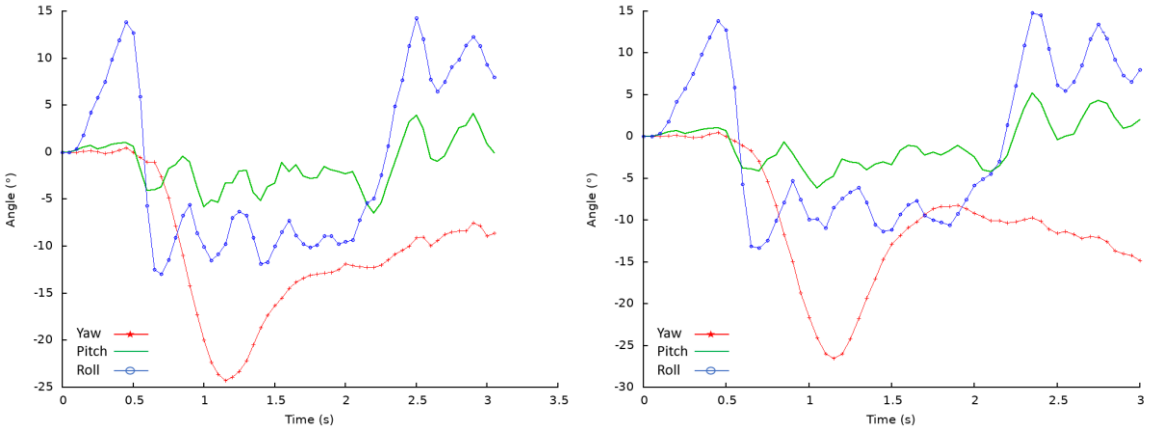

(a) At a post (b) At mid-span

Figure 4.61: Yaw, pitch, and roll angles of the Ford F250 impacting the "Four-cable Design Retrofit" from backside.

Figure 4.62 shows the time histories of the transverse velocities measured at the CG point of the Ford F250 impacting the "*Four-cable Design Retrofit*" from backside. The transverse velocities were approximately 12 km/hr (7.46 mph) after the vehicle was redirected in the both cases, indicating a small chance of getting involved in a secondary collision.

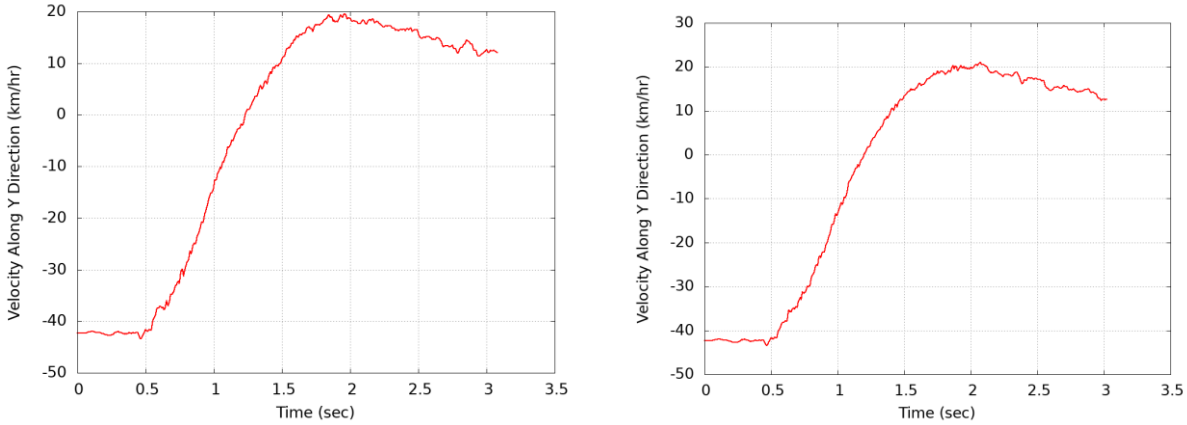

(a) At a post (b) At mid-span

Figure 4.62: Transverse velocities of the Ford F250 impacting the "Four-cable Design Retrofit" from backside.

4.4 Comparison of All Three CMB Designs Placed on a 6H:1V Sloped Median

In Sections 4.1 to 4.3, the performance of the current CMB design, the "*Sixth Design Retrofit*," and the "*Four-cable Design Retrofit*" were evaluated on a 6H:1V sloped median and under impacts by a Dodge Neon and Ford F250 from both the front-side and backside. In this section, the three CMB designs were compared side by side so the overall performance of each design can be easily determined. Tables 4.6 and 4.7 summarize the simulation results of impacts on the three CMB designs by the Dodge Neon and Ford F250, respectively. The MASH evaluation criteria used in Tables 4.6 and 4.7 are summarized as follows:

MASH Evaluation Criterion A:	*The Article should contain and redirect the vehicle or bring the vehicle to a controlled stop, the vehicle should not penetrate, underride, or override the installation although controlled lateral deflection of the test article is acceptable.*
MASH Evaluation Criterion D:	*Detached elements, fragments, or other debris from the test article should not penetrate or show potential for penetrating the occupant compartment, or present undue hazard to other traffic, pedestrians, or personnel in a work zone.*
MASH Evaluation Criterion F:	*The vehicle should remain upright during and after collision. The maximum roll and pitch angles are not to exceed 75 degrees.*

It can be seen from Table 4.6 that under impacts by the Dodge Neon, the two retrofit designs performed better than the current CMB design. In the two backside impact cases on the current CMB design, the vehicle penetrated the CMB and thus failed to meet the MASH exit box criterion and the Evaluation Criterion *A*. The "*Four-cable Design Retrofit*" met all the MASH requirements and performed better than the "*Sixth Design Retrofit*," which failed to meet the MASH exit box criterion in one case. In the two backside impact cases on the "*Four-cable Design Retrofit*", the vehicle remained in contact with the CMB and the MASH exit box criterion was not needed.

Under impacts by the Ford F250, the current CMB design failed the MASH Evaluation Criterion A in the two backside impact cases, and the "*Sixth Design Retrofit*" failed to meet the MASH exit box criterion and Evaluation Criterion *A* due to vehicle penetration in the two front-side impact cases. The "*Four-cable Design Retrofit*" was capable of redirecting the Ford F250 in both front-side and backside impacts, and meet with all the MASH evaluation criteria except for the two backside impact cases in which the MASH exit box criterion was not met by a small margin. Considering the relatively small exit angles, transverse displacements, transverse velocities, and passing all other criteria, the "*Four-cable Design Retrofit*" was considered to be safe in the four impacts by the Ford F250.

Table 4.6: Summary of simulation results for Dodge Neon

CMB Design	Impact Side	Impact Location	Vehicle Response	MASH Evaluation Criteria				
				Exit Box	Exit Angle	A	D	F
The Current Design	Front-side	Post	RD	P	6°	P	P	P
		Mid-span	RD	P	5°	P	P	P
	Backside	Post	PE	F	N/A	F	P	P
		Mid-span	PE	F	N/A	F	P	P
The "*Sixth Design Retrofit*"	Front-side	Post	RD	F	54°	P	P	P
		Mid-span	RD	P	7°	P	P	P
	Backside	Post	RD	P	12°	P	P	P
		Mid-span	RD	P	7°	P	P	P
The "*Four-cable Design Retrofit*"	Front-side	Post	RD	P	5°	P	P	P
		Mid-span	RD	P	7°	P	P	P
	Backside	Post	RC	N/A	N/A	P	P	P
		Mid-span	RC	N/A	N/A	P	P	P

* Notations:
  – Vehicular Responses: **RD**: Redirected, **PE**: Penetrated, **RC**: Remained in Contact
  – Evaluation Criteria A, D, F: **P**: Pass, **F**: Fail
  – Exit Box Criterion: **P**: Pass, **F**: Fail, **N/A**: Not Applicable
  – Exit Angle: **N/A**: Not Applicable

Table 4.7: Summary of simulation results for Ford F250

CMB Design	Impact Side	Impact Location	Vehicle Response	MASH Evaluation Criteria				
				Exit Box	Exit Angle	A	D	F
The Current Design	Front-side	Post	RC	N/A	N/A	P	P	P
		Mid-span	RD	P	7°	P	P	P
	Backside	Post	RD	P	13°	F	P	P
		Mid-span	RD	P	12°	F	P	P
The Sixth Design Retrofit	Front-side	Post	PE	F	N/A	F	P	P
		Mid-span	PE	F	N/A	F	P	P
	Backside	Post	RD	P	7°	P	P	P
		Mid-span	RD	P	9°	P	P	P
The Four-cable Design Retrofit	Front-side	Post	RD	P	12°	P	P	P
		Mid-span	RD	P	11°	P	P	P
	Backside	Post	RD	F §	12°	P	P	P
		Mid-span	RD	F §	14°	P	P	P

* Notations:
  – Vehicular Responses: **RD**: Redirected, **PE**: Penetrated, **RC**: Remained in Contact
  – Evaluation Criteria A, D, F: **P**: Pass, **F**: Fail
  – Exit Box Criterion: **P**: Pass, **F**: Fail, **N/A**: Not Applicable
  – Exit Angle: **N/A**: Not Applicable

§: In these impact cases, the exit box criterion was slightly violated.

5. Findings and Conclusions

In this project, finite element (FE) modeling and simulations were used to evaluate the performance of the current NCDOT cable median barrier (CMB) design with two retrofit CMB designs, namely the "*Sixth Design Retrofit*" and the "*Four-cable Design Retrofit*." All three CMB designs were evaluated on a 6H:1V sloped median and under MASH TL-3 conditions, i.e., under impacts by a passenger car and a pick-up truck at 100 km/hr (62 mph) and a 25° angle. A 1996 Dodge Neon and a 2006 Ford F250 were selected as the test vehicles, which impacted the three CMBs from the front-side and backside at a post and at mid-span. A total of 24 simulations were run and the vehicular responses were obtained on exit angles, yaw, pitch and roll angles, and residual transverse velocities. The performance of the CMBs were evaluated based on the abovementioned vehicular responses as well as the MASH exit box criterion and the MASH Evaluation Criteria *A, D,* and *F*. The simulation results also provided insights into the vehicles' redirection characteristics. Some of the major research findings were summarized as follows:

- Under impacts by the Dodge Neon from the front-side, the current CMB design was capable of redirecting the vehicle and satisfying the MASH requirements. For backside impacts by the Dodge Neon, the current CMB design failed to stop the vehicle from penetrating the CMB and failed to pass the MASH exit box criterion and MASH Evaluation Criterion *A*. This penetration on the CMB in the backside impacts by the Dodge Neon was consistent with previous research findings as well as field observations. Under impacts by the Dodge Neon, both the "*Sixth Design Retrofit*" and the "*Four-cable Design Retrofit*" could redirect the vehicle, though the "*Sixth Design Retrofit*" failed to pass the MASH exit box criterion in one of the front-side impact cases. The "*Four-cable Design Retrofit*" met all MASH requirements in both front-side and backside impacts by the Dodge Neon and thus outperform the other two CMB designs.

- Under impacts by the Ford F250, the "*Sixth Design Retrofit*" failed to stop the vehicle from penetrating the CMB in front-side impacts and thus failed to pass the MASH exit box criterion and MASH Evaluation Criterion *A*. The current CMB design could redirect or retain the vehicle in both front-side and backside impacts, but failed to pass the MASH Evaluation Criterion *A* in the two backside impacts. The "*Four-cable Design Retrofit*" could redirect the vehicle in both front-side and backside impacts and pass all MASH criteria except for the two backside impact cases in which the MASH exit box criterion was violated by a small margin. Considering vehicular responses and all MASH criteria, the four impact cases for the "*Four-cable Design Retrofit*" were considered safe and the "*Four-cable Design Retrofit*" was determined to outperform the other two CMB designs.

- The simulation results showed that cable heights affected the vehicle-cable engagements and thus the CMB performance when placed on a 6H:1V sloped median. For example, lowering the middle and bottom cables could prevent vehicle penetration for backside impacts by the Dodge Neon (as seen in the "*Sixth Design Retrofit*" compared to the current design), but caused the Ford F250 to penetrate the CMB in front-side impacts (as seen in in the "*Sixth Design Retrofit*" compared to the current design). To this end, adding a fourth cable to the current CMB design, i.e., the "Four-cable Design Retrofit," was shown to be effective for impacts by both a small and large vehicles: preventing the Dodge Neon from

penetrating the CMB from backside, and preventing the Ford F250 from penetrating from backside.

In summary, the simulation results suggested that replacing the current CMB design with the "*Four-cable Design Retrofit*" could improve the CMB performance on a 6H:1V sloped median under impacts at MASH TL-3 conditions. It should be noted that the simulation results of this project can be used to interpret the performance trends of CMB designs. They should not be used to draw definitive conclusions about the CMB performance for a specific crash event because some factors, e.g., soil conditions and driver behaviors, that could affect the performance were not considered in the simulations of this project. Nevertheless, finite element analysis was demonstrated to be a useful tool in crash analysis and could be used in future investigations of other research issues.

6. Recommendations

Based on the simulation results of this project, it was determined that the "*Four-cable Design Retrofit*" could safely redirect or retain the vehicles when placed on a 6H:1V sloped median and impacted by a Dodge Neon and Ford F250 from both front-side and backside. Therefore, the "*Four-cable Design Retrofit*" was recommended to be crash tested so that it can be used to replace the current design when deemed necessary by NCDOT officials.

7. Implementation and Technology Transfer Plan

The simulation results of this project will be submitted to NCDOT for consideration in future projects to install or retrofit cable median barriers when allowed by site conditions and deemed necessary by NCDOT personnel. Detailed simulation results will be provided to NCDOT engineers for a comprehensive understanding in evaluating proposed roadside features and/or improving the safety performance of the current system. The modeling and simulation work, along with research findings, will be presented at technical conferences and submitted for publication in technical journals to help researchers and DOT engineers nationwide with similar needs. The research results of this project will be distributed to the public through this report, which will be made available by NCDOT.

References

1. AASHTO (2006). *Roadside Design Guide*, 3rd edition, American Association of State Highway and Transportation Officials, Washington, D.C.
2. Abdel-Aty, M., Pemmanaboina, R., and Hsia, L. (2006). "Assessing crash occurrence on urban freeways by applying a system of interrelated equations," *Transportation Research Record*, 1953, 1-9.
3. Alberson, D.C., Bligh, R.P., Buth, C.E., and Bullard, D.L., Jr. (2003). "Cable and wire rope barrier design considerations: review," *Transportation Research Record*, 1851, 95-104.
4. Alberson, D.C., Sheikh, N.M., and Chatham, L.S. (2007). "Guidelines for the selection of cable barrier systems," *NCHRP 20-7 (210) Final Report*, Transportation Research Board, National Research Council, Washington, D.C.
5. Albin, R. B., Bullard, D. L., and Menges, W. L. (2001). "Washington State cable median barrier," *Transportation Research Record*, 1743, 71-79.
6. Alluri, P., Haleem, K., Gan, A., and Mauthner, J. (2015). "Safety performance evaluation of cable median barriers on freeways in Florida", *Traffic Injury Prevention*, DOI: 10.1080/15389588.2015.1101079
7. Atahan, A.O. (2002). "Finite element simulation of a strong-post W-beam guardrail system," *Simulation*, 78(10), 587-599.
8. Atahan, A.O. (2003). "Impact behavior of G2 steel weak-post W-beam guardrail on nonlevel terrain," *International Journal of Heavy Vehicle Systems*, 10(3), 209-223.
9. Atahan, A.O. (2007). "Crashworthiness analysis of a bridge rail-to-guardrail transition," *Accident Analysis and Prevention*, in press.
10. Atahan, A.O., and Cansiz, O.F. (2005). "Crashworthiness analysis of a bridge rail-to-guardrail transition," *Finite Elements in Analysis and Design*, 41, 371-396.
11. Bi, J., Fang, H., and Weggel, D.C. (2010). "Finite element modeling of cable median barriers under vehicular impacts," *The 11th International Conference on Structures under Shock and Impact*, Tallinn, Estonia, July 28-30.
12. Bligh, R.P., Abu-Odeh, A.Y., Hamilton, M.E., and Seckinger, N.R. (2004). "Evaluation of roadside safety devices using finite element analysis," *Report 0-1816-1*, Texas Transportation Institute, College Station, TX.
13. Bligh, R.P., and Mak, K.K. (1999). "Crashworthiness of roadside features across vehicle platforms," *Transportation Research Record*, 1690, 68-77.
14. Bligh, R.P., Miaou, S.P., Lord, D., and Cooner, S. (2006). "Median barrier guidelines for Texas," *Report 0-4254-1*, Texas Transportation Institute, College Station, TX.
15. BMI-SG (2004). "Improved Guidelines for Median Safety," *NCHRP 17-14(2) Draft Report of Analysis Findings*, Transportation Research Board, National Research Council, Vienne, VA.
16. Bullard, D.L., and Menges, W.L. (1996). "Crash testing and evaluation of the WSDOT three strand cable rail system," Texas Transportation Institute, College Station, TX.
17. Bullard, D.L., and Menges, W.L. (2000). "NCHRP Report 350 Test 3-11 of the Washington three-strand cable barrier with New York cable terminal," Texas Transportation Institute, College Station, TX.

18. Caliendo, C., Guida, M., and Parisi, A. (2007). "A crash-prediction model for multilane roads," *Accident Analysis and Prevention*, 39, 657-670.

19. Choi, J., Kim, S., Heo, T.Y., and Lee, J. (2010). "Safety effects of highway terrain types in vehicle crash model of major rural roads," *KSCE Journal of Civil Engineering*, 15(2), 405-412.

20. Donnell, E.T., Harwood, D.W., Bauer, K.M., Mason, J.M., and Pietrucha, M.T. (2002). "Cross-median collisions on Pennsylvania interstates and expressways," *Transportation Research Record*, 1784, 91-99.

21. ESI (2003). *PAM-CRASH Solver Reference Manual, v2003.1*, ESI Group.

22. Fang, H., Wang, Q., and Weggel, D.C. (2015). "Crash analysis and evaluation of cable median barriers on sloped medians using an efficient finite element model," *Advances in Engineering Software*, 82, 1-13.

23. Fang, H., Li., N., DiSogra, M., and Gutowski, M. (2012). "Recommendations for placement cable median barriers on 6:1 and 4:1 sloped median with horizontal curvatures." *NCDOT, Final Report, FHWA/NC-2011-09.*

24. Gabauer, D.J. and Gabler, H.C. (2009). "Differential rollover risk in vehicle-to-traffic barrier collisions," *Annals of Advances in Automotive Medicine*, Vol. 53.

25. Gabler, H.C., Gabauer, D.J., and Bowen, D. (2005). "Evaluation of cross median crashes," *Final Report FHWA-NJ-2005-004*, Rowan University, Glassboro, NJ.

26. Gutowski, M., Palta, E., and Fang, H. (2017a). "Crash analysis and evaluation of vehicular impacts on W-beam guardrails placed behind curbs using finite element simulations," *Advances in Engineering Software*, 114, 85-97.

27. Gutowski, M., Palta, E., and Fang, H. (2017b). "Crash analysis and evaluation of vehicular impacts on W-beam guardrails placed on sloped medians using finite element simulations," *Advances in Engineering Software*, 112, 88-100.

28. Hiser, N.R., and Reid, J.D. (2005). "Modeling slip base mechanisms," *International Journal of Crashworthiness*, 10(5), 463-472.

29. Hiss, J.G. F., Jr., and Bryden, J.E. (1992). "Traffic barrier performance," *Report 155*, New York State Department of Transportation, Albany, NY.

30. Hu, W. and Donnell, E.T. (2010). "Median barrier crash severity: Some new insights," *Accident Analysis and Prevention*, 42, 1697-1704.

31. Hunter, W.W., Stewart, J.R., Eccles, K.A., Huang, H.F., Council, F.M., and Harkey, D.L. (2001). "Three-strand cable median barrier in North Carolina: in-service evaluation," *Transportation Research Record*, 1743, 97-103.

32. Jehu, V. J. (1968). "Paper 1: Crash Barrier Developments," *Proceedings of the Institution of Mechanical Engineers*, 183 (1), 93-101.

33. Kan, C.D., Marzougui, D., Bahouth, G.T., and Bedewi, N.E. (2001). "Crashworthiness evaluation using integrated vehicle and occupant finite element models," *International Journal of Crashworthiness*, 6, 387-398.

34. Lewis, B. A. (2004). "Manual for LS-DYNA soil material model 147," *FHWA-HRT-04-095*, U.S. Department of Transportation, Federal Highway Administration, McLean, VA.

35. Li, N., Fang, H., Zhang, C., Gutowski, M., Palta, E., and Wang, Q. (2015). "A numerical study of occupant responses and injuries in vehicular crashes into roadside barriers based on finite element simulations," *Advances in Engineering Software*, 90, 22-40.

36. LSTC (2007). *LS-DYNA Keyword User's Manual, version 971*, Livermore Software Technology Corporation (LSTC), Livermore, CA.

37. Lu, G., Chitturi, M.V., Ooms, A.W. and Noyce, D.A. (2010). "Ordinal discrete choice analyses of wisconsin cross-median crash severities," *Transportation Research Record*, 2148, 47-58.

38. Lynch, J.M., Crowe, N.C., and Rosendahl, J.F. (1993). "Interstate across median accident study: a comprehensive study of traffic accidents involving errant vehicles which cross the median divider strips on North Carolina interstate highways," *In: 1993 AASHTO Annual Meeting Proceedings*, Publisher American Association of State Highway and Transportation Officials, 125-133.

39. MacDonald, D.B. and Batiste, J.R. (2007). "Cable Median Barrier - Reassessment and Recommendations," *WSDOT Report*, Washington State Department of Transportation, Olympia, WA.

40. Mackerle, J. (2003). "Finite element crash simulations and impact-induced injuries: an addendum. a bibliography (1998–2002)," *The Shock and Vibration Digest*, 35(4), 273-280.

41. Marzougui, D., Bahouth, G., Eskandarian, A., Meczkowski, L., and Taylor, H. (2000). "Evaluation of portable concrete barriers using finite element simulation," *Transportation Research Record*, 1720, 1-6.

42. Marzougui, D., Kan, C.D., and Opiela, K. (2010). "Comparison of the crash test and simulation of an angle impact of a 2007 Chevrolet Silverado pick-up truck into a New Jersey-shaped concrete barrier for MASH conditions," *The National Crash Analysis Center*, The George Washington University.

43. Marzougui, D., Kan, C.D., McGinnis, R.G., and Opiela, K. (2009). "Analyzing the effects of end-anchor spacing & initial tension on cable barrier deflection using computer simulation," *NCAC 2009-W-007*.

44. Marzougui, D., Mahadevaiah, U., Kan, C.D., Opiela, K. (2009). "Analyzing the effects of cable barriers behind curbs using computer simulation," *NCAC 2009-W-008*.

45. Marzougui, D., Mahadevaiah, U., Tahan, F., Kan, C.D., McGinnis, R., Powers, R. (2012). "Guidance for the selection, use, and maintenance of cable barrier systems," *NCHRP Report 711*, Transportation Research Board, National Research Council, Washington, D.C.

46. Marzougui, D., Mohan, P., Kan, C.D., and Opiela, K. (2007). "Performance evaluation of low-tension three-strand cable median barriers," *Transportation Research Record*, 2025, pp. 34–44.

47. Marzougui, D., Mohan, P., Kan, C.D., and Opiela, K. (2007a). "Performance evaluation of low-tension three-strand cable median barriers," *Transportation Research Record*, to be published.

48. Marzougui, D., Mohan, P., Kan, C.D., and Opiela, K. (2007b). "Evaluation of rail height effects on the safety performance of W-beam barriers," *2007 TRB Annual Meeting*, Washington, D.C.

49. Marzougui, D., Samaha, R.R., Cui, C., and Kan, C.D. (2012). "Extended validation of the finite element model for the 2007 Chevrolet Silverado pick-up truck," *NCAC 2012-W-003*.

50. Marzougui, D., Zink, M., Zaouk, A.K., Kan, C.D., and Bedewi, N.E. (2004). "Development and validation of a vehicle suspension finite element model for use in crash simulations," *International Journal of Crashworthiness*, 9(6), 565-576.

51. MASH-1 (2009). *Manual for Assessing Safety Hardware*, 1st ed., American Association of State and Highway Transportation Officials, Washington, D.C.

52. Medina, J.C. and Benekohal, R.F. (2006) “High Tension Cable Median Barrier: A Scanning Tour Report”.

53. Medina, J.C. and Benekohal, R.F. (2006). “A scanning tour to identify effective and efficient approaches of reducing the number and severity of freeway median crossover crashes,” *Report No, FHWA-IL/UI-TOL-18*, Department of Civil and Environmental Engineering, University of Illinois at Urbana-Champaign.

54. Miaou, S.P., Bligh, R.P., and Lord, D. (2005). “Developing guidelines for median barrier installation: benefit-cost analysis with Texas data,” *Transportation Research Record*, 1904, 3-19.

55. Miaou, S.P., Hu, P.S., Wright, T., Rathi, A.K., and Davis, S.C. (1992). “Relationship between truck accidents and highway geometric design: a poisson regression approach,” *Transportation Research Record*, 1376, 10-18.

56. Mohamedshah, Y.M., Paniati, J.F., and Hobeika, A.G. (1993). “Truck accident models for interstates and two-lane rural roads,” *Transportation Research Record*, 1407, 35-41.

57. Mohan, P., Marzougui, D., and Kan, C.D. (2007). “Validation of a single unit truck model for roadside hardware impact,” *International Journal of Vehicle Systems Modelling and Testing*, 2(1), 1-15.

58. Mohan, P., Marzougui, D., Meczkowski, L., and Bedewi, N. (2005). “Finite element modeling and validation of a 3-strand cable guardrail system,” *International Journal of Crashworthiness*, 10, 267-273.

59. Murphy, B. (2006). “Cable Median Barrier/Rumble Strips in North Carolina,” *In: 57th Annual Traffic and Safety Conference*, Missouri Department of Transportation, Columbia, MO.

60. Murray, Y. D. (2007). “User’s manual for LS-DYNA concrete material model 159,” *FHWA-HRT-05-062*, U.S. Department of Transportation, Federal Highway Administration, McLean, VA.

61. Murray, Y.D., Reid, J.D., Faller, R.K., Bielenberg, B.W., and Paulsen, T.J. (2005). “Evaluation of LS-DYNA Wood Material Model 143,” *FHWA-HRT-04-096*, U.S. Department of Transportation, Federal Highway Administration, McLean, VA.

62. Mussa, R. and Chimba, D. (2006). “Analysis of crashes occurring on Florida six-lane roadways,” *Advances in Transportation Studies*, 8, 43-56.

63. NCAC (web1). “NCAC Finite Element Models,” <*http://www.ncac.gwu.edu/vml/models.html*>.

64. NCAC. (web2). “NCAC Publications,” <*http://www.ncac.gwu.edu/filmlibrary/publications.html*>.

65. NCDOT (2002). *Roadway design manual*, North Carolina Department of Transportation, Raleigh, NC.

66. NCDOT (2005). “Median Barriers in North Carolina – Long Term Evaluation,” *NCDOT Safety Evaluation Group*, Traffic Safety Systems Management Section, AASHTO TIG Initiative for “Cable Median Barrier” (TIG-CMB), Raleigh, NC.

67. NCDOT (2006). *Roadway Standard Drawings*, North Carolina Department of Transportation, Raleigh, NC.

68. Opiela, K., Kan, C.D., and Marzougui, D. (2009). “Development & initial validation of a 2007 Chevrolet Silverado finite element model,” National Crash Analysis Center, George Washington University.

69. Orengo, F., Ray, M.H., and Plaxico, C.A. (2003). "Modeling tire blow-out in roadside hardware simulations using LS-DYNA," In: *2003 ASME International Mechanical Engineering Congress & Exposition*, Washington, D.C., IMECE2003-55057.

70. Pandea, A. and Abdel-Aty, M. (2009). "A novel approach for analyzing severe crash patterns on multilane highways," Accident Analysis and Prevention, 41, 985-994.

71. Patzner, G.S., Plaxico, C.A., and Ray, M.H. (1999). "Effects of post and soil strength on performance of modified eccentric loader breakaway cable terminal," *Transportation Research Record*, 1690, 78-83.

72. Plaxico, C.A., Hackett, R. M., and Uddin, W. (1997). "Simulation of a vehicle impacting a modified thrie-beam guardrail," *Transportation Research Record*, 1599, 1-10.

73. Plaxico, C.A., Mozzarelli, F., and Ray, M.H. (2003). "Tests and simulation of a w-beam rail-to-post connection," *International Journal of Crashworthiness*, 8(6), 543-551.

74. Plaxico, C.A., Patzner, G. S., and Ray, M.H. (1998). "Finite element modeling of guardrail timber posts and the post-soil interaction," *Transportation Research Record*, 1647, 139-146.

75. Plaxico, C.A., Ray, M.H., and Hiranmayee, K. (2000). "Impact Performance of the G4(1W) and G4(2W) guardrail systems: comparison under NCHRP Report 350 Test 3-11 conditions," *Transportation Research Record*, 1720, 7-18.

76. Ray, M.H. (1996a). "Repeatability of full-scale crash tests and criteria for validating simulation results," *Transportation Research Record*, 1528, 155-160.

77. Ray, M.H. (1996b). "Use of finite element analysis in roadside hardware design," *Transportation Research Circular*, 453, 61-71.

78. Ray, M.H., and McGinnis, R. G. (1997). "NCHRP Synthesis of Highway Practice 244: Guardrail and Median Barrier Crashworthiness," *Transportation Research Board*, National Research Council, Washington, D.C.

79. Ray, M.H., and Patzner, G. S. (1997). "Finite element model of modified eccentric loader terminal (MELT)," *Transportation Research Record*, 1599, 11-21.

80. Ray, M.H., and Weir, J. A. (2001). "Unreported collisions with post-and-beam guardrails in Connecticut, Iowa, and North Carolina," *Transportation Research Record*, 1743, 111-119.

81. Ray, M.H., Oldani, E., and Plaxico, C.A. (2004). "Design and analysis of an aluminum F-shape bridge railing," *International Journal of Crashworthiness*, 9(4), 349-363.

82. Ray, M.H., Weir, J., and Hopp, J. (2003). "In-service performance of traffic barriers," *NCHRP Report 490*, Transportation Research Board, National Research Council, Washington, D.C.

83. Reid, J. D., and Coon, B.A. (2002). "Finite element modeling of cable hook bolts," In: *7th International LS-DYNA User Conference*, Dearborn, MI.

84. Reid, J.D. (1996). "Towards the understanding of material property influence on automotive crash structures," *Thin-Walled Structures*, 24, 285-313.

85. Reid, J.D. (1998). "Admissible modeling errors or modeling simplifications," *Finite Elements in Analysis and Design*, 29, 49-63.

86. Reid, J.D. (1998). "Critical Impact Point for Longitudinal Barriers," Highway Division.

87. Reid, J.D. (2004). "LS-DYNA simulation influence on roadside hardware," *Transportation Research Record*, 1890, 34-41.

88. Reid, J.D., and Bielenberg, B.W. (1999). "Using LS-DYNA simulation to solve a design problem: bullnose guardrail example," *Transportation Research Record,* 1690, 95-102.

89. Reid, J.D., and Hiser, N.R. (2004). "Friction modelling between solid elements," *International Journal of Crashworthiness,* 9(1), 65-72.

90. Reid, J.D., and Hiser, N.R. (2005). "Detailed modeling of bolted joints with slippage," *Finite Elements in Analysis and Design,* 41, 547-562.

91. Reid, J.D., and Marzougui, D. (2002). "Improved truck model for roadside safety simulations: Part I - structural modeling," *Transportation Research Record,* 1797, 53-62.

92. Reid, J.D., Coon, B.A., Lewis, B.A., Sutherland, S.H., and Murray, Y.D. (2004). "Evaluation of LS-DYNA Soil Material Model 147," *FHWA-HRT-04-094,* U.S. Department of Transportation, Federal Highway Administration, McLean, VA.

93. Reid, J.D., Kuipers, B.D., Sicking, D.L., and Faller, R.K. (2009). "Impact performance of W-beam guardrail installed at various flare rates," *International Journal of Impact Engineering,* 36, 476-485.

94. Ross Jr, H. E., and Sicking, D.L. (1984). "Guidelines for placement of longitudinal barriers on slopes," *Transportation Research Record,* 970, 3-9.

95. Ross, H.E., Jr., Sicking, D.L., Zimmer, R.A., and Michie, J.D. (1993). "Recommended procedures for the safety performance evaluation of highway features," *NCHRP Report 350,* Transportation Research Board, National Research Council, Washington, D.C.

96. Savolainen, P., Kirsch, R., Johari M.U.M., and Nightingale, E. (2018). "In-service performance evaluation of median cable barriers in Iowa." *Institute for Transportation, Final Report, InTrans Project 15-546.*

97. Sheikh, N.M., Alberson, D.C., and Chatham, L.S. (2008). "State of the practice of cable barrier systems," *Transportation Research Record,* 2060, 84–91.

98. Sposito, B., and Johnston, S. (1999). "Three-cable median barrier," *Final Report OR-RD-99-03,* Oregon Department of Transportation, Salem, OR.

99. Stasburg, G., and Crawley, L.C. (2005). "Keeping Traffic on the Right Side of the Road," In: *Public Road.*

100. Stine, J.S., Hamblin, B.C., Brennan, S.N., Donnell, E.T. (2010). "Analyzing the influence of median cross-section design on highway safety using vehicle dynamics simulations," *Accident Analysis and Prevention,* 42, 1769-1777.

101. Stolle, C.S., Sicking, D.L., Faller, R.K., and Reid, J.D. (2013). "Cable median barrier failure analysis and remediation phase II.", *Midwest Roadside Safety Facility, TRP-03-313-13.*

102. Tiso, P., Plaxico, C., and Ray, M. (2002). "Improved truck model for roadside safety simulations: Part II - suspension modeling," *Transportation Research Record,* 1797, 63-71.

103. Troy, S. A. (2007). "Median barriers in North Carolina," In: *TRB-AFB20 Committee Summer Meeting,* Rapid City, SD.

104. Venkataraman, N.S. Ulfarsson, G.F., Shankar, V., Oh, J., and Park, M. (2011). "Model of relationship between interstate crash occurrence and geometrics: exploratory insights from random parameter negative binomial approach," *Transportation Research Record,* 2236, 41-48.

105. Wang, Q., Fang, H., Li, N., Weggel, D.C., and Wen, G. (2013). "An efficient FE model of slender members for crash analysis of cable barriers," *Engineering Structures,* 52, 240-256.

106. Whitworth, H. A., Bendidi, R., Marzougui, D., and Reiss, R. (2004). “Finite element modeling of the crash performance of roadside barriers,” *International Journal of Crashworthiness*, 9(1), 35-43.

107. WSDOT. (2006). “I-5 Marysville cable median barrier,” *WSDOT Report*, Washington State Department of Transportation, Olympia, WA.

108. WSDOT. (2007). "Cable median barrier report." WSDOT Report, Washington State Department of Transportation, Olympia, WA

109. WSDOT. (2008). "Cable median barrier report." WSDOT Report, Washington State Department of Transportation, Olympia, WA

110. WSDOT. (2009). "Cable median barrier report." WSDOT Report, Washington State Department of Transportation, Olympia, WA

111. Yin, H., Xiao, Y., Wen, G., and Fang, H. (2017). “Design Optimization of a New W-beam Guardrail for Enhanced Highway Safety Performance,” *Advances in Engineering Software*, 112, 154-164.

112. Yin, H., Fang, H., Wang, Q., and Wen, G. (2016). “Design optimization of a MASH TL-3 concrete barrier using RBF-based metamodels and nonlinear finite element simulations,” *Engineering Structures*, 114, 122-134.

113. Zaouk, A.K., Bedewi, N. E., Kan, C.D., and Marzouigui, D. (1997). “Development and evaluation of a C-1500 pickup truck model for roadside hardware impact simulation,” *FHWA-RD-96-212*, Federal Highway Administration, Washington, D.C.

114. Zaouk, A.K., Marzougui, D., and Bedewi, N.E. (2000a). “Development of a detailed vehicle finite element model, Part I: methodology,” *International Journal of Crashworthiness*, 5(1), 25-36.

115. Zaouk, A.K., Marzougui, D., and Kan, C.D. (2000b). “Development of a detailed vehicle finite element model, Part II: material characterization and component testing,” *International Journal of Crashworthiness*, 5(1), 37-50.

116. Zegeer, C.V., Stewart, J.R., Council, F.M., Reinfurt, D.W., and Hamilton, E. (1992). “Safety effects of geometric improvements on horizontal curves,” *Transportation Research Record*, 1356, 11-19.

117. Zhu, L. and J. Rohde (2010). “Development of guidelines for anchor design for high-tension cable guardrails,” *Transportation Research Record*, 2195, 115-120.

118. Zweden, J.V. and Bryden, J.E. (1977). “In-service Performance of Highway Barriers,” *Report NYSDOT-ERD-77-RR51*, New York State Department of Transportation, Albany, NY.

APPENDIX A. Performance Evaluation of Three CMB Designs on a Flat Terrain under MASH TL-3 Conditions

In this section, the three CMB designs, i.e., the current CMB, "*Sixth Design Retrofit*" and "*Four-cable Design Retrofit*," are evaluated on a flat terrain and under MASH TL-3 test conditions, i.e., under impacts of a small passenger car and a pickup truck. For each CMB design, two impact locations were used, i.e., at a post and at mid-span, and both front-side and backside impacts were evaluated. The simulation results of the three CMBs on a flat terrain and impacted by a 1996 Dodge Neon (i.e., the small passenger car) and a 2006 Ford F250 (i.e., the pickup truck) are summarized in Tables A.1 and A.2, respectively. It can be seen that the CMB performance on a flat terrain is slightly better than the same CMBs on a 6H:1V sloped median (see Tables 4.6 and 4.7). This indicates that in-service CMBs on a sloped median could underperform even if they have passed the MASH TL-3 tests that are typically performed on a flat terrain. It is thus suggested that new CMB systems be tested on a sloped median to determine their performance under in-service conditions.

Table A.1: Summary of simulation results of the three CMBs on a flat terrain and impacted by a Dodge Neon

CMB Design	Impact Side	Impact Location	Vehicle Response	MASH Evaluation Criteria				
				Exit Box	Exit Angle	A	D	F
The Current Design	Front-side	Post	RD	F §	14°	P	P	P
		Mid-span	RD	P	7°	P	P	P
	Back-side	Post	RD	P	7°	P	P	P
		Mid-span	PE	F	N/A	F	P	P
The Sixth Design Retrofit	Front-side	Post	RD	P	6°	P	P	P
		Mid-span	RC	N/A	N/A	P	P	P
	Back-side	Post	RD	P	9°	P	P	P
		Mid-span	RD	P	15°	P	P	P
The Four-cable Design Retrofit	Front-side	Post	RD	P	5°	P	P	P
		Mid-span	RD	P	7°	P	P	P
	Back-side	Post	RD	F §	15°	P	P	P
		Mid-span	RD	P	6°	P	P	P

* Notations:
- – Vehicular Responses: **RD**: Redirected, **PE**: Penetrated
- – Evaluation Criteria A, D, F: **P**: Pass, **F**: Fail
- – Exit Box Criterion: **P**: Pass, **F**: Fail, **N/A**: Not Applicable
- – Exit Angle: **N/A**: Not Applicable

§: In these impact cases, the exit box criterion was slightly violated.

Table A.2: Summary of simulation results of the three CMBs on a flat terrain and impacted by a Ford F250

CMB Design	Impact Side	Impact Location	Vehicle Response	MASH Evaluation Criteria				
				Exit Box	Exit Angle	A	D	F
The Current Design	Front-side	Post	RD	P	8°	P	P	P
		Mid-span	RD	P	4°	P	P	P
	Back-side	Post	RD	P	6°	P	P	P
		Mid-span	RD	P	9°	P	P	P
The Sixth Design Retrofit	Front-side	Post	RD	P	4°	P	P	P
		Mid-span	RD	P	11°	P	P	P
	Back-side	Post	RD	P	7°	P	P	P
		Mid-span	RD	P	7°	P	P	P
The Four-cable Design Retrofit	Front-side	Post	RD	P	5°	P	P	P
		Mid-span	RD	P	9°	P	P	P
	Back-side	Post	RD	P	6°	P	P	P
		Mid-span	RD	P	8°	P	P	P

* Notations:
– Vehicular Responses: **RD**: Redirected
– Evaluation Criteria A, D, F: **P**: Pass, **F**: Fail
– Exit Box Criterion: **P**: Pass, **F**: Fail

Figures A1 to A8 give the top-view vehicle trajectories of the Dodge Neon and Ford F250 impacting the current CMBs. Figures A9 to A16 give the top-view vehicle trajectories of the Dodge Neon and Ford F250 impacting the "*Sixth Design Retrofit*." Figures A17 to A24 give the top-view vehicle trajectories of the Dodge Neon and Ford F250 impacting the "*Four-cable Design Retrofit*." Other simulation results such as vehicle-barrier interactions, yaw, pitch, and roll angles, time histories of transverse displacements, and time histories of transverse velocities are not included in this report but will be submitted to NCDOT electronically.

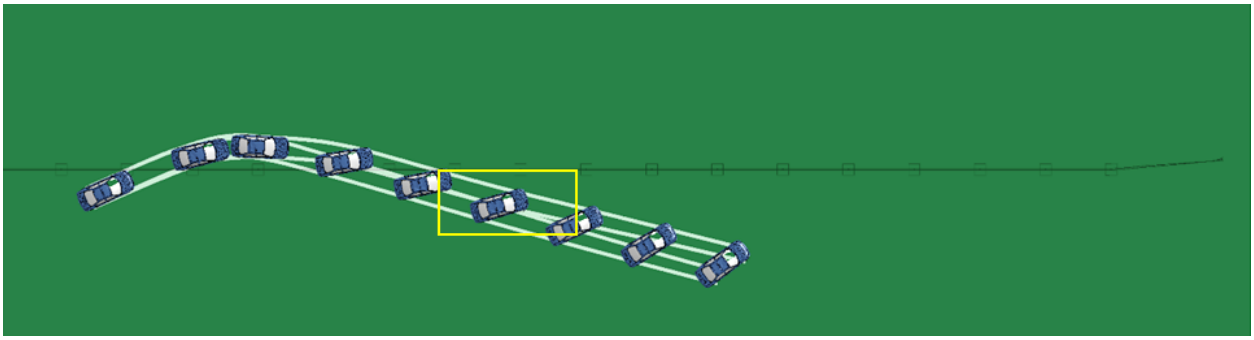

Fig. A.1: A Dodge Neon impacting the current CMB design at a post from front-side.

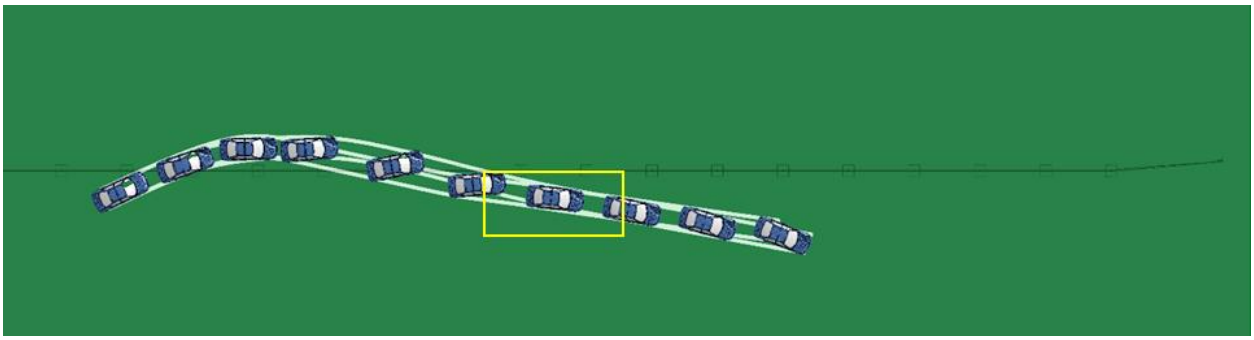

Fig. A.2: A Dodge Neon impacting the current CMB design at mid-span from front-side.

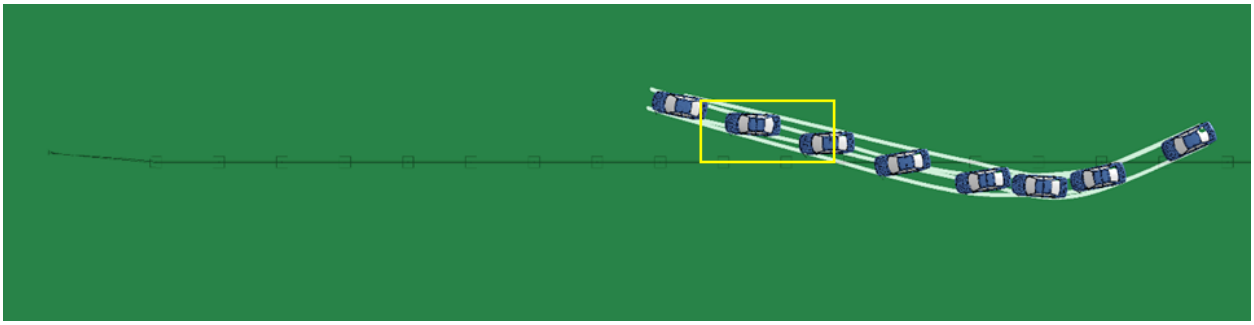

Fig. A.3: A Dodge Neon impacting the current CMB design at a post from backside.

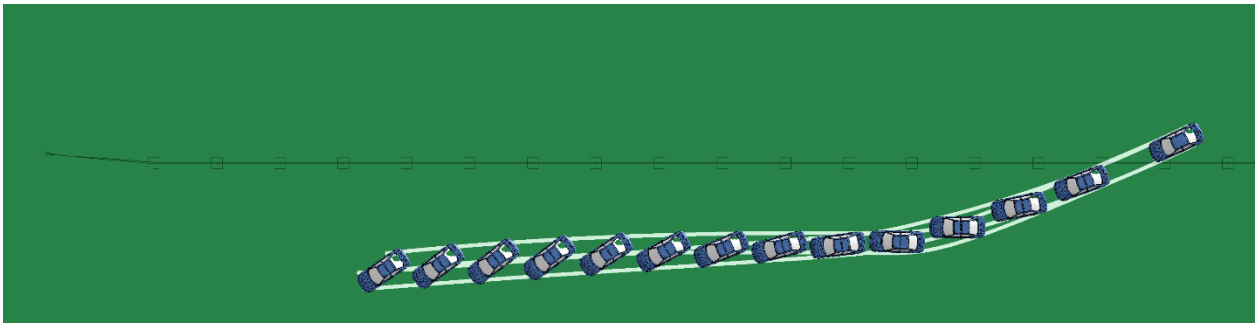

Fig. A.4: A Dodge Neon impacting the current CMB design at mid-span from backside.

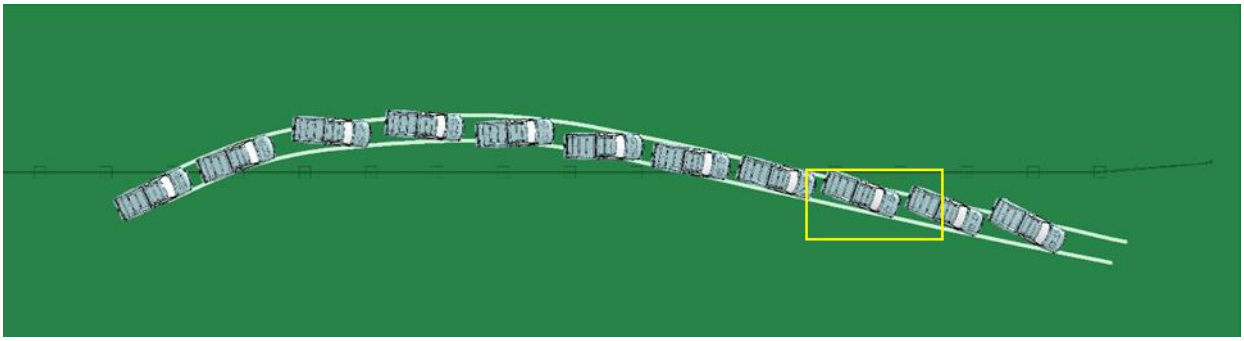

Fig. A.5: A Ford F250 impacting the current CMB design at a post from front-side.

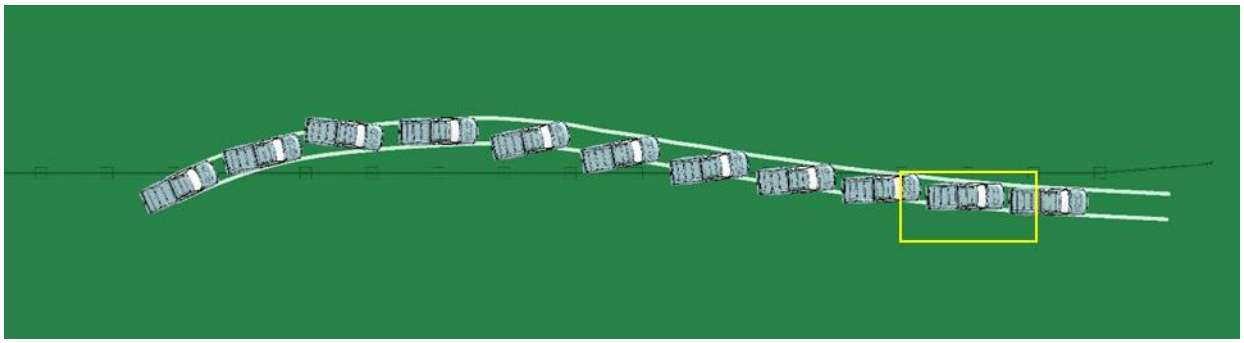

Fig. A.6: A Ford F250 impacting the current CMB design at mid-span from front-side.

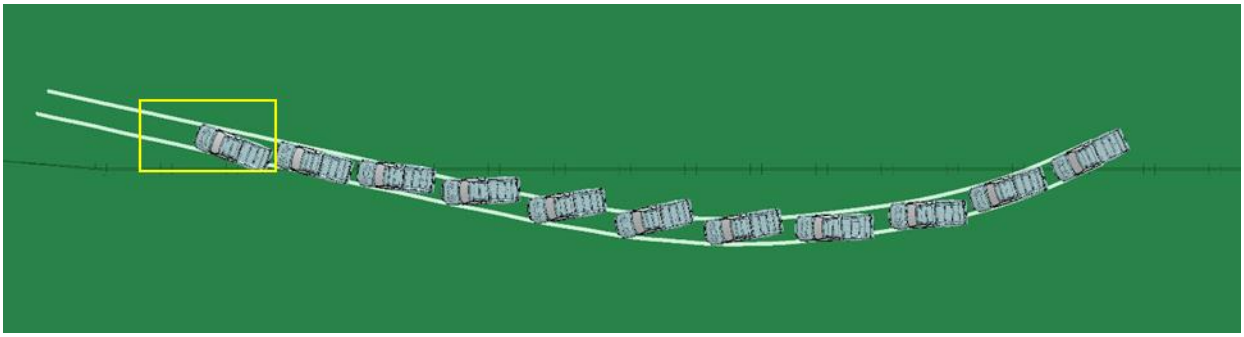

Fig. A.7: A Ford F250 impacting the current CMB design at a post from backside.

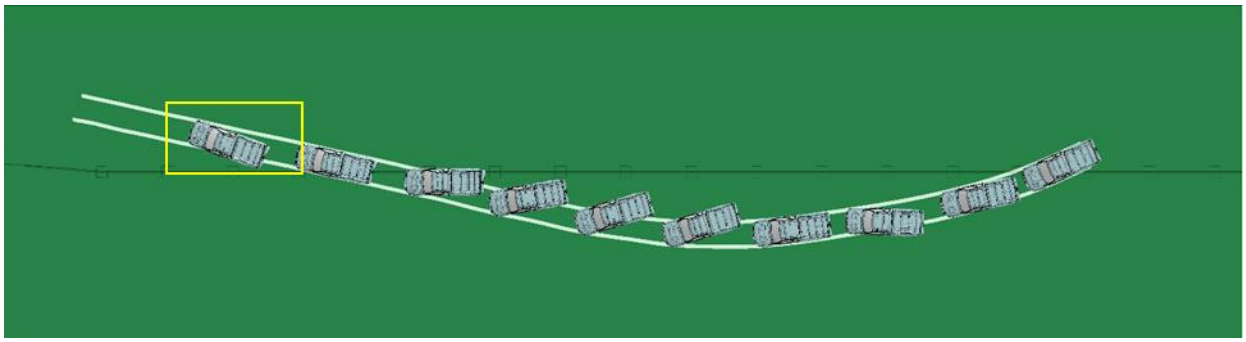

Fig. A.8: A Ford F250 impacting the current CMB design at mid-span from backside.

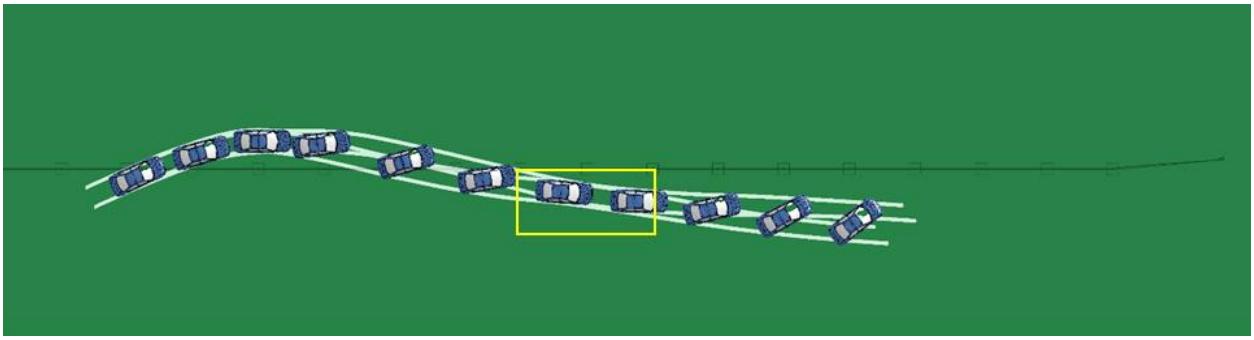

Fig. A.9: A Dodge Neon impacting the "*Sixth Design Retrofit*" at a post from front-side.

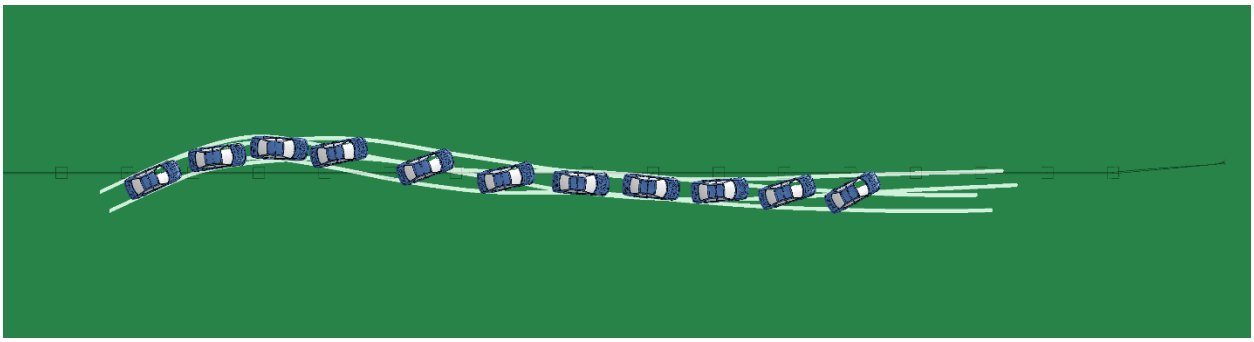

Fig. A.10: A Dodge Neon impacting the "*Sixth Design Retrofit*" at mid-span from front-side.

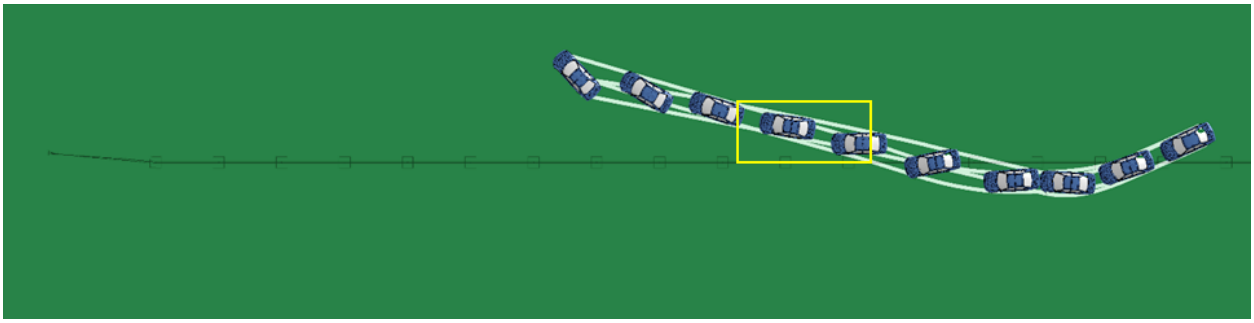

Fig. A.11: A Dodge Neon impacting the "*Sixth Design Retrofit*" at a post from backside.

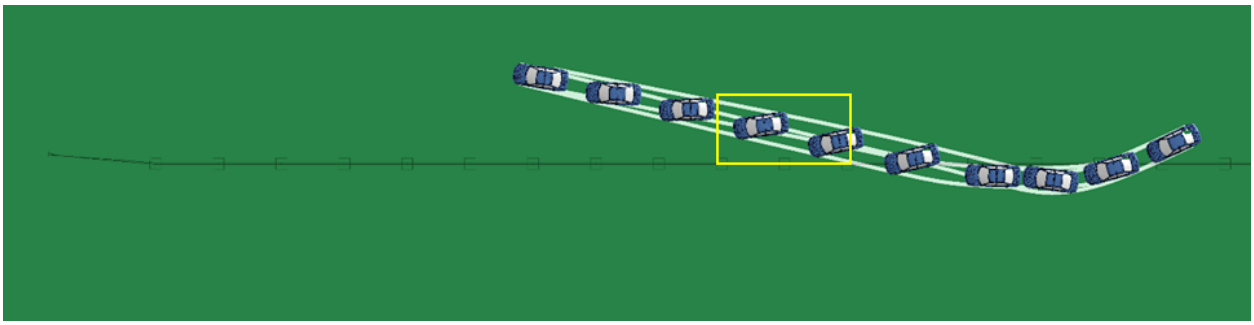

Fig. A.12: A Dodge Neon impacting the "*Sixth Design Retrofit*" at mid-span from backside.

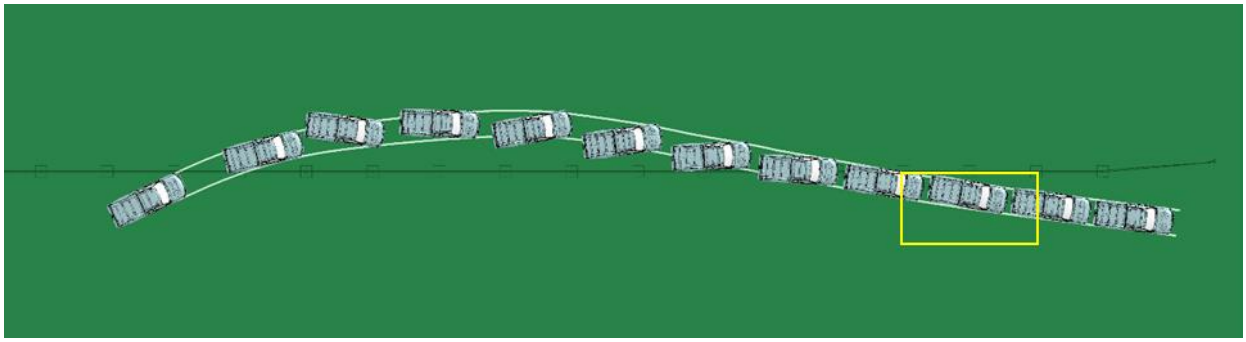

Fig. A.13: A Ford F250 impacting the "*Sixth Design Retrofit*" at a post from front-side.

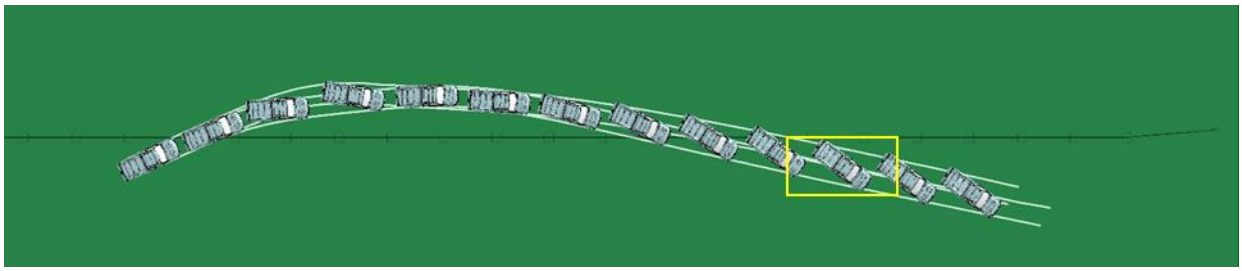

Fig. A.14: A Ford F250 impacting the "*Sixth Design Retrofit*" at mid-span from front-side.

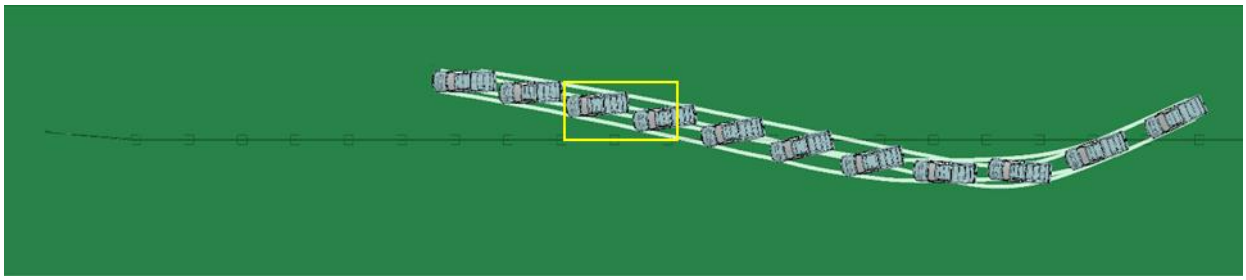

Fig. A.15: A Ford F250 impacting the "*Sixth Design Retrofit*" at a post from backside.

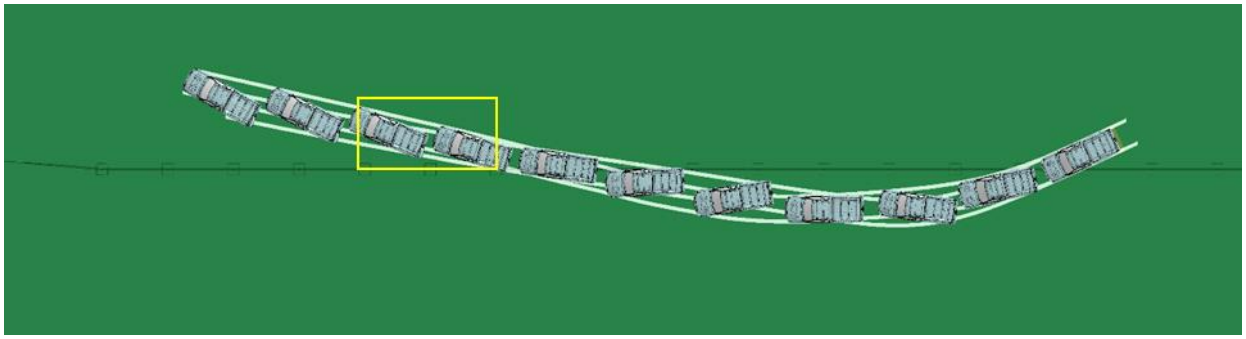

Fig. A.16: A Ford F250 impacting the "*Sixth Design Retrofit*" at mid-span from backside.

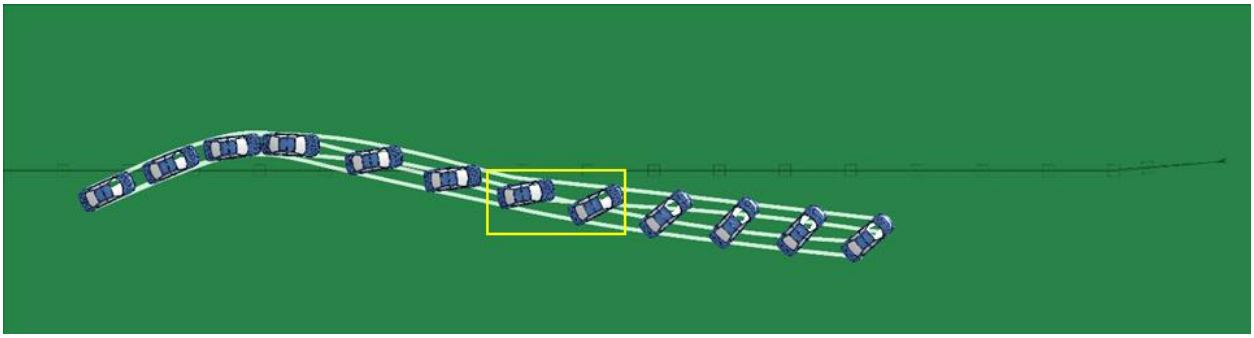

Fig. A.17: A Dodge Neon impacting the "*Four-cable Design Retrofit*" at a post from front-side.

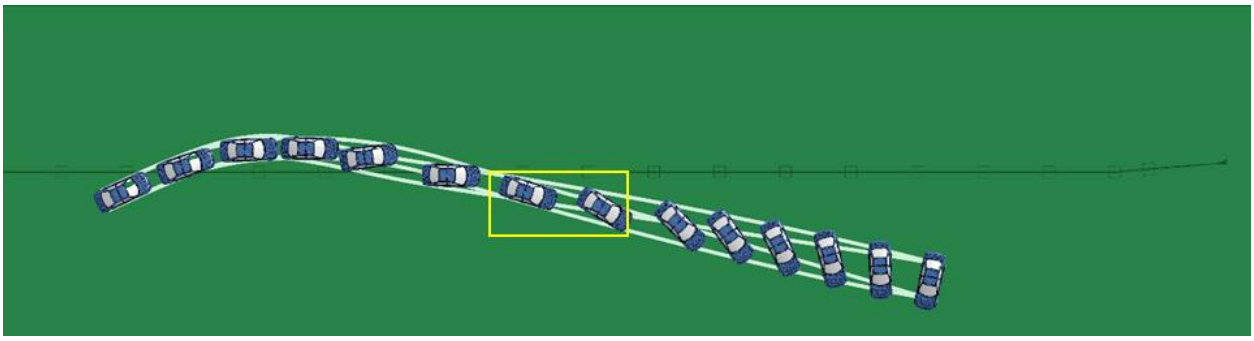

Fig. A.18: A Dodge Neon impacting the "*Four-cable Design Retrofit*" at mid-span from front-side.

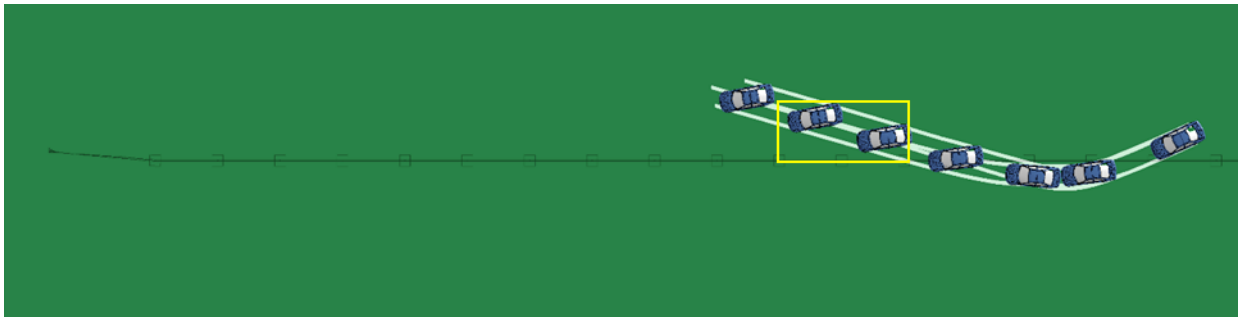

Fig. A.19: A Dodge Neon impacting the "*Four-cable Design Retrofit*" at a post from backside.

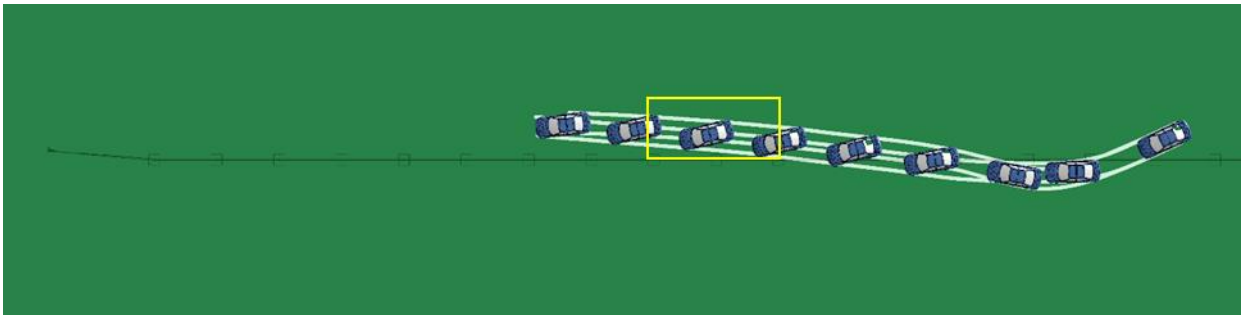

Fig. A.20: A Dodge Neon impacting the "*Four-cable Design Retrofit*" at mid-span from backside.

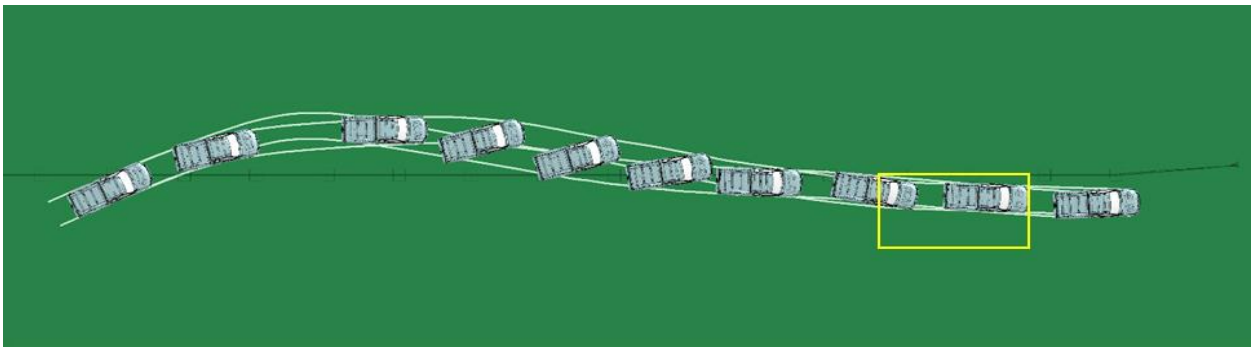

Fig. A.21: A Ford F250 impacting the "*Four-cable Design Retrofit*" at a post from front-side.

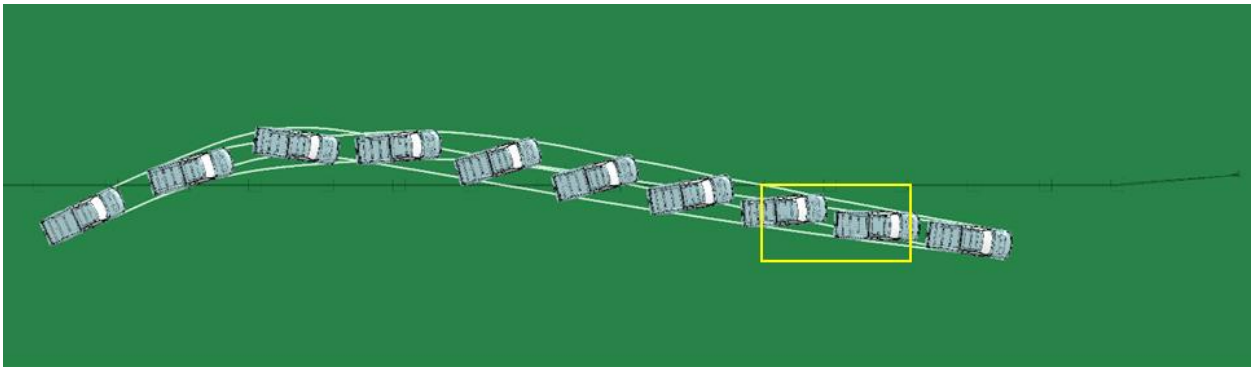

Fig. A.22: A Ford F250 impacting the "*Four-cable Design Retrofit*" at mid-span from front-side.

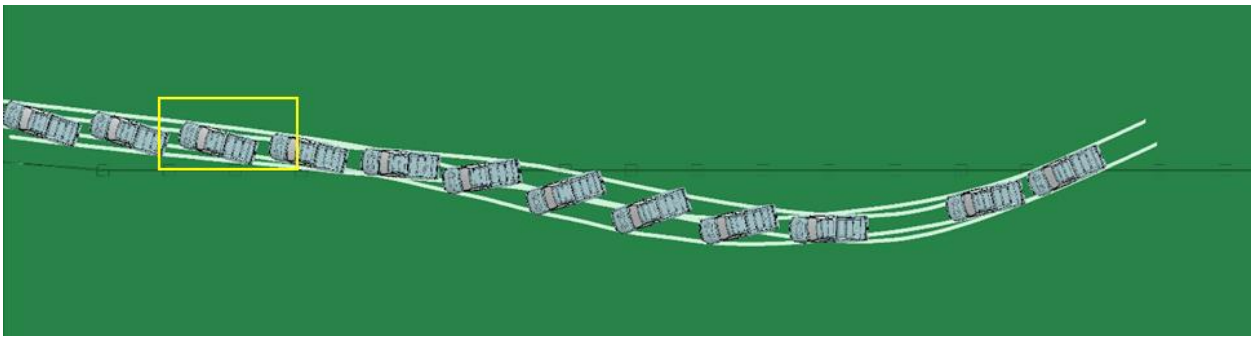

Fig. A.23: A Ford F250 impacting the "*Four-cable Design Retrofit*" at a post from backside.

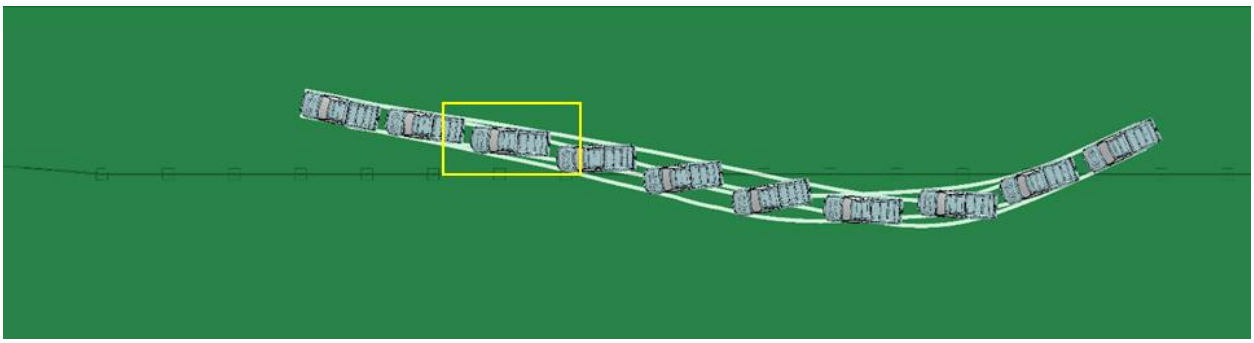

Fig. A.24: A Ford F250 impacting the "*Four-cable Design Retrofit*" at mid-span from backside

APPENDIX B. Performance Evaluation of Two CMB Designs on a Flat Terrain under Impacts by a MASH 1500A Vehicle

In this section, a preliminary study was performed on the current CMB desing and the "*Sixth Design Retrofit*" placed on a flat terrain and under impacts by a Toyota Camry, a TL-3 test vehicle (1500A) required by the new edition of MASH. Figure B.1 shows the FE model of the Toyota Camry used in this study.

Fig. B.1: FE model of a Toyota Camry.

Figures B.2 and B.3 show the top-view vehicle trajectories of the Toyota Camry impacting the current CMB design and "Sixth Design Retrofit," respectively, from front-side. It can be seen from Figures B.2 and B.3 that both the current CMB design and "Sixth Design Retrofit" could safety redirect the vehicle and pass the MASH exit box criterion.

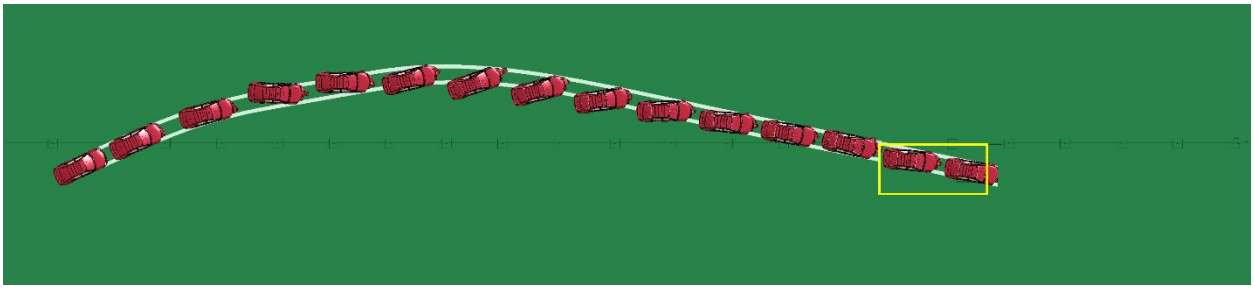

Fig. B.2: A Toyota Camry impacting the current CMB from front-side.

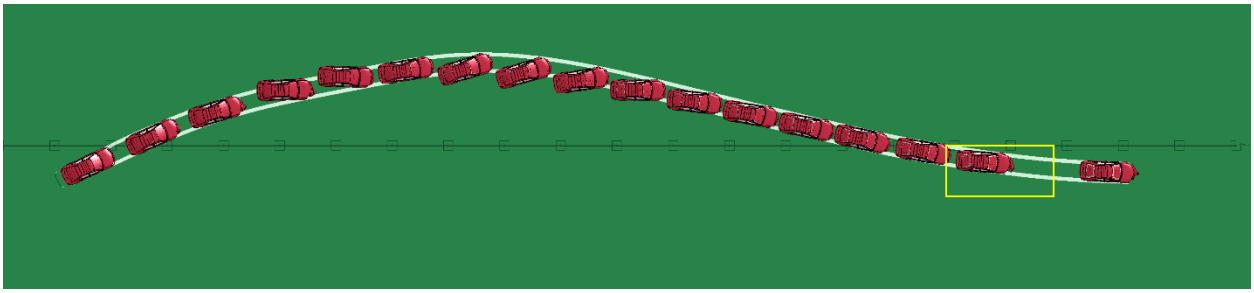

Fig. B.3: A Toyota Camry impacting the "*Sixth Design Retrofit*" from front-side.

The exit angles were determined to be 8° for the current CMB design and 5° for the "*Sixth Design Retrofit*." Figure B.4 shows the yaw, pitch, and roll angles of the Toyota Camry impacting the two CMB designs from front-side. It can be seen that the MASH Evaluation Criterion *F*, which specified a maximum of 75° of roll or pitch angle, was met in both impact cases.

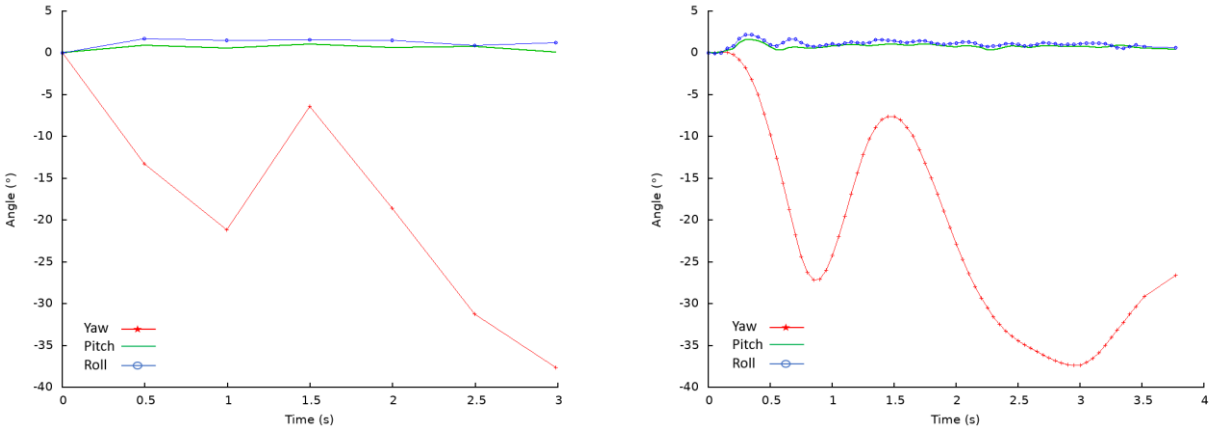

(a) Current CMB design (b) "*Sixth Design Retrofit*"

Fig. B.4: Yaw, pitch, and roll angles of a Toyota Camry impacting the current design and "*Sixth Design Retrofit*" from front-side.

Figures B5 and B6 show the time instants when the maximum dynamic deflections occured on the current CMB design and the "*Sixth Design Retrofit*," respectively, under impacts by the Toyota Camry from front-side. The maximum CMB deflection was 6.74 m (22.11 ft) on the current CMB design and 7.61 m (24.96 ft) on the "*Sixth Design Retrofit*." Although both impact cases met the MASH exit box criterion, the large maximum CMB deflections raised concerns for narrow medians where the CMBs were to be installed.

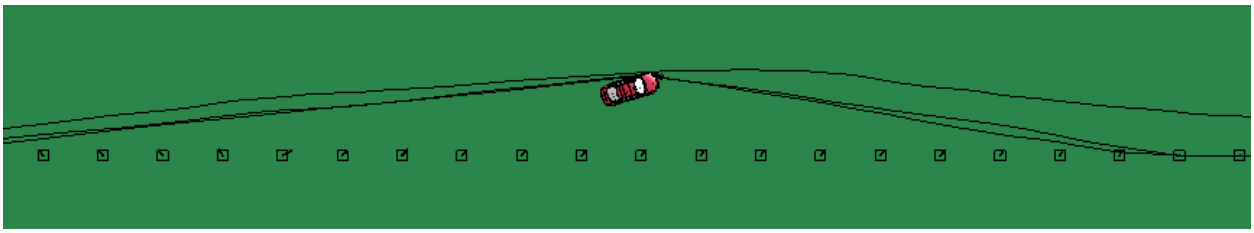

Fig. B.5: Maximum deflection of the current CMB design impacted by a Toyota Camry from front-side.

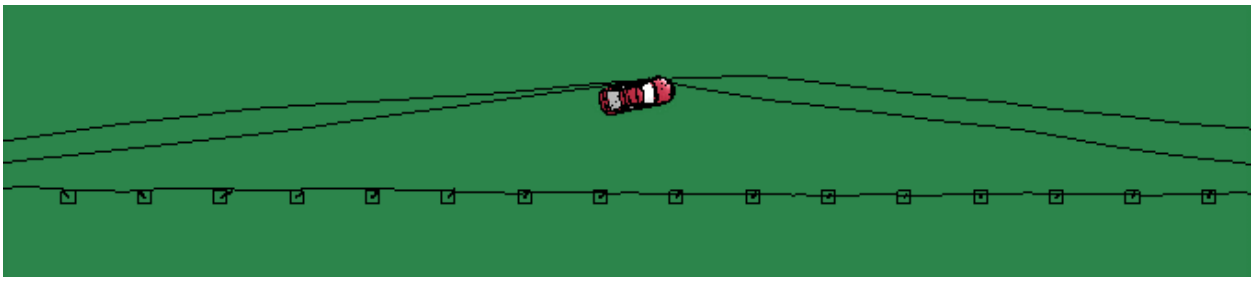

Fig. B.6: Maximum deflection of the "*Sixth Design Retrofit*" impacted by a Toyota Camry from front-side.